

Role of evolutionary conserved MAP kinase
C-terminal regions in transcriptional activation in
Arabidopsis thaliana

Inaugural-Dissertation

zur

Erlangung des Doktorgrades
der Mathematisch-Naturwissenschaftlichen Fakultät
der Universität zu Köln

vorgelegt von

María Claudia Salazar Rondón

aus Bogotá - Kolumbien

Köln

2019

Die vorliegende Arbeit wurde am Max-Planck-Institut für Pflanzenzüchtungsforschung in Köln in der Abteilung für Pflanze-Mikroben Interaktionen (Direktor: Prof. Dr. Paul Schulze-Lefert), in der Arbeitsgruppe von Dr. Kenichi Tsuda angefertigt.



MAX-PLANCK-GESELLSCHAFT



Max-Planck-Institut für
Pflanzenzüchtungsforschung



IMPRS Cologne

Berichterstatter:

Prof. Dr. Jane E. Parker

Prof. Dr. Alga Zuccaro

Prüfungsvorsitzender:

Prof. Dr. Stanislav Kopriva

Tag der mündlichen Prüfung:

23.07.2019

Publications

Mine, A., Nobori, T., **Salazar-Rondon, M.C.**, Winkelmüller, T.M., Anver, S., Becker, D. and Tsuda, K., 2017. An incoherent feed-forward loop mediates robustness and tunability in a plant immune network. *EMBO reports*, p.e201643051.

Table of Contents

Publications	I
Table of Contents	III
List of Figures	VII
List of Tables	VIII
List of Abbreviations	IX
Abstract	XIII
Zusammenfassung	XIV
1. Introduction	1
1.1. The plant immune system.....	1
1.2. Arabidopsis MAPKs.....	2
1.2.1. Regulation of TFs by <i>AtMPK3/6</i> during plant immunity.....	5
1.2.2. Interactions between <i>AtMPK3/6</i> and phytohormones in plant immunity	8
1.2.3. <i>AtMPK3/6</i> modulate RNA-Pol II phosphorylation	9
1.3. MAPKs in other eukaryotes.....	11
1.3.1. MAPK cascades and scaffold proteins in yeast.....	12
1.3.2. MAPK cascades and scaffold proteins in mammals	13
1.3.3. Arabidopsis scaffold proteins associated with MAPKs during immunity	16
1.4. Thesis aims	17
2. Results	19
2.1. Y2H screening for MAPK interactors	19
2.1.1. <i>AtMPK3</i> and <i>AtMPK6</i> C-termini are responsible for autoactivity in yeast	20
2.1.2. Twenty-three TFs were identified as candidate interactors of <i>AtMPK3</i> and <i>AtMPK6</i> in Y2H.....	22
2.1.3. The C-terminus of <i>AtMPK3</i> and <i>AtMPK6</i> works as a trans-activation domain in yeast	26
2.2. <i>AtMPK3</i> and <i>AtMPK6</i> C-terminal domain induces transcription independently from their kinase activity <i>in planta</i>	28
2.2.1. <i>AtMPK3</i> and <i>AtMPK6</i> C-terminal domain present transcriptional activity <i>in planta</i>	28

2.2.2. Sequence-specific <i>AtMPK3</i> and <i>AtMPK6</i> C-termini activate transcription <i>in planta</i>	30
2.2.3. Transcriptional activation of <i>AtMPK3</i> and <i>AtMPK6</i> C-termini is independent of protein accumulation.....	32
2.3. <i>AtMPK3</i> and <i>AtMPK6</i> C-terminal domain is evolutionary conserved across plant species	35
2.3.1. Angiosperms and non-plant kinases possess a conserved C-terminal domain	35
2.3.2. MAPK C-terminal domains are conserved among the Viridiplantae clade.....	36
2.3.3. MAPKs C-terminal domain transcriptional activation is conserved across kingdoms	38
2.4. Physiological function of <i>AtMPK3</i> C-terminal domain in <i>A. thaliana</i>	41
3. Discussion.....	43
3.1. Newly identified <i>AtMPK3</i> and <i>AtMPK6</i> interacting TFs	43
3.2. <i>AtMPK3</i> and <i>AtMPK6</i> C-terminal domain as trans-activation domain.....	46
3.3. Evolutionary conserved trans-activation domain in MAPK C-terminal domains	48
3.4. Developmental phenotype of <i>Atmpk3 Atmpk6</i> double mutant was not complemented by <i>AtMPK3-GFP</i>	50
3.5. Concluding remarks and future perspectives	51
4. Materials and Methods	53
4.1. Materials.....	53
4.1.1. Plant material and growth conditions	53
4.1.2. Bacteria and Yeast material and growth conditions.....	53
4.1.3. Primer information.....	58
4.1.4. Chemicals, and kits	63
4.1.5. Media, buffers and solutions.....	64
4.2. Methods.....	67
4.2.1. Cloning of MAPKs for Y2H and transient assays <i>in planta</i>	67
4.2.2. Y2H assays for <i>AtMPK3</i> and <i>AtMPK6</i> interactors	70
4.2.3. Biomolecular fluorescence complementation (BiFC) assays in <i>N. benthamiana</i>	72
4.2.4. Particle bombardment transient assay in <i>Arabidopsis</i> leaves	72
4.2.5. Transient expression assays in <i>Arabidopsis</i> mesophyll protoplast	73
4.2.6. Dual luciferase assays	74
4.2.7. <i>AtMPK3/6</i> short peptides protein accumulation	75
4.2.8. Promoter activity assays with GUS reporter.....	75
4.2.9. Phylogenetic analysis.....	76

4.2.10. Transformation of <i>A. thaliana</i> <i>Atmpk3</i> <i>Atmpk6</i> double mutant by floral dipping.....	76
5. References.....	79
6. Supplementary Material	93
Acknowledgments	99
Erklärung	101
Curriculum Vitae.....	103

List of Figures

Figure 1: MPK3/6 signaling cascade mediates immune responses in Arabidopsis	9
Figure 2: MAPK activation modules and scaffold proteins in yeast, mammals, and plants	15
Figure 3: <i>AtMPK3</i> and <i>AtMPK6</i> baits show autoactivity in Y2H	19
Figure 4: Schematic representation of <i>AtMPK3</i> and <i>AtMPK6</i> constructs	20
Figure 5: The C-terminus of <i>AtMPK3</i> and <i>AtMPK6</i> is necessary and sufficient for autoactivity in Y2H	21
Figure 6: Confirmation of <i>AtMPK3/6</i> - TFs interactions through Y2H assays.....	25
Figure 7: Baits containing <i>AtMPK3</i> and <i>AtMPK6</i> C-termini show autoactivity without a prey	27
Figure 8: <i>AtMPK3</i> and <i>AtMPK6</i> C-terminus shows transcriptional activation activity in Arabidopsis	29
Figure 9: Transcriptional activation activity of <i>AtMPK3</i> and <i>AtMPK6</i> C-terminus is sequence specific	31
Figure 10: Protein expression does not explain transcriptional activation.....	33
Figure 11: MAPKs phylogenetic tree and C-terminal protein profile reveal conserved residues.....	36
Figure 12: Phylogenetic analysis of 713 MAPKs from the Viridiplantae clade	37
Figure 13: MAPK C-terminal domains across kingdoms induce transcriptional activity <i>in planta</i>	39
Figure 14: C-terminal MAPKs sequence analysis determined a potential conserved motif among eukaryotes	40
Figure 15: <i>AtMPK3prom::AtMPK3-GFP</i> did not complement the embryo-lethal phenotype in <i>Atmpk3 Atmpk6</i> double mutants.	42
Supplementary Figure 1: <i>AtMPK3</i> and <i>AtMPK6</i> show autoactivity in Y2H LexA system.....	93
Supplementary Figure 2: YFP fluorescence caused by expression of n-YFP and <i>AtMPK3</i> and <i>AtMPK6</i> fused to c-YFP in BiFC assay	94
Supplementary Figure 3: Amino sequences of the new <i>AtMPK3</i> and <i>AtMPK6</i> deletion constructs.	95
Supplementary Figure 4: Protein accumulations of effector proteins are not detectable by α -GAL4-DBD antibody	96
Supplementary Figure 5: Co-expression of <i>AtMPK3</i> and <i>AtWRKY33</i> does not lead to <i>AtPROPEP2</i> promoter induction.....	97

List of Tables

Table 1: Candidate TFs that interacted with AtMPK3 and/or AtMPK6 in Y2H screens	23
Table 2: Confirmed TFs interacting with AtMPK3 and AtMPK6 in Y2H.....	26
Table 3: Bacteria and yeast strains used in this study	53
Table 4: Vectors used in this study	54
Table 5: Vectors generated in this study	55
Table 6: List of primers used in this study for PCR amplification	59
Table 7: List of primers used for sequencing.....	62
Table 8: List of chemicals used during this study.....	63
Table 9: Kits used in this study.....	63
Table 10: Media used for bacteria and yeast growth	64
Table 11: Solutions and buffers used in this study	65
Table 12: PrimeSTAR HS Takara master mix.....	67
Table 13: PCR Program for AtMPK3 and AtMPK6 deletion constructs	67
Table 14: PrimeSTAR HS Takara master mix for oligo-amplification	69
Table 15: Y2H transformation mix.....	71
Table 16: Selective media used for co-transformations or single transformations in yeast.....	71
Table 17: Antibodies used for immunoblotting	75
Table 18: Fusion PCR components and program for AtMPK3/6 promoter and coding sequences	77
Table 19: PCR components and program for <i>Atmpk6</i> genotyping	78
Supplementary Table 1: Molecular weight of effectors containing HA tag	98

List of Abbreviations

%	Percentage
μg	Microgram
μl	Microliter
3AT	3-Amino-1,2,4-triazole
ΔC	C-terminus-deletion
A	Adenine
aa	Amino acid
ABA	abscisic acid
ACC	1-amino-cyclopropane-1-carboxylic acid
ACS	ACC synthase
AD	Activation domain
Amp	Ampicillin
<i>At</i>	<i>Arabidopsis thaliana</i>
bp	Base pairs
BS	Binding site
bZIP	basic region/leucine zipper motif
Carb	Carbenicillin
CCB	Coomassie Brilliant Blue
CDK	cyclin-dependent kinases
Chlo	Chloramphenicol
cm	centimeter
Col-0	Columbia-0
CTD	RNA-Pol II C-terminal domain
DBD	DNA-binding domain

EGF	Epidermal growth factors
ERK	Extracellular-signal-regulated kinase
ET	Ethylene
ETI	Effector-trigger immunity
EtOH	Ethanol
ETS	Effector trigger-susceptibility
Gent	Gentamicin
GPCR	G protein-coupled receptor
H	Histidine
HADCs	histone deacetylation by histone deacetylases
<i>Hs</i>	<i>Homo sapiens</i>
JA	Jasmonic acid
JNK	Jun amino N-terminal kinase
Kan	Kanamycin
kDa	Kilo dalton
KSR	Kinase suppressor of Ras
L	Leucine
LB	Luria-Bertani
LPS	Lipopolysaccharides
LRR	Leucin-reach repet
LysM	Lysine-motif
M	Molar
MAMPs	Microbe-associated molecular patterns
MAPK	Mitogen-activated protein kinases
MAPKK	MAP kinase kinase
MAPKKK	MAP kinase kinase kinase

mg	Milligram
min	Minutes
MKI	MAP kinase insert
ML	Maximum likelihood
ml	milliliter
mm	millimeter
mM	Millimolar
<i>Mp</i>	<i>Marchantia polymorpha</i>
MTI	MAMPs-triggered immunity
NJ	Neighbor-joining
NLS	Nuclear localization sequence
OD	Optical density
P-def	Phospho-deficient
PGNs	Peptidoglycans
PRRs	Pattern recognition receptors
<i>Pto</i>	<i>Pseudomonas syringae</i>
R	Resistant proteins
RACK1	Receptor for activated C-kinase 1
rcf	relative centrifugal force
RLCK	Receptor-like cytoplasmic kinases
RNA-Pol II	RNA Polymerase II
rpm	Revolutions per minute
RT	Room temperature
RTK	Receptor tyrosine kinases
s	Seconds
SA	Salicylic acid

<i>Sc</i>	<i>Saccharomyces cerevisiae</i>
SD	Synthetic defined medium
tAD	trans-activation domain
TF	Transcription factor
TTSS	Type III secretion system
V	Volts
W	Tryptophan
WB	Western blot
WT	Wild type
Y2H	Yeast two-hybrid
YPD	Yeast extract-peptone-dextrose

Abstract

Mitogen-activated protein kinase (MAPK) cascades are central signaling components among eukaryotes that mediate intracellular signaling in numerous physiological processes. MAPKs cascades consist of three kinases, MAPKKKs, MAPKKs, and MAPKs whose activity is regulated through phosphorylation. The *Arabidopsis thaliana* MAPKs *AtMPK3* and *AtMPK6* modulate the function of substrates through phosphorylation and are positive immune regulators. However, *AtMPK3* and *AtMPK6* substrates are not fully understood, especially for transcription factors (TFs) that control immune transcriptional reprogramming. Only a few TFs (e.g., *AtWRKY33*, *AtVIP1*, *AtERF6*, *AtERF104*, and *AtMYB44*) are known to be phosphotargets of *AtMPK3/6* during plant immunity. Here I identified 12 novel TFs interactors of *AtMPK3* and or *AtMPK6* through a large-scale yeast two-hybrid (Y2H) screening with a library composed of ~ 1500 *Arabidopsis* TFs. Moreover, I found that when fused to a DNA binding protein, *AtMPK3/6* activated transcription of reporter genes in yeast and that the C-terminus region of *AtMPK3/6* was necessary and sufficient for this activation. Notably, this novel MAPK function was preserved in two transient expression systems of *Arabidopsis*. This MAPK C-terminus-mediated transcriptional activation was sequence-specific. Furthermore, consistently with the highly conserved amino acid sequences of MAPK C-terminal regions across kingdoms, all tested C-terminal domains of MAPKs from *Arabidopsis thaliana*, the early-diverged bryophyte *Marchantia polymorpha*, mammals, and yeast exhibited the ability for transcriptional enhancement. These results imply that MAPKs can activate transcription via the evolutionary conserved MAPK C-terminal domains when close to DNA. Taken together, this study broadens the knowledge of MAPKs immune signaling networks by identifying 12 TFs interactors of *AtMPK3* and or *AtMPK6* and revealing a novel kinase-independent MAPK function, which may be conserved across eukaryotes.

Zusammenfassung

Mitogen-aktivierte Proteinkinase (MAPK) Kaskaden sind zentrale Signalkomponenten der Eukaryonten, die die intrazelluläre Signalübertragung in zahlreichen physiologischen Prozessen vermitteln. MAPK Kaskaden bestehen aus drei Kinasen, MAPKKKs, MAPKKs und MAPKs, deren Aktivität durch Phosphorylierung reguliert wird. Die *Arabidopsis thaliana* MAPK *AtMPK3* und *AtMPK6* verändern die Funktion von Substraten durch Phosphorylierung und sind positive Regulatoren der Immunantwort. Die Substrate von *AtMPK3*- und *AtMPK6* sind jedoch nicht vollständig bekannt, insbesondere für Transkriptionsfaktoren (TFs), die die Reprogrammierung der Immuntranskription steuern. Es ist bekannt, dass nur einige TFs (z. B. *AtWRKY33*, *AtVIP1*, *AtERF6*, *AtERF104* und *AtMYB44*) Phosphorylierungsziele von *AtMPK3/6* während der pflanzlichen Immunantwort sind. In dieser Arbeit identifizierte ich 12 neue TF-Interaktoren von *AtMPK3* und/oder *AtMPK6* durch den Yeast-Two-Hybrid (Y2H) -Screen einer Bibliothek, die aus ~1500 *Arabidopsis*-TFs bestand. Darüber hinaus stellte ich fest, dass *AtMPK3/6* bei Fusion mit einem DNA-bindenden Protein die Transkription von Reporter genen in Hefe aktivierte, und dass die C-terminale Region von *AtMPK3/6* für diese Aktivierung notwendig und ausreichend war. Bemerkenswerterweise blieb diese neuartige MAPK-Funktion in zwei transienten Expressionssystemen von *Arabidopsis* erhalten. Diese, durch den MAPK C-terminus vermittelte Transkriptionsaktivierung war sequenzspezifisch. In Übereinstimmung mit den hohen Aminosäuresequenzkonservierung zwischen den MAPK C-termini von *Arabidopsis thaliana*, dem früh divergierten Bryophyten *Marchantia polymorpha*, Säugetieren und Hefe wiesen diese C-termini ebenfalls die Fähigkeit zur Transkriptionsaktivierung auf. Diese Ergebnisse weisen darauf hin, dass MAPK die Transkription über die evolutionär konservierten MAPK C-terminalen Domänen aktivieren können, wenn sie sich in der Nähe von DNA befinden. Zusammenfassend erweitert diese Studie das Wissen über das MAPK Signaltransduktionsnetzwerk während der Immunantwort, indem 12 TF Interaktoren von *AtMPK3* and *AtMPK6* identifiziert werden und eine neue Kinase-unabhängige MAPK Funktion entschlüsselt wird, welche möglicherweise innerhalb der Eukaryoten konserviert ist.

1. Introduction

1.1. The plant immune system

In nature, plants constantly face numerous abiotic and biotic stresses that force them to evolve suitable strategies to recognize and respond to these pressures. Biotic stress is caused by numerous pathogens such as bacteria, fungi, oomycetes, nematodes or viruses. Plants rely on their cellular innate immunity to defend against potential pathogenic microbes. During their coevolution with microbes, plants had acquired two main layers of innate immunity. The first layer of immunity is activated by the recognition of Microbial Associated Molecular Patterns (MAMPs) like flagellin, lipopolysaccharides (LPS), chitin, peptidoglycans (PGN), and the elongation factor Tu (EF-Tu). MAMPs perception occurs at the plasma membrane by specialized Pattern Recognition Receptors (PRRs) that activate MAMPs-triggered immunity (MTI) (Jones and Dangl, 2006; Chisholm et al., 2006; and Dodds and Rathjen, 2010). These PRRs consist of an intracellular kinase domain, a transmembrane domain, and an ectodomain for ligand binding and recognition. The PRRs ectodomains relevant for plant immunity are the leucine-rich repeat (LRR) that recognize flagellin or EF-Tu, the lysine-motif (LysM) that identifies chitin or PGNs, and the S-lectin domain that senses bacterial metabolites medium-chain 3-hydroxy fatty acid (mc-3-OH-FA) (Tena et al., 2011; Couto and Zipfel, 2016; and Kutschera et al., 2019). The PRRs containing LRRs identified in *Arabidopsis thaliana* are the FLAGELLIN SENSING 2 (*AtFLS2*) and the EF-TU RECEPTOR (*AtEFR*) (Gómez-Gómez and Boller, 2000; Chinchilla et al., 2007; and Zipfel et al., 2006). Among the LysM there are the CHITIN ELICITOR RECEPTOR KINASE 1 (*AtCERK1*), the LysM-CONTAINING RECEPTOR-LIKE KINASE 5 (*AtLYK5*), and the LysM DOMAIN-CONTAINING GPI-ANCHORED PROTEIN 1 (*AtLYM1*) and (*AtLYM3*) (Miya et al., 2007; Willmann et al., 2011; and Cao et al., 2014). As for S-lectin domain, only the LIPOOLIGOSACCHARIDE-SPECIFIC REDUCED ELICITATION (*AtLORE*) receptor has been identified (Ranf et al., 2015; and Kutschera et al., 2019).

After MAMPs perception, receptor-like cytoplasmic kinases (RLCK) BOTRYTIS-INDUCED KINASE 1 (*AtBIK1*), and PBS1-Like 27 (*AtPBL27*), which are activated by flagellin and chitin, respectively, dissociate from PRRs and activate intracellular signaling of Mitogen-activated protein kinase (MAPK) cascades (Lu et al., 2010; and Yamada et al., 2016).

Introduction

Nevertheless, pathogens evolved mechanisms for interfering with MTI by delivering the so-called effectors (virulence proteins) into plants. One mechanism of effector delivery is through a molecular syringe known as the type III secretion system (TTSS) from bacteria (Galán and Collmer, 1999). The interference of the immune response by the effectors (e.g., *Pseudomonas syringae* HopAI and HopF2) causes Effector triggered-susceptibility (ETS) (Jones and Dangl, 2006; Chisholm et al., 2006; Zhang et al., 2007; Dodds and Rathjen, 2010; Wang et al., 2010; Zhang et al., 2012; and Meng and Zhang, 2013).

Moreover, plants have evolved the second layer of immunity, where effectors are recognized by resistant (R) proteins and elicit robust immunity known as Effectors-triggered immunity (ETI) (Jones and Dangl, 2006; Chisholm et al., 2006; Dodds and Rathjen, 2010; and Cui et al., 2015). R proteins are often nucleotide-binding/leucine-rich repeat (NB-LRR or NLR), which can be classified according to their N-terminal domain into coil-coil (CC) domain or Toll-interleukin 1 receptor (TIR) so-called CNLs or TNLs, respectively. The NLRs can interact with effectors directly at the C-terminal (LRR) or indirectly (Mackey et al., 2003; Takken and Goverse, 2012; Cui et al., 2015; and Le Roux et al., 2015). Both MTI and ETI require immune-responsive MAPKs, *AtMPK3* and *AtMPK6*, for effective resistance against pathogens, pointing to their significant roles in plant immunity (Su et al., 2017).

1.2. Arabidopsis MAPKs

In response to stimuli, eukaryotic cells mediate responses via intracellular signaling components such as MAPK cascades. They have been broadly studied in yeast, animal, and plants. These kinases cascades are in general composed of three kinases known as MAPKKKs, MAPKKs, and MAPKs. Signal transduction of MAP kinase cascades is mediated by phosphorylation, where active MAPKKKs phosphorylate its downstream MAPKKs, which subsequently phosphorylate MAPKs. In plants, MAPKKKs and MAPKKs activation occur at the serine (S) - threonine (T) motif (S/T)-X₃₋₅-(S/T). Differently from MAPKKKs and MAPKKs, MAPKs dual phosphorylation takes place at threonine (T) - tyrosine (Y) residues in the so-called TEY or TDY motif (Ichimura et al., 2002; Colcombet and Hirt, 2008; and Taj et al., 2010). In Arabidopsis, there are 60 MAPKKKs, 10 MAPKKs, and 20 MAPKs (Ichimura et al., 2002; Dodds and Rathjen, 2010; Meng and Zhang, 2013; and Vidhyasekaran, 2014). MAPKs are characterized by a kinase domain and a common docking (CD) domain. The kinase domain contains the ATP binding pocket important for ATP interaction and substrate phosphorylation, and the conserved MAP kinase insert (MKI), which regulates protein

localization in animals, but whose function in plants remains unknown. On the other hand, the CD domain serves as a recognition site for upstream kinases. Additionally, MAPKs have an N-terminal and C-terminal domain, but their functions remain unknown (Ichimura et al., 2002; Roskoski, 2012; and Wang et al., 2016).

In plant immunity, MAPKs cascades mediate intracellular signaling for both MTI and ETI upon pathogen perception by PRRs. MAPKs interact with and activate by phosphorylation numerous substrates that mediate defense response (Tsuda et al., 2013). In response to the bacterial MAMP flg22 (22 amino acids of flagellin), the Arabidopsis MAPKs *AtMPK3*, *AtMPK4*, *AtMPK6* and *AtMPK11* are activated (Nühse et al., 2000; Bethke et al., 2011; Suarez-Rodriguez et al., 2007; Colcombet and Hirt, 2008; and Meng and Zhang, 2013). The main kinases modules for *AtMPK4*, and *AtMPK3/6* have been studied. *AtMPK4* is downstream *AtMEKK1-AtMKK1/2* and is genetically a negative regulator of immunity (Petersen et al., 2000). However, upon flg22 treatment, active *AtMPK4* dissociate the molecular complex formed by MPK4 substrate 1 (*AtMSK1*) and the transcription factor (TF) *AtWRKY33*. In turn, *AtWRKY33* induced the gene expression of *PHYTOALEXIN DEFICIENT3 (AtPAD3)* required for the biosynthesis of the phytoalexin, camalexin. Camalexin biosynthesis is performed by two main enzymatic reactions. The principal precursor for camalexin production is the tryptophan deviate indole-3-acetaldoxime (IAOx). IAOx is then converted into indole-3-acetonitrile (IAN) by *AtCYP71B15*, and *AtPAD3* mediates the final enzymatic reaction that converts IAN into camalexin (Schuhegger et al., 2006). Thereby, *AtMPK4* mediates the biosynthesis of the antimicrobial compound (Qiu et al., 2008). Furthermore, it was reported that *Atmpk4* autoimmune phenotype is caused by activation of the NLR *AtSUMM2* that monitors the disruption of the *AtMEKK1-AtMKK1/2-AtMPK4* cascade. The *Atmpk4* autoimmune phenotype was rescued in *Atmpk4 Atsumm2* double mutant. Additionally, *Atsumm2 Atmkk1/2* double mutant, which disrupts the kinase cascade that regulates *AtMPK4* activation, was more susceptible than *Atsumm2* single mutant. These results demonstrate that this MAPK cascade functions indeed as a positive regulator of immunity. (Kong et al., 2012; Zhang et al., 2012; and Zhang et al., 2017).

After pathogen perception by PRRs, the RLCKs *AtBIK1* and *AtPBL27* activate a second kinase cascade, this is comprised of *AtMAPKKK3/5-AtMKK4/5-AtMPK3/6* (Asai et al., 2002; Liu and Zhang, 2004; Yamada et al., 2016; and Bi et al., 2018). *AtMPK3/6*, which have been described as redundant in function, are positive regulators of plant immunity (Beckers et al., 2009 ; and Su et al., 2017). They interact with and phosphorylate several

Introduction

substrates like transcription factors (TFs), enzymes and other kinases, for transcriptional reprogramming of defense genes (Meng et al., 2013; Li et al., 2014; Tsuda and Somssich, 2015; and Bigeard and Hirt, 2018). To counteract plant defense, bacterial pathogens evolved effectors that target and inhibit this kinase cascade. The effectors HopF2 and HopAI1 from *P. syringae* target *AtMKK5* and *AtMPK3/6*, respectively. HopF2 interacts with and ADP-ribosylate the C-terminus of *AtMKK5* blocking its kinase activity. Moreover, HopAI1 is a phosphothreonine lyase that dephosphorylates active *AtMPK3/6*, inhibiting defense response and promoting bacterial virulence (Zhang et al., 2007; and Wang et al., 2010) (Figure 1). Additionally, *P. syringae* exploits the plant hormone signaling pathway to induce the expression of *AtHAI1*, a phosphatase that dephosphorylates *AtMPK3/6* (Mine et al., 2017a).

Besides their role in immunity, MAPK cascades play an important role in development. They regulate cell proliferation and cell fate required for the development of organs. One of the main developmental kinase cascades composed by MAPKKK YODA (*AtYDA*), *AtMKK4/5*, and *AtMPK3/6* regulates stomata development. This kinase cascade is activated upon the recognition of EPIDERMAL PATTERNING FACTOR 1 (*AtEPF1/2*) ligand by RLKs, and *AtMPK3/6* phosphorylates the TF SPEECHLESS (*AtSPCH*) (Meng et al., 2012). Activation of *AtSPCH* induces the entry of cell differentiation, which is the first step in stomatal development. *AtMUTE* and *AtFAMA* TFs regulate the other two steps in stomata development progression and termination of differentiation, respectively (Lampard et al., 2009). Even though, *AtMUTE* and *AtFAMA* are not under the regulation of *AtYDA-AtMKK4/5-AtMPK3/6* kinase cascade, the interference of any of this kinases results in the abolition of pavement cells, and stomata cluster. Moreover, the deletion of both *AtMPK3* and *AtMPK6* causes embryo lethality (Bergmann et al., 2004; and Wang et al., 2007).

To overcome this embryo lethality, an excellent system was developed. In this system, *Atmpk3 Atmpk6* double mutant were complemented with a MAPK transgene *AtMPK3SR* (genotype: *Atmpk3 Atmpk6 P_{AtMPK3}::AtMPK3^{TG}*) or *AtMPK6SR* (genotype: *Atmpk3 Atmpk6 P_{AtMPK6}::AtMPK6^{YG}*). These transgenes have a point mutation at the Thr116 for Gly (*AtMPK3^{TG}*) or Tyr144 for Gly (*AtMPK6^{YG}*) residues that cause an enlargement of the ATP-binding pocket groove in *AtMPK3^{TG}* or *AtMPK6^{YG}*, making them sensitive to the reversible inhibitor NA-PP1. Once the transgenic lines are in contact with the inhibitor, the NA-PP1 actively competes with ATP for the ATP-binding pocket and inhibits the kinase activity of *AtMPK3^{TG}* or *AtMPK6^{YG}*, resulting in conditional double *Atmpk3 Atmpk6* mutants only in the

presence of the inhibitor. These plants allowed researchers to demonstrate that *AtMPK3* and *AtMPK6* function redundantly in immunity (Su et al., 2017).

Considering their importance in development and immunity, researchers have studied the potential crosstalk between *AtYDA-AtMKK4/5-AtMPK3/6* and *AtMAPKKK3/5-AtMKK4/5-AtMPK3/6* cascades, and suggest that *AtYDA* may antagonize the immune cascade (Zhang et al., 2018; Sun et al., 2018). Nevertheless, it would be interesting to investigate how plants prioritize between development and immunity.

One of the major steps in signal transduction is the regulation of substrates by MAPKs. Several publications showed that *AtMPK3/6* are proline-directed kinases that phosphorylate their substrates at serine (S) or threonine (T) residues followed by a proline (P) (Beckers et al., 2009; Sörensson et al., 2012; Pitzschke, 2015; and Bigeard and Hirt, 2018). Nevertheless, while phosphorylation sites by MAPK show a certain signature, predicting *AtMPK3/6* substrates in silico has not been sufficiently accurate. Therefore, researchers have been using empirical approaches to screen MAPK substrates such as large scale protein-protein interactions.

1.2.1. Regulation of TFs by *AtMPK3/6* during plant immunity

In plant immunity, *AtMPK3/6* interact with and phosphorylates TFs from different families, like the basic region/leucine zipper motif (bZIP), the Helix-turn-Helix (HTH) MYB, zinc-coordinating protein WRKY, and APETALA2/ETHYLENE-RESPONSE ELEMENT BINDING FACTOR (AP2/ERF) families (Figure 1) (Andreasson and Ellis, 2010; Weirauch and Hughes, 2011; Tsuda and Somssich, 2015; and Peng et al., 2017). bZIP family is characterized by its DNA binding region, which targets the DNA sequences with ACGT core, and the leucine zipper dimer motif. In Arabidopsis, this family includes around 74 proteins, which are subdivided into 10 groups according to their sequence similarity. The TF VirE2-interacting protein (*AtVIP1*) belonging to group I. The group I proteins present an amino acid modification on the conserved bZIP domain, which might be involved in the recognition of specific binding sites (Jakoby et al., 2002). Previous reports showed that upon flg22 treatment, *AtMPK3* phosphorylates cytoplasmic *AtVIP1*, causing its relocalization into the nucleus (Figure1). Once in the nucleus, *AtVIP1* mediates the expression of *PATHOGENESIS-RELATED1 (AtPRI)* gene and *AtMYB44* TF (Djamei et al., 2007; and Pitzschke et al., 2009).

MYB transcription factors are characterized by their DNA binding MYB domain, which is composed of one or more imperfect repeats. Each repeat is formed by a sequence of

Introduction

52 amino acids and a helix-turn-helix conformation structure, and they are known as the R1, R2, R3 repeats. Arabidopsis presents around 190 genes belonging to the MYB family, and around 120 of them belong to the R2R3-MYB class (Yanhui et al., 2006; and Dubos et al., 2010). It is known that the R2R3-MYB *AtMYB30* induces cell death in response to bacteria, and *AtMYB15* mediates defense-induced lignification upon flg22 treatment (Vaillau et al., 2002; and Chezem et al., 2017). Nevertheless, interaction with and phosphorylation by *AtMPK3/6* have only been reported for *AtMYB44* (Nguyen et al., 2012a; and Persak and Pitzschke, 2013). *AtMYB44* induces the expression of *AtWRKY70*, which confers resistance against *P. syringae* through regulation of SA-mediated response (Li et al., 2004; and Shim et al., 2013). Moreover, *AtMPK3/6* regulates *AtMYB44* activation by phosphorylation, and gene expression through *AtVIP1* activation (Figure 1).

The WRKY TF family represents a large TF family specific to plants. Members of this family present a conserved WRKY (WRKYGQK) domain and a zinc-finger-like motif, and they bind DNA mainly at W-boxes (C/TTGAC/T) through the WRKY domain. These TFs are classified into three groups. Group I presents two WRKY domains, different to group II and III that contain only one, and a C₂-H₂ zinc-finger-motif (C-X₄₋₅-C-X₂₂₋₂₃-H-X₁-H) that is shared with group II. Group III presents a variation on the zinc-finger-motif, instead of a C₂-H₂ motif, it contains a C₂-HC motif (C-X₇-C-X₂₃-H-X₁-C) (Eulgem et al., 2000; Pandey and Somssich, 2009; and Tsuda and Somssich, 2015). In Arabidopsis over 70 WRKY TFs have been identified, and numerous are positive or negative immune regulators (Eulgem and Somssich, 2007; Rushton et al., 2010; Tsuda and Somssich, 2015; Birkenbihl et al., 2017; and Mine et al., 2018). The heterocomplex formed by *AtWRKY18*, *AtWRKY40*, and *AtWRKY60* mediates resistance against necrotrophic pathogen *Botrytis cinerea* by inducing the expression of jasmonic acid (JA) regulated *AtPDF1.2* gene (Xu et al., 2006). Additionally, a recent study showed that upon flg22 treatment *AtWRKY18*, *AtWRKY40*, and *AtWRKY33* associate with more than 1000 genes, several of which are related to plant immunity (Birkenbihl et al., 2017). Several WRKYs have been identified as potential targets of MAPKs (Popescu et al., 2009). Among them, *AtWRKY33* has been confirmed as a phosphorylation target of *AtMPK3/6* (Figure 1). *AtMPK3/6* phosphorylate *AtWRKY33*, which activate the expression of camalexin biosynthetic genes (*AtCYP71A13* and *AtPAD3*). Moreover, *AtWRKY33* binds to the W-boxes in the *AtACS2/6* promoter regions, and mediate the expression of the *AtACS2/6* enzymes, required for the biosynthesis of the phytohormone ethylene (ET). Thus, *AtMPK3/6* mediates the biosynthesis of camalexin and ET through phosphorylation of *AtWRKY33*, thereby

confering plant resistance against the necrotrophic pathogen *B. cinerea* (Ren et al., 2008; Mao et al., 2011; and Li et al., 2012).

Another TF family relevant for plant immunity is the APETALA2/ETHYLENE-RESPONSE ELEMENT BINDING FACTOR (AP2/ERF) superfamily, which is subdivided into four families according to their conserved AP2 DNA binding domain (60 amino acids long). The four families are the AP2, RAV, ERF, and Soloist. The AP2 family contains two tandem sequences of the AP2 domain, which bind DNA at non-canonical AT-rich elements (Dinh et al., 2012; and Licausi et al., 2013). The RAV has one AP2 domain that binds DNA at the CACCA motif and an additional B3 DNA-binding domain that binds the CACCTG motif (Kagaya et al., 1999; and Licausi et al., 2013). The ERF and Soloist families are characterized by only one AP2 domain. Moreover, the ERF family is subdivided into two, the ERF and the DREB. They differ in their DNA binding motifs, DREB TFs recognize the A/GCCGAC element, and ERFs bind to the GCC-box (AGCCGCC) (Ohme-Takagi and Shinshi, 1995; Stockinger et al., 1997; and Ohme-Takagi et al., 2000). ERF TFs have been reported to regulate the production of the phytohormones JA and ET, in response to biotic stress (Licausi et al., 2013; and Tsuda and Somssich, 2015). Arabidopsis presents around 120 ERF genes and numerous have been reported to be induced upon chitin treatment (Nakano et al., 2006; and Libault et al., 2007). Moreover, a high-density functional microarray containing around 2158 proteins, identified ETHYLENE RESPONSE FACTOR13 (*AtERF13*), ETHYLENE RESPONSE FACTOR104 (*AtERF104*), ETHYLENE RESPONSE FACTOR109 (*AtERF109*) and ETHYLENE RESPONSE FACTOR6 (*AtERF6*) as MAPKs substrates (Popescu et al., 2009). It has been confirmed that *AtERF6* and *AtERF104* are phospho-targets of *AtMPK3/6* (Figure 1). Active *AtMPK6* stabilizes *AtERF104* through its phosphorylation, which enhances *AtERF104* activity to regulate expression of target genes (Bethke et al., 2009). Similarly, *AtMPK3/6* phosphorylate *AtERF6*, which leads to *AtERF6* stabilization, thereby enhancing expression of JA-marker gene *AtPDF1.2* and conferring resistance against the necrotroph *B. cinerea* (Meng et al., 2013). Additionally, it has been reported that *AtERF6* mediates gene expression of *AtMPK3* and *AtWRKY33* during ETI (Mine et al., 2018), suggesting a regulatory mechanism in which active *AtMPK3* mediates its own gene expression by phosphorylation of *AtERF6*. Additionally, *AtMPK3*, besides activating *AtWRKY33* by phosphorylation, regulates *AtWRKY33* gene expression through activation of *AtERF6*. These complex regulatory mechanisms place the MAPKs as central hubs in complex immune networks.

Introduction

1.2.2. Interactions between *AtMPK3/6* and phytohormones in plant immunity

Plant hormones play an essential role in immunity. The phytohormone SA signaling network regulates resistance against biotrophic and hemibiotrophic pathogens like *P. syringae*. In contrast, JA and ET signaling pathways mediate resistance against necrotrophs such as the fungus *B. cinerea* (Glazebrook, 2005). Additionally, it is known reported that phytohormones abscisic acid (ABA), auxin, cytokinins, gibberellin, and brassinosteroids are modulators of hormone-regulated plant immunity networks (Pieterse et al., 2009; and Berens et al., 2017). Nevertheless, it is known that SA and JA/ET are not only antagonistic, but they also cooperate to confer resistance against both biotrophs and necrotrophs (Tsuda et al., 2009). Moreover, it has been reported that the crosstalk between SA and JA/ET is context-dependent. Upon flg22 treatment, JA signaling mediates the repression of *PHYTOALEXIN-DEFICIENT 4* (*AtPAD4*), required for SA accumulation, through TFs *AtMYC2/3/4*. Nevertheless, in perturbation of *AtPAD4* at high temperature or by mutation, JA mediates SA accumulation by coordinating the transcription of *ENHANCED DISEASE SUSCEPTIBILITY 5* (*AtEDS5*) via *AtMYC2*. This provides robustness and tunability to this immune network (Mine et al., 2017b). Additionally, it is known that sustained MAPK activation during ETI mediates transcriptional reprogramming of SA-responsive genes independent of SA, thereby demonstrating that MAPKs regulate redundantly the gene expression of genes mediated by SA. This dual regulation of gene expression by phytohormone network and MAPK signaling work in a compensatory way contributing to robust immune responses during ETI (Tsuda et al., 2013).

Ethylene biosynthesis has two main precursors S-adenosylmethionine (S-AdoMet) and 1-amino-cyclopropane-1-carboxylic acid (ACC). Cellular methionine is converted into S-AdoMet by the S-AdoMet synthase, and subsequently, the conversion of S-AdoMet into ACC is mediated by the ACC synthase (ACS). The last step for the biosynthesis of ethylene is ACC oxidation performed by the ACC oxidase (Wang et al., 2002). During plant immunity, MAPKs mediate ethylene biosynthesis through the accumulation of the ethylene precursor ACC. Upon flg22 treatment *AtMPK3/6* phosphorylates *AtACS2/6*, increasing their protein accumulation required for the production of the ethylene precursor ACC (Figure 1) (Liu and Zhang, 2004; and Joo et al., 2008). Thus, increased *AtACS2/6* enhances ethylene production, which in turn confers immunity against necrotrophic pathogens (Meng and Zhang, 2013; and Tsuda and Somssich, 2015).

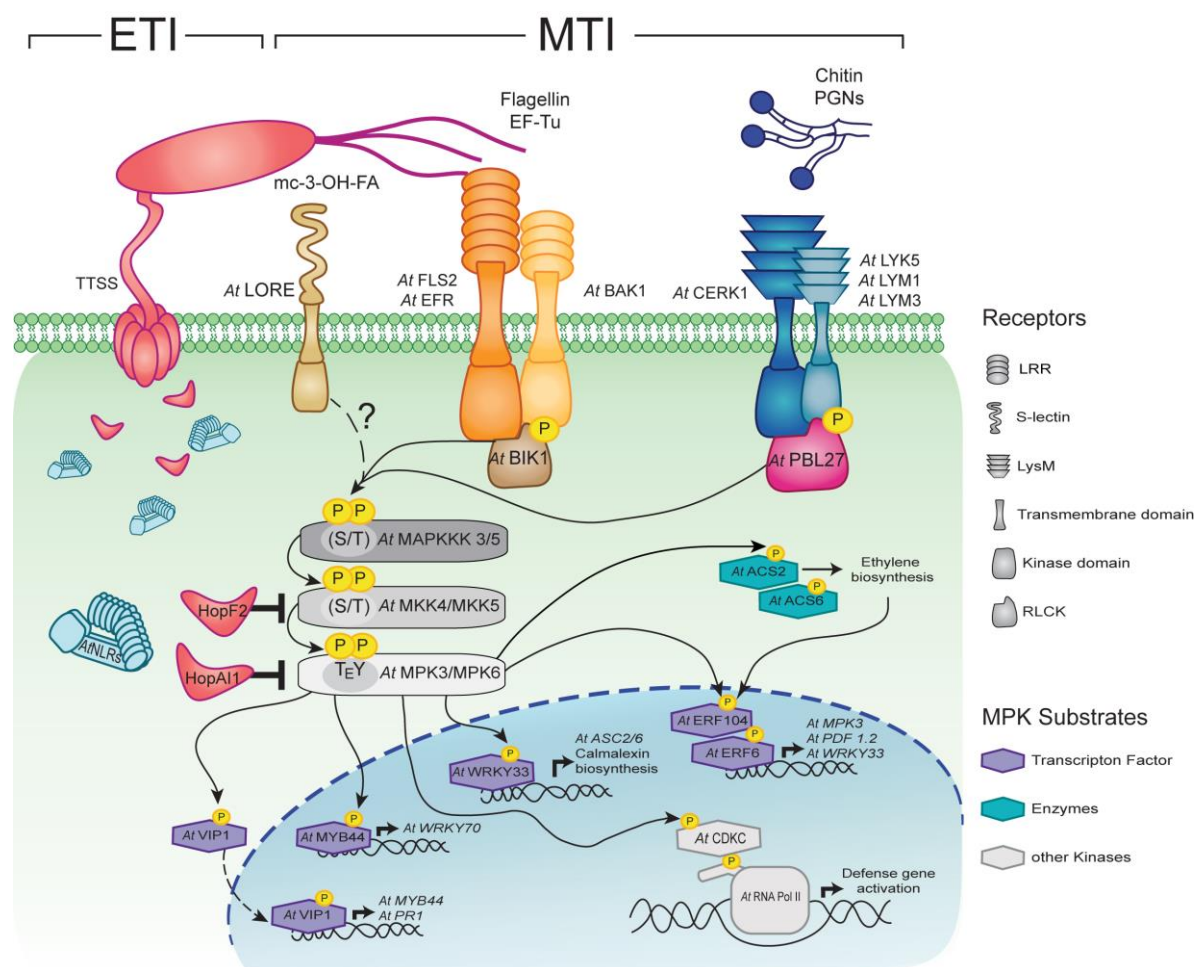


Figure 1: MPK3/6 signaling cascade mediates immune responses in Arabidopsis

Pattern recognition receptors (PRRs) sense Microbe-associated molecular patterns (MAMPs), and recruit receptor-like cytoplasmic kinases (RLCKs) that activate MAPKs cascades, thereby triggering MAMPs-triggered immunity (MTI). Pathogenic bacteria (*P. syringae*) releases effectors such as HopF2 and HopA1 that target and inactivate MAPKs, causing Effector trigger-susceptibility (ETS). Plants recognize bacterial effectors by resistant (R) proteins NLRs and trigger Effector-triggered immunity (ETI). ETI activation leads to restored MAPK activity. Active *AtMPK3/6* regulates plant immunity by phosphorylation of *AtVIP1* (causing nuclear translocation), *AtMYB44*, *AtWRKY33*, *AtERF104* and *AtERF6* transcription factors (TFs), *AtACS2* and *AtACS6* enzymes, and cyclin-dependent kinases *AtCDKC*. *AtMPK3/6* phosphorylation targets regulate various downstream events such as transcription of immune-related genes (*AtPR1*, *AtMYB44*, *AtWRKY70*, *AtACS2/6*, *AtMPK3*, *AtPDF1.2*, and *AtWRKY33*), camalexin production, ethylene (ET) biosynthesis, and phosphorylation of the C-terminal tail of the RNA-Pol II.

1.2.3. *AtMPK3/6* modulate RNA-Pol II phosphorylation

Transcriptional activation of gene expression is a fundamental process in organisms. In eukaryotes, the majority of gene transcription requires the recruitment of the RNA Polymerase II (RNA-Pol II) to the promoter regions. However, RNA-Pol II proximity to promoter regions

Introduction

does not guarantee an efficient and specific transcription. Therefore, TF activation at *cis*-regulatory sequences in the promoter regions or enhancers is required for targeted gene expression (Spitz and Furlong, 2012; Shlyueva et al., 2014; and Weber et al., 2016). TFs then mediate the locus-specific recruitment of the RNA Polymerase II (RNA-Pol II) for gene expression, through interaction with cofactor proteins. TFs present a DNA binding domain (DBD), important for recognition and target of specific DNA binding motifs present at promoter regions (e.g., W-boxes), and a trans-activation domain (tAD) that interplays with different cofactors involved in the recruitment of RNA-Pol II (Smith and Matthews, 2016; and Arnold et al., 2018). Recruitment of cofactor proteins and activation of RNA-Pol II by phosphorylation leads to transcriptional activation. RNA-Pol II phosphorylation occurs at the heptapeptide (Y₁S₂P₃T₄S₅P₆S₇) of the RNA-Pol II C-terminal domain (CTD). The CDT sequence presents a degree of conservation among eukaryotes. In Arabidopsis, *At*RNA-Pol II has 19 divergent heptapeptide repeats, and 15 of them are conserved in animals and yeast (Koiwa et al., 2004; Hajheidari et al., 2013; and Li et al., 2014). Specifically, phosphorylation of animal RNA-Pol II CTD threonine-4 (Ther4) residue is associated with post-transcriptional termination of splicing, and serine-5 (Ser5) residue is associated to co-transcriptional recruitment of spliceosome (Harlen et al., 2016). RNA-Pol II recruitment is followed by the adherence of the basal transcription factor IIIH (TIFIIIH), which in turn is associated in a complex with cyclin-dependent kinases (CDK). In Arabidopsis, *At*TIFIIIH is associated with CDK type D and F, *At*CDKD1, *At*CDKD2, *At*CDKD3, and *At*CDKDF (Shimotohno et al., 2004; Hajheidari et al., 2012; and Hajheidari et al., 2013). Additionally, these CDKs regulate the phosphorylation of specific residues (Ser2 and Ser5) present at the *At*RNA-Pol II CTD heptapeptide repeats to guarantee the mediation of 5' capping nascent RNA. Subsequently, the elongation factor *At*Spt5L mediates the recruitment of enzymes required for chromatin remodeling (Hajheidari et al., 2013). Finally, 3' polyadenylated RNA is cleaved by Pcf11p-similar protein 4 (*At*PCFS4) (Xing et al., 2008; and Hajheidari et al., 2013), and transcriptional termination is mediated mainly by phosphatases that inhibit CTD RNA-Pol II. In Arabidopsis, the C-terminal domains of phosphatase-like *At*CPL1/3 have been reported to interact and dephosphorylate *At*RNA-Pol II, in a stress-dependent context (Koiwa et al., 2002; and Li et al., 2014).

Active plant MAPKs orchestrate a massive transcriptional reprogramming during plant immunity (Tsuda et al., 2013). The mechanism by which these kinases trigger immunity has been associated with their ability to interact and phosphorylate mainly with TFs and enzymes.

Nevertheless, *AtMPK3/6* have additional phosphorylation targets that mediate the phosphorylation of the *AtRNA*-Pol II, and chromatin remodeling during plant immunity (Li et al., 2014; and Latrasse et al., 2017).

Upon flg22 treatment, *AtMPK3/6* interact with and phosphorylate cyclin-dependent kinases (CDK) *AtCDKC1* and *AtCDKC2* that phosphorylate the conserved serine residues (Ser2, Ser5, and Ser7) present in the heptapeptide of the *AtRNA*-Pol II CTD, herewith activating *AtRNA*-Pol II for transcriptional activation (Li et al., 2014). Thus, in response to biotic stresses *AtMPK3/6* interplay with basal transcriptional machinery. Nevertheless, the molecular mechanism by which *AtMPK3/6-AtCDKC1/2-AtRNA*-Pol II specifically mediates the expression of defense-related genes remains unsolved.

Additionally, gene expression can be regulated by rapid and reversible chromatin post-translational modifications such as methylation, phosphorylation, ubiquitination, and acetylation, among others. Nucleosomes are the basic units of chromatin. They are formed by a histone octamer, which contains two copies of the core histones H2A, H2B, H3, and H4, wrapped in around 147 bp of DNA (Luger et al., 1997; and Ding and Wang, 2015). Chromatin remodeling by post-translational modifications plays an important role in plant immunity. The post-transcriptional modification generated by histone acetylation induces transcriptional activation. In contrast, histone deacetylation by histone deacetylases (HDACs), suppresses transcription. In *Arabidopsis* *AtHAD19* and *AtHAD6*, regulate the transcription of genes involved in the JA/ET signaling pathway (Zhou et al., 2005; and Ding and Wang, 2015). Recent studies propose that *AtMPK3* phosphorylates histone deacetylase *AtHD2B*, thereby, mediating chromatin remodeling (Latrasse et al., 2017). Upon flg22 treatment, phosphorylated *AtHD2B*, which has been reported as a plant-specific type-II HDACs (Ding and Wang, 2015), deacetylates the lysine 9 residue from histone 3 (H3K9) leading to the regulation of biotic stress-related genes (Latrasse et al., 2017).

1.3. MAPKs in other eukaryotes

MAPK cascades are conserved signaling components among eukaryotes. However, despite their conservation, MAPKs present some differences, like the phosphorylation motif. Besides conserved TEY motif, yeast present kinases with a TGY motif, animals have a TPY and TGY motif, and plants have kinases with a TDY motif (Ichimura et al., 2002; Chen and

Introduction

Thorner, 2007; Cargnello and Roux, 2011; and Meng and Zhang, 2013). Even though plant MAPKs have been broadly studied, little is known in comparison to yeast and animal field. Therefore, understanding conserved molecular mechanisms within yeast and mammalian MAPKs may improve the comprehension of the plant MAPK field.

Eukaryotic cells have to coordinate numerous and simultaneous intracellular signaling pathways in response to changing environments. Signaling pathways involve the mobilization of molecules or molecular complexes through different compartments of the cell. Therefore, the spatial-temporal coordination of proteins within cells is crucial to guarantee a successful cellular response. MAPK cascades as master regulators of intracellular signaling, present different variants of kinase cascades in response to one environmental stimulus. Therefore, to mediate selectivity, signal amplitude, and regulate the duration of signaling pathways, kinase cascades associate with scaffold proteins.

1.3.1. MAPK cascades and scaffold proteins in yeast

The yeast *Saccharomyces cerevisiae* possess four main MAPKs that mediate mating, cell fate during nutrient limitation conditions, osmoregulation, and cell wall repair. The MAPKs involved in these processes are *ScFus3*, *ScKss1*, *ScHog1*, and *ScSlit2/Mkp1*. MAPKs, *ScFus3* and *ScKss1*, orthologs of the extracellular-signal-regulated ERK1/2 in mammals, are downstream of the MAPKKK *ScSte11* and the MAPKK *ScSte7* (Chen and Thorner, 2007). Nevertheless, *ScFus3* and *ScKss1* signaling cascades work under different transmembrane receptors, mediating different responses. The MAPK cascade *ScSte11-ScSte7-ScFus3* is activated upon the perception of pheromones, and *ScSte11-ScSte7-ScKss1* is activated upon nutrient starvation (Reményi et al., 2005; and Good et al., 2009). The most characterized module in yeast is the *ScSte11-ScSte7-ScFus3*. Yeast can reproduce asexually through binary fission, or sexually by mating. During the mating process, the recognition of pheromones is crucial. Perception occurs through membrane G protein-coupled receptor (*ScGPCR*). This receptor is associated with heterotrimeric G proteins (*ScG α* , *ScG β* , and *ScG γ*). Upon pheromone perception, heterotrimeric G proteins *ScG β -ScG γ* dissociate and recruit the protein kinase *ScSte20* (Inouye et al., 1997; Klein et al., 2000; and Good et al., 2011). Simultaneously, *ScSte11-ScSte7* associated with the scaffold protein *ScSte5* are recruited from the cytoplasm to the plasma membrane (Choi et al., 1994; Yablonski et al., 1996; and Pryciak and Huntress, 1998). *ScG β -ScG γ* interacts with *ScSte5*, and *ScSte20* mediates the phosphorylation of the

MAPKKK *ScSte11*, which in turn phosphorylates *ScSte7* (Chen and Thorner, 2007; and Good et al., 2011). Then *ScFus3* is recruited into the scaffold protein and phosphorylated by *ScSte7* (Good et al., 2009). Active *ScFus3* is then released from the complex and relocates into the nucleus, where TFs are phosphorylated, and activate transcription of mating genes (Elion et al., 1993; and Blackwell et al., 2007). Additionally, *ScFus3* negatively regulates its own activity independent from pheromone stimulation. Inactive *ScFus3* can bind to *ScSte5* in a second motif, different from the one required for assembling MAPK cascade. After binding, *ScFus3* mediates its own activation through unconventional phosphorylation, then this active *ScFus3* phosphorylates *ScSte5*, causing a disruption of the functional MAPK signaling cascade (Figure 2A) (Bhattacharyya et al., 2006; and Good et al., 2009).

1.3.2. MAPK cascades and scaffold proteins in mammals

In mammals, MAPKs mediate cell proliferation, differentiation, and apoptosis and are classified into three families: 1) the extracellular-signal-regulated kinases (ERKs), 2) the stress-activated protein kinases (p38/SAPKs), and 3) the Jun amino N-terminal kinases (JNKs). These families present different phosphorylation motifs, ERKs have a TEY motif, p38/SAPKs contain a TGY motif, and JNKs have a TPY motif (Cargnello and Roux, 2011). Among mammalian ERKs, there are some conventional and non-conventional kinases. The conventional kinases are ERK1, ERK2, and ERK5. ERK5 presents an unconventional elongated C-terminal domain that contains a nuclear localization signal (NLS) and a tAD (Kasler et al., 2000; and Morimoto et al., 2007). The ERK5 tAD was identified through reporter-effector assays, where the ERK5 C-terminal domain fused to the GAL4 DNA-binding domain (DBD), or the ERK5 interactor, myocyte enhancer-binding factor (MEF2) DBD, showed enhanced reporter activity (Kasler et al., 2000). Additionally, it is known that the unphosphorylated ERK5 reduces the C-terminal tAD activity. However, these kinases count with extra phosphorylation motifs within the C-terminal domain that allows them autophosphorylation and enhance transcription when TEY motif is not phosphorylated (Morimoto et al., 2007). Different from the conventional kinases, the non-conventional kinases ERK3, ERK4, ERK7, ERK8, and Nemo-like kinase (NLK) characterized by the presence of different phosphorylation motifs, and they do not associate in canonical kinases cascades. (Cargnello and Roux, 2011). The kinase cascade that comprises ERK1/2, has been broadly studied considering their high conservation across animals, their importance in cell

Introduction

proliferation, and their relevance in oncogenesis (Buscà et al., 2016; Yang and Liu, 2017; Imperial et al., 2019).

ERK1/2, orthologues of *ScFus3* and *SsKss1* in yeast, belong to the Ras-Raf-MEK-ERK kinase module. They are activated after the perception of epidermal growth factors (EGFs), which are perceived by the receptor tyrosine kinases (RTKs) (Cargnello and Roux, 2011; Witzel et al., 2012; and McCubrey et al., 2015). Recognition of EGFs induces dimerization and autophosphorylation of the receptors at the intracellular tyrosine residues. This phosphorylation allows the binding of the growth factor receptor-bound protein2 (Grb2) at the plasma membrane. Subsequently, the son of sevenless (SOS) which is a guanine nucleotide exchange factor (GEF), is mobilized from the cytosol to the plasma membrane for interaction with Grb2.

Simultaneously, Ras is recruited to the plasma membrane and activated by SOS (Witzel et al., 2012; and McCubrey et al., 2015), mediating the activation of the downstream kinases. Similar to yeast, the kinase module Raf-MEK-ERK is bound together by the scaffold protein Kinase Suppressor of Ras (KSR) (Therrien et al., 1996; and McKay et al., 2009). Nevertheless, the molecular mechanism by which the scaffold protein KSR interacts with the kinase cascade is different. In resting conditions, KSR is present in a molecular complex with MEK (Brennan et al., 2011), and the regulatory protein 14-3-3. The cytosolic localization of this complex is mediated by 14-3-3, which upon EGFs perception is dephosphorylated and dissociated. KSR-MEK are then relocalized to the plasma membrane, where they associate with Raf (Ory et al., 2003; and Müller et al., 2001). Once the kinases and scaffold proteins are assembled, Ras phosphorylates Raf, which mediates the phosphorylation of MEK and the recruitment of ERK into the scaffold protein (Yu et al., 1998). Active MEK phosphorylates ERK, and differently from yeast, active ERK dimerizes and relocalizes into the nucleus where it interacts with TFs, and mediate transcription of proliferation genes (Chen et al., 1992; and Canagarajah et al., 1997). Additionally, active ERK phosphorylates four serine/threonine (S/T) sites present in KSR and in Raf, disrupting the interaction between the scaffold protein (KSR) and the Raf kinase. Hence, active ERK disrupts the KSR-Raf complex through feedback phosphorylation as self-regulatory mechanisms (McKay et al., 2009). (Figure 2B).

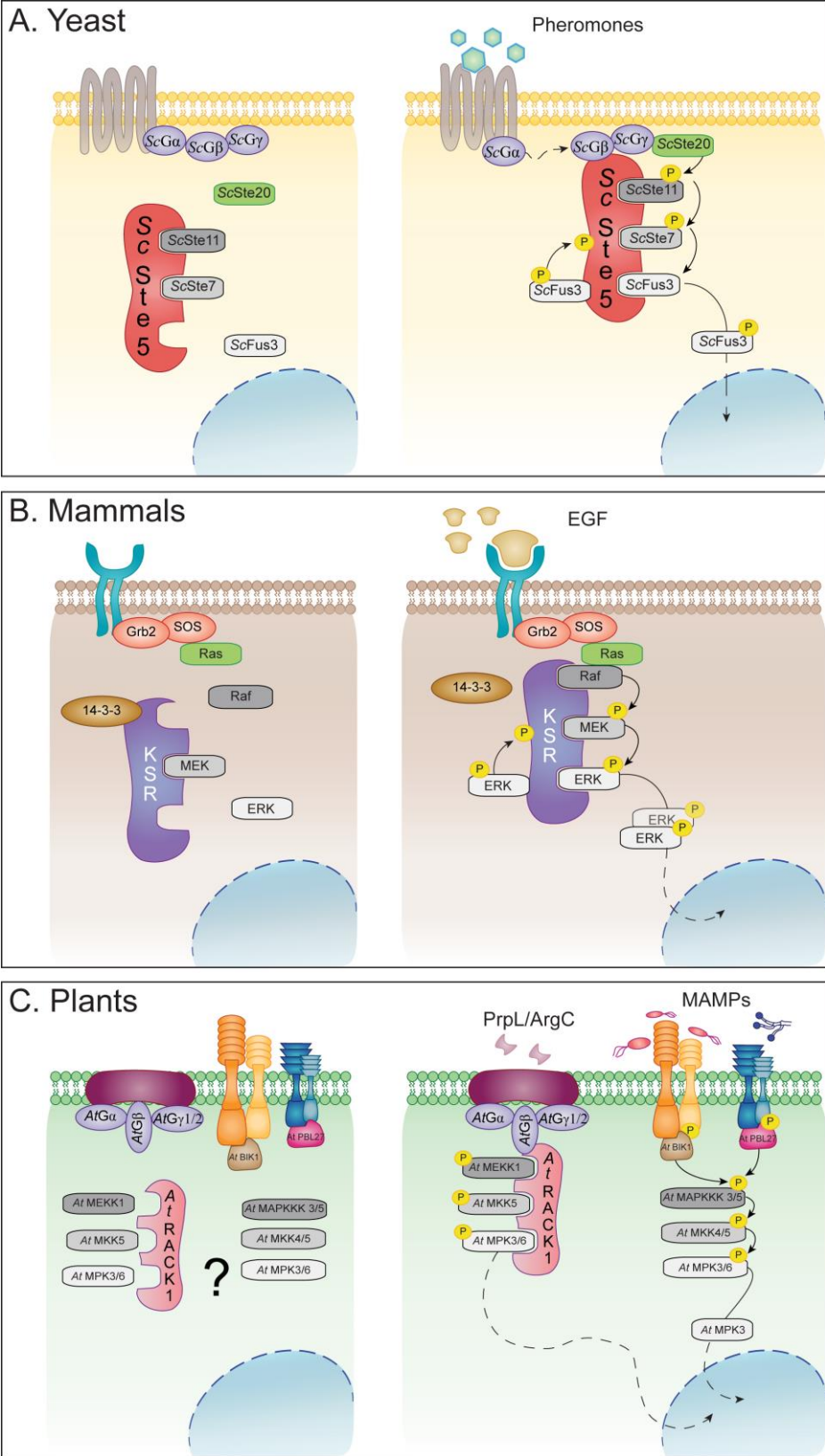


Figure 2: MAPK activation modules and scaffold proteins in yeast, mammals, and plants

(A) During resting conditions, *Saccharomyces cerevisiae* MAPKs and their scaffold protein ScSte5 are located at the cytosol. After pheromone perception, ScGβ-ScGγ dissociates from ScGα and recruits ScSte20, and ScSte5-ScSte11-ScSte7. Activation of ScSte11 by phosphorylation induces the recruitment of ScFus3 to the scaffold

Introduction

protein. Once active *ScFus3* translocate into the nucleus and activate transcription factors (TFs). Additionally, *ScFus3* self-regulate the activity of the kinase module, by phosphorylation of *ScSte5*. (B) In the absence of stimuli, mammalian kinases Raf, EKR, and the complex formed by the scaffold protein KSR, MEK and the protein regulator 14-3-3 are in the cytosol. Sensing epidermal growth factor (EGF) induces the dissociation of 14-3-3 from the scaffold protein, and plasma membrane translocation of KSR-MEK, Raf, and ERK. Once the kinases are associated with the scaffold protein, they are activated by phosphorylation. Active ERK dimerizes and translocates into the nucleus where they interact with TFs. Similar to yeast, active EKR phosphorylates KSR and thereby terminating the kinase cascade. (C) The spatial organization of Arabidopsis kinases in the absence of stimuli is unknown. After proteases perception (PrpL/ArgC) by an unknown receptor, the *AtMEKK1-AtMKK4/5-AtMPK3/6* kinase module and their scaffold protein *AtRACK1* associate with the plasma membrane with *AtGβ-AtGγ*. MAPKs cascade is then activated, and *AtMPK3/6* mediate transcription of immune-related genes through phosphorylation of TFs. Additionally, Arabidopsis plants present a second kinase cascade that is induced upon Microbe-Associated Molecular Patterns (MAMPs) perception. The receptor-like cytoplasmic kinases *AtBAK1* and *AtPBL27* phosphorylate *AtMAPKKK3/5* activating the kinase cascades. Active *AtMPK3/6* phosphorylates numerous substrates that regulate transcriptional reprogramming of defense genes. Additionally, the nuclear localization of *AtMPK3* is necessary to confer resistance against necrotroph pathogens. Nevertheless, the nuclear translocation of MAPKs is unknown.

1.3.3. Arabidopsis scaffold proteins associated with MAPKs during immunity

As mention previously, scaffold proteins regulate the function of MAPK cascades (Figure 2A and 2B). In 2015, the scaffold protein receptor for activated C-kinase 1 (*AtRACK1*) was identified for the kinase module *AtMEKK1-AtMKK4/5-AtMPK3/6* in response to pathogens in Arabidopsis (Cheng et al., 2015, and Su et al., 2015). Their study revealed that the opportunistic bacterial *P. aeruginosa* secretes proteases PrpL and ArgC, that activate *AtMPK3/6* kinase signaling. Additionally, they found that this *AtMPK3/6* activation requires *AtRACK1* and the heterotrimeric G protein *AtGβ*. Moreover, interactions between the scaffold protein and the *AtMEKK1-AtMKK4/5-AtMPK3/6* cascade were confirmed (Cheng et al., 2015). Nevertheless, several questions remain unsolved; for instance, there is no information about the sensor that perceives the proteases PrpL and ArgC (Figure 2C).

Compared to yeast and animal, the mechanisms by which MAPKs regulate downstream responses and are regulated in plants are far from the complete. Aspects like cellular localization of kinase cascade components (e.g., MAPKKKK, MAPKK, MAPK) and scaffold proteins during resting conditions, mechanisms for plasma membrane translocation and activation upon stimuli, MAPK mobilization or nuclear relocation upon activation, MAPKs dimerization, and self-regulatory mechanisms to disrupt kinase signaling remain unsolved in plants.

1.4. Thesis aims

Despite the studies on MAPK functions during plant immunity, little is known about how *Arabidopsis thaliana* AtMPK3 and AtMPK6 mediate the massive transcriptional reprogramming observed upon their activation (Tsuda et al., 2013). Gene transcriptional activation requires the recruitment of TF(s) to the gene promoter region. Thus, identifying TFs involved in a biological process is crucial to comprehend the process. Therefore, to understand MAPK-mediated plant immune networks, my first aim was to identify candidates for TF interactors of AtMPK3 and AtMPK6. I implemented a Y2H screening approach with a library containing around ~1500 Arabidopsis TFs (Mitsuda et al., 2010a) and confirmed the interaction between the TFs candidates and AtMPK3 and AtMPK6.

During the course of this study using the Y2H system, I unexpectedly found that the C-terminal region of AtMPK3 and AtMPK6 promotes transcription of reporter genes in yeast, independently of their kinase activity. The importance of MAPKs as major regulatory components in numerous physiological processes has been well evidenced. However, researchers have focused on identifying MAPK-regulatory mechanisms based on their kinase activity with a few exceptions in animals and yeast, where some kinase-independent functions have been reported. Nevertheless, there are no reports for MAPK functions beyond their kinase activity in plants. Therefore, the second goal of my thesis was to study this kinase-independent function of AtMPK3 and AtMPK6 via the C-terminal region as transcriptional co-activators. To achieve this aim, I performed two different reporter-effector transient expression assays in *A. thaliana*. This system allowed me to test if the C-terminal domain of AtMPK3/6 was able to activate transcription *in planta*. Transient expression assays performed with different reporter genes in yeast and Arabidopsis came to the same conclusion that the MAPK C-terminal domain can activate transcription. Therefore, I decided to investigate if this novel function for transcriptional activation is conserved in MAPKs among eukaryotes, including *A. thaliana*, bryophytes, yeast, and human. To address this question, I analyzed the protein sequences of numerous eukaryotic kinases and identified that the conserved MAPK C-terminal domains from different organisms activate transcription similar to AtMPK3 and AtMPK6. Finally, I decided to study the physiological relevance of the MAPK C-terminal region by complementing the embryo-lethal phenotype of the *Atmpk3 Atmpk6* double mutant with AtMPK3/6 full-length, C-terminus-deletion (Δ C), and C-terminus proteins, driven by their

Introduction

native promoters. This approach aimed to identify whether the *AtMPK3/6* C-terminus is required for development or immunity.

In summary, this Ph.D. thesis provides novel TFs that interact with the plant MAPKs *AtMPK3* and *AtMPK6*, and a novel function for the MAPK C-terminus in promoting transcription in a kinase-independent manner.

2. Results

2.1. Y2H screening for MAPK interactors

To gain more insights into how MAPKs coordinate plant immunity, I decided to identify TFs that are targets of Arabidopsis MAPKs *AtMPK3* and *AtMPK6*, through large-scale Y2H screens with a library of approximately 1,500 TFs from *A. thaliana* (Mitsuda et al., 2010b). In these Y2H assays, the bait contained the full-length *AtMPK3* or *AtMPK6* fused to the DNA-binding domain (DBD), and a prey contained a TF fused to the transcriptional activation domain (AD). I used two different DBDs; one from LexA of *Escherichia coli* and the other from GAL4 from *Saccharomyces cerevisiae* (Brent and Ptashne, 1985). Thus, Y2H assays were performed in two different systems, LexA and GAL4. Both systems have histidine (*HIS3*) and α -galactosidase (*MEL1*) as reporter genes, and the GAL4 system additionally presents adenine (*ADE2*) as a reporter gene. The interaction between MAPKs and TFs activates the expression of these reporter genes, which can be monitored by yeast growth on nutrition deficient media and generation of a blue precipitate in the presence of X- α -gal substrate. Unexpectedly, yeast cells carrying the full-length *AtMPK3* or *AtMPK6* bait construct (BD) together with an empty prey vector control (AD) grew on selective media lacking histidine (H) and showed X-gal activity for both GAL4 and LexA systems (Figure 3). These results were congruent with the ones obtained by our collaborator Dr. Nobutaka Mitsuda (AIST, Japan) (Supplementary Figure 1).

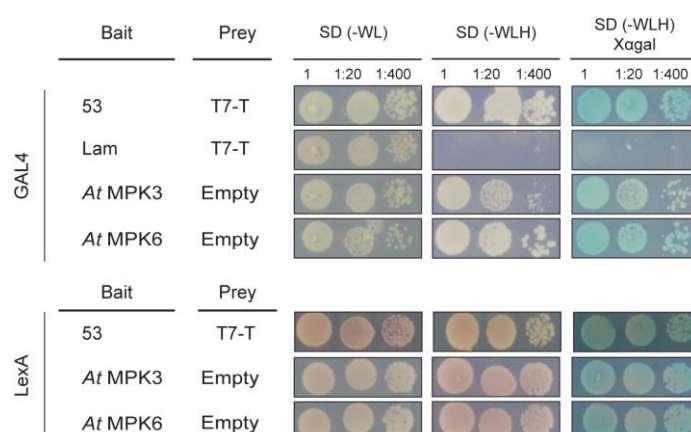


Figure 3: *AtMPK3* and *AtMPK6* baits show autoactivity in Y2H

In both GAL4 and LexA systems, the combination of the bait p53 (53) and the prey SV40 large T-antigen (T7-T) was used as a positive control of interaction. In GAL4 system, the combination of the bait lamin (Lam) and the

Results

prey SV40 large T-antigen (T7-T) was used as a negative control of interaction. Autoactivity of the bait containing the full-length *AtMPK3* or *AtMPK6* was detected in combination with the empty prey containing only AD, as indicated by yeast growth on SD (-WLH) and SD (-WLH) X- α -gal selection media. Dilutions were performed starting from an $OD_{600} = 1$. Pictures were taken 3 days after incubation at 30°C. Same results were obtained for the other two independent experiments.

In this study, autoactivity is defined as the growth on selective media of yeast expressing the bait protein (*AtMPK3/6*) fused to GAL4-DBD or LexA-DBD and the prey containing only AD. The autoactivity of *AtMAPKs* baits prevented us to screen for MAPK-interacting TFs. Therefore, eight different deletion constructs of *AtMPK3* and *AtMPK6* were generated to identify the cause of the autoactivity in the *AtMAPKs* (Figure 4). These constructs included different parts of the MAPKs; some presented a truncated version of the ATP-binding pocket, the TEY motif (dual phosphorylation site), the kinase domain, the common docking domain (CD) and the C-terminal domain.

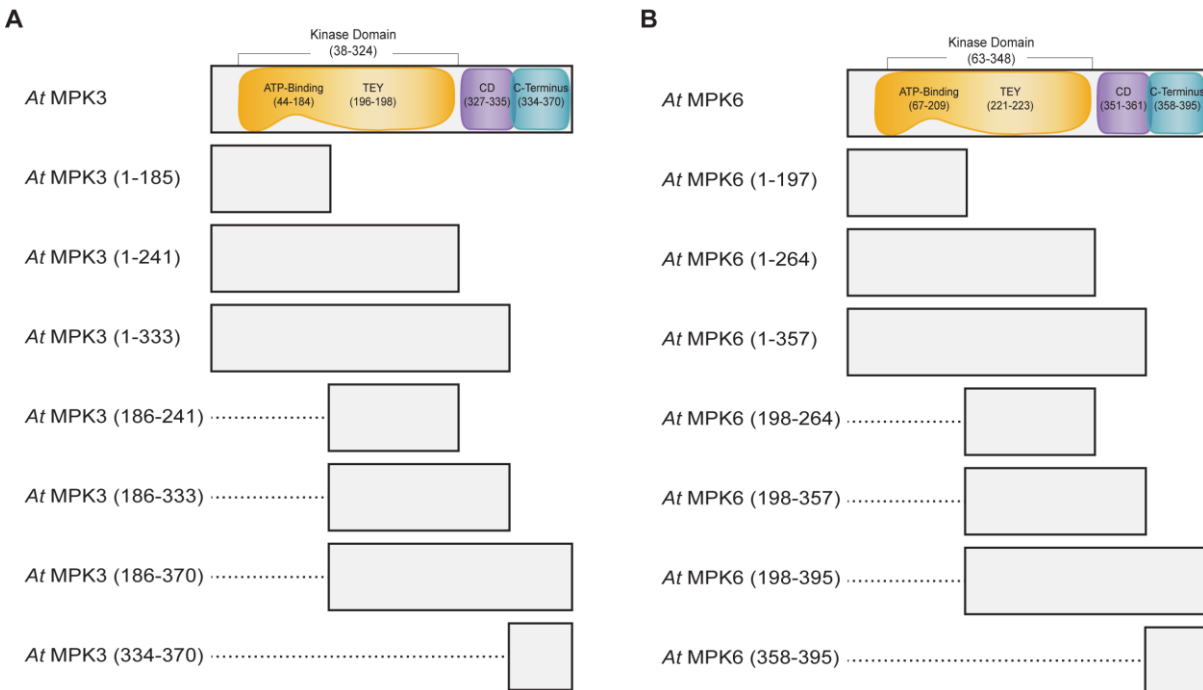


Figure 4: Schematic representation of *AtMPK3* and *AtMPK6* constructs

(A) *AtMPK3* and (B) *AtMPK6* full lengths contain a kinase domain (orange), which is comprised of an ATP-Binding domain and a TEY phosphorylation motif, a Common Docking (CD) domain (purple), and a C-terminus (turquoise).

2.1.1. *AtMPK3* and *AtMPK6* C-termini are responsible for autoactivity in yeast

All constructs were tested for autoactivity in both GAL4 and LexA systems. Results on the selective medium (-WLH) medium showed that for both systems, the C-terminus of these

*At*MAPKs was necessary and sufficient for autoactivity (Figure 5). These results suggest that the autoactivity of *At*MPK3 and *At*MPK6 in Y2H is associated with their C-terminal domain (*At*MPK3 (333-375) and *At*MPK6 (358-395)). Thus, their C-terminal deleted baits could be used for Y2H screen. However, I did not detect the autoactivity for the full-length of *At*MPK3 and *At*MPK6 in a more stringent selective media (-WLHA) in the GAL4 system (Figure 5A). Therefore, to increase the chance to detect MAPK-interacting TFs in Y2H screen, the full-length *At*MPK3 and *At*MPK6 bait constructs were also used for the GAL4 system (Figure 5A) in addition to the *At*MPK3 and *At*MPK6 C-terminal-deletion constructs (*At*MPK3 (1-333) and *At*MPK6 (1-357)) for both systems (Figure 5B). From here, I would refer to the *At*MPK3/6 C-terminal-deletion constructs *At*MPK3/6 Δ C, and the *At*MPK3/6 C-termini as the *At*MPK3/6 C-ter.

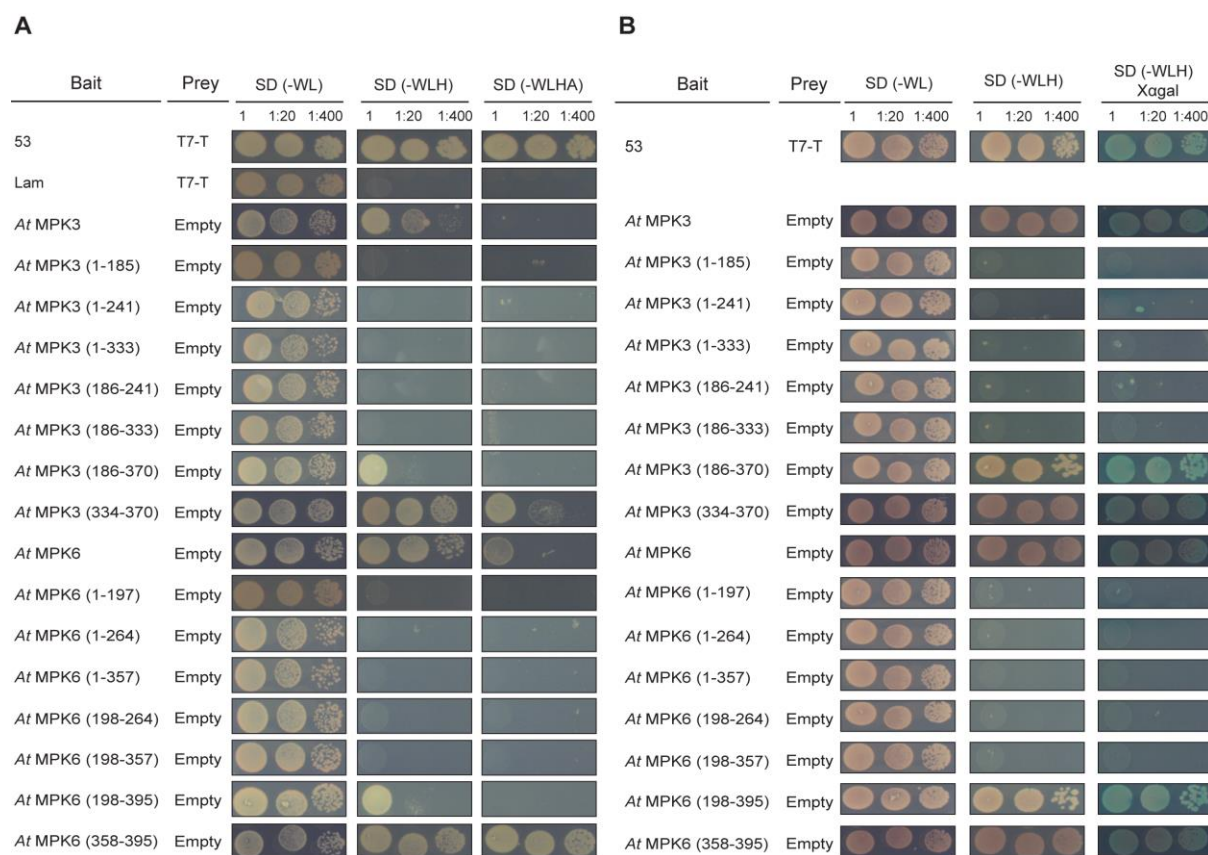


Figure 5: The C-terminus of *At*MPK3 and *At*MPK6 is necessary and sufficient for autoactivity in Y2H

Yeast-two-hybrid (Y2H) analysis of *At*MPK3/6 deletions constructs autoactivity. Y2H controls used for the GAL4 (A) and LexA (B) systems were the same as described in Figure 3. Autoactivity of the bait containing the *At*MPK3/6 deletion constructs was detected in combination with the empty vector of the prey containing only the AD, as indicated by yeast growth on selective media SD (-WLHA) and SD (-WLH) X- α -gal for GAL4 (A) and LexA (B), respectively. Dilutions were performed starting from an OD₆₀₀ = 1. Pictures were taken 3 days after incubation at 30°C. Same results were obtained for the other two independent experiments.

2.1.2. Twenty-three TFs were identified as candidate interactors of *AtMPK3* and *AtMPK6* in Y2H

The Y2H screens identified 23 candidates that interact with *AtMPK3* and/or *AtMPK6* and belong to different TF families. These are the TCP, VOZ, zinc finger (C2H2ZnF), bZIP, WRKY, and GATA (Table 1). From the TCP family *AtTCP8*, *AtTCP14*, *AtTCP15*, *AtTCP19*, *AtTCP20*, and *AtTCP21* are implicated in plant immunity (Kim et al., 2014; Lopez et al., 2015; and Wang et al., 2015). Nevertheless, their interaction with MAPKs remains unknown. *AtVOZ1*, as well as its functional homolog *AtVOZ2*, have been described as positive regulators of plant immunity since knock-out mutants are susceptible against pathogenic bacteria *Pseudomonas syringae* pv. *tomato* (*Pto* DC3000) and *Pto* DC3000 carrying the effector gene *avrRpt2* (*Pto* DC3000 (*AvrRpt2*)) (Nakai et al., 2013). *AtZAT10*, whose gene expression is induced by biotic stress, interacts with and is phosphorylated by *AtMPK3/6* (Nguyen et al., 2012b). Nonetheless, its role in plant immunity is unknown. And the zinc finger TF *AtAZF2* is a transcriptional repressor involved in abiotic stress (Sakamoto et al., 2004).

The WRKY TFs *AtWRKY10* and *AtWRKY25* differ in function. *AtWRKY10* is involved in endosperm development, and *AtWRKY25* is a negative regulator of immunity against *Pseudomonas syringae* pv. *maculicola* (Luo et al., 2005 and Zheng et al., 2007). The GATA-type zinc TFs *AtTIFY2A* and *AtTIFY2B*, which possess conserved ZIM domain, have been reported to interact with TFs involved in the JA pathway. Nevertheless, little is known about their function in immunity. (Arabidopsis Interactome Mapping Consortium, 2011; and Kazan and Manners, 2012).

Because of their potential relevance in plant immunity, I confirmed the interactions between *AtMPK3* and *AtMPK6* with *AtTCP8*, *AtTCP14*, *AtTCP15*, *AtTCP19*, *AtTCP20*, *AtTCP21*, *AtVOZ1*, *AtVOZ2*, *AtTIFY2A*, *AtTIFY2B*, *AtWRKY10* and *AtWRKY25* TFs. Interaction and phosphorylation of *AtVIP1* by *AtMPK3* and their role in immunity has been previously reported (Djamei et al., 2007). Therefore, *AtVIP1* was excluded from my confirmation assay. Moreover, WRKY TFs, *AtWRKY33* and *AtWRKY40*, which have been reported to be phospho-targets of *AtMPK3* and *AtMPK6* (Mao et al., 2011; Lassowskat et al., 2014), were included as positive controls. I also included two additional WRKY TFs, *AtWRKY18* and *AtWRKY60* which are homologs of and form protein complex with *AtWRKY40* (Xu et al., 2006).

Table 1: Candidate TFs that interacted with AtMPK3 and/or AtMPK6 in Y2H screens

Yeast System	AtMAPKs	AGI	TF Common Name	TF Classification
GAL4	AtMPK3 full length	AT1G43700	AtVIP1	bZIP
		AT1G51600	AtTIFY2A/AtGATA28	GATA
	AtMPK6 full length	AT3G21175	AtTIFY2B/AtGATA24	GATA
		AT1G55600	AtWRKY10	WRKY
		AT2G30250	AtWRKY25	WRKY
		AT1G28520	AtVOZ1	VOZ
		AT1G27730	AtZAT10	C2H2ZnF
		AT1G67260	AtTCP1	TCP
		AT1G53230	AtTCP3	TCP
		AT3G15030	AtTCP4	TCP
		AT1G58100	AtTCP8	TCP
	AtMPK3 ΔC and AtMPK6 ΔC	AT3G47620	AtTCP14	TCP
		AT1G69690	AtTCP15	TCP
		AT3G45150	AtTCP16	TCP
		AT5G51910	AtTCP19	TCP
		AT3G27010	AtTCP20	TCP
		AT5G08330	AtTCP21	TCP
		AT1G72010	AtTCP22	TCP
		AT1G35560	AtTCP23	TCP
		AtMPK6 ΔC	AT3G19580	AtAZF2
LexA		AtMPK3 ΔC and AtMPK6 ΔC	AT2G40620	AtZIP18
	AT4G38900		AtZIP29	bZIP
	AtMPK3 ΔC	AT2G40470	AtLBD15	AS2

TF interactions were validated only in the GAL4 system, because of the reduction of autoactivity of the full-length AtMPK3/6 under stringent conditions. Autoactivity of AtMPK3 was abolished on selective medium (-WLH) supplemented with 5mM of histidine biosynthesis inhibitor 3-amino-1,2,4-triazole (3-AT). AtMPK6, autoactivity was reduced on selective medium (-WLHA) allowing me to identified positive interactions, when compared to the positive control of the Y2H system (bait p53 (53) and the prey SV40 large T-antigen) (Figure 6A). Therefore, positive interactions between TFs and AtMPK3/6 were assessed in these selective media. Under these criteria, I found that AtMPK3 interacts with AtTIFY2A, AtTIFY2B, AtTCP8, AtTCP14, and AtTCP21 TFs and that AtMPK6 interacts with AtVOZ1, AtTIFY2A, AtTIFY2B, AtTCP8, AtTCP14, AtTCP15, AtTCP20 and AtTCP21 (Figure 6B - Figure 6K). As for the WRKY TFs, I confirmed the interaction of both AtMAPKs with AtWRKY10, AtWRKY25, and the positive control AtWRKY33. Moreover, AtMPK6 interacted with AtWRKY18 and AtWRKY60 (Figure 6L – Figure 6Q).

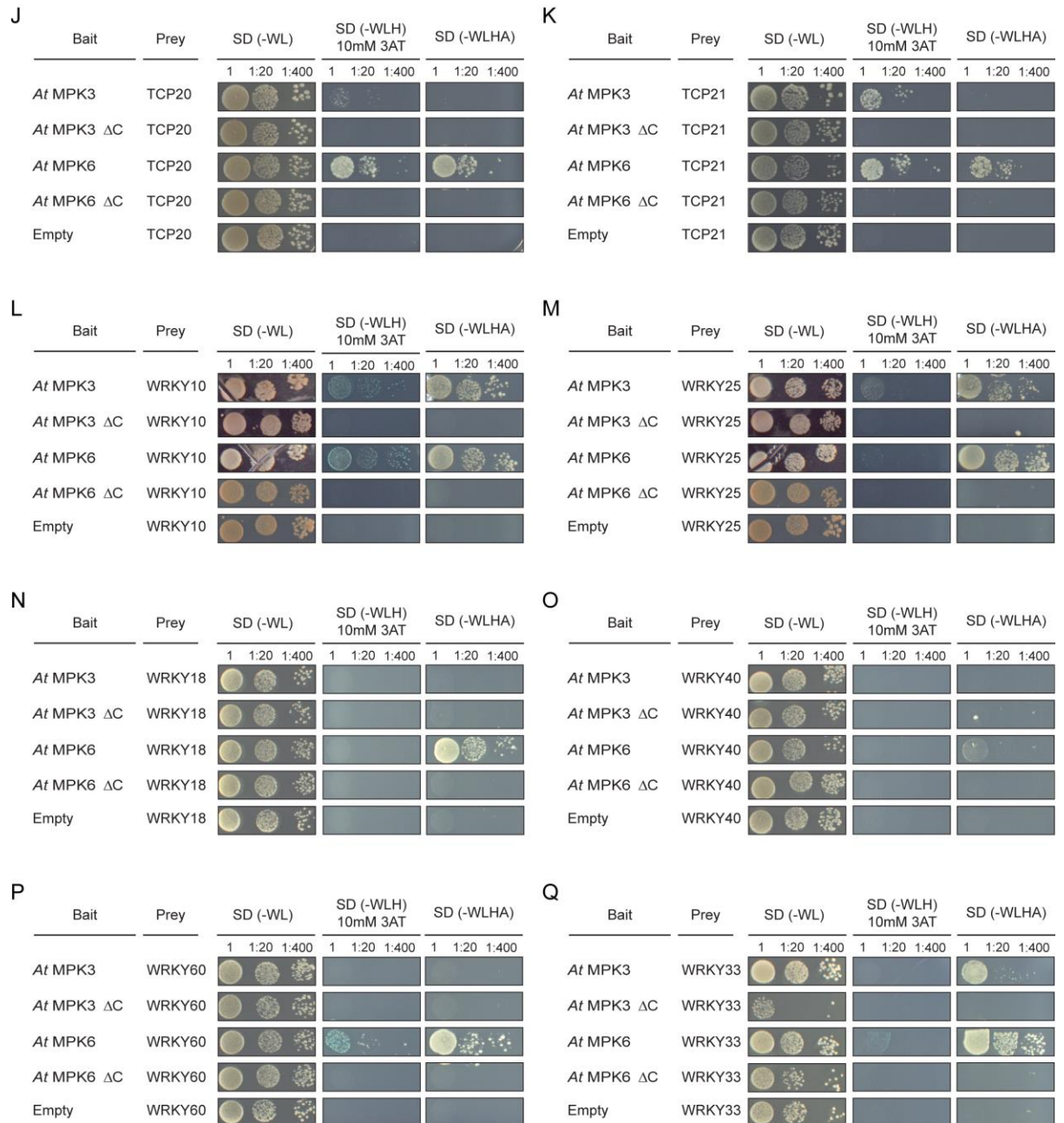


Figure 6: Confirmation of *At*MPK3/6 - TFs interactions through Y2H assays

(A) Y2H analysis of *At*MPK3/6 deletions constructs autoactivity for the GAL4 system. Positive and negative controls were the same as used in Figure 3. Assays were performed with bait containing the *At*MPK3/6 constructs, and the empty vector of the prey with only the AD. Autoactivity abolition is indicated by yeast growth on selective media SD (-WLH) with 10mM of 3-amino-1,2,4-triazole (3-AT), a histidine biosynthesis inhibitor, and SD (-WLHA). (B-Q) Y2H analysis of *At*MPK3/6 – TFs interaction. The assays were performed with the bait containing the *At*MPK3/6 constructs in combination with the prey containing the TFs. Additionally, bait empty vector with only the DBD was included as a negative control. Interactions are indicated by yeast growth on selective media SD (-WLH) with 10mM 3AT, and SD (-WLHA). Dilutions were performed starting from an OD₆₀₀= 1. Pictures were taken 3 days after incubation at 30°C. Same results were obtained for the other two independent experiments.

Results

Overall, I identified 12 novel TFs that interact with *AtMPK3/6* in yeast. Next, I decided to test whether the MAPKs and these TFs interact *in planta*, by *Agrobacterium*-mediated transient bimolecular fluorescence complementation (BiFC) assays in *Nicotiana benthamiana*. *AtMPK3* and *AtMPK6* full-length and C-terminal were fused to the C-terminal YFP fragment (c-YFP), and the TFs to the N-terminal YFP (n-YFP). To determine if the BiFC approach was suitable, I first tested the interaction between *AtMPK3/6* c-YFP constructs and the n-YFP without an interacting protein as controls. Unexpectedly, YFP fluorescence was observed for samples expressing the MAPKs-c-YFP and n-YFP (Supplementary Figure 2), making this method inappropriate for further interaction confirmation. Further experiments are required to investigate the physiological significance of their interactions in plants by different methods

Table 2: Confirmed TFs interacting with *AtMPK3* and *AtMPK6* in Y2H

<i>AtMAPKs</i>	TF Common Name	TF Classification	AGI
<i>AtMPK3</i>	<i>AtTIFY2A/AtGATA28</i>	GATA	AT1G51600
	<i>AtTIFY2B/AtGATA24</i>	GATA	AT3G21175
	<i>AtTCP8</i>	TCP	AT1G58100
	<i>AtTCP14</i>	TCP	AT3G47620
	<i>AtTCP21</i>	TCP	AT5G08330
	<i>AtWRKY10</i>	WRKY	AT1G55600
	<i>AtWRKY25</i>	WRKY	AT2G30250
<i>AtMPK6</i>	<i>AtVOZ1</i>	VOZ	AT1G28520
	<i>AtTIFY2A/AtGATA28</i>	GATA	AT1G51600
	<i>AtTIFY2B/AtGATA24</i>	GATA	AT3G21175
	<i>AtTCP8</i>	TCP	AT1G58100
	<i>AtTCP14</i>	TCP	AT3G47620
	<i>AtTCP15</i>	TCP	AT1G69690
	<i>AtTCP20</i>	TCP	AT3G27010
	<i>AtTCP21</i>	TCP	AT5G08330
	<i>AtWRKY10</i>	WRKY	AT1G55600
	<i>AtWRKY25</i>	WRKY	AT2G30250
	<i>AtWRKY18</i>	WRKY	AT4G31800
<i>AtWRKY60</i>	WRKY	AT2G25000	

2.1.3. The C-terminus of *AtMPK3* and *AtMPK6* works as a trans-activation domain in yeast

Results obtained from the Y2H assays (Figure 5) showed that the C-terminal sequence of *AtMPK3/6* was sufficient to cause autoactivity. This autoactivity could be caused by direct interaction of *AtMPK3/6* with the AD, which in turn activates transcription of reporter genes

or a direct mediation of transcriptional activation by the C-terminus of *AtMPK3/6*. To distinguish these two possibilities, I tested the *AtMPK3/6* deletion constructs in the absence of the AD for autoactivity. Results showed that autoactivity mediated by *AtMPK3/6* C-terminal domains does not require AD (Figure 7) for both *HIS3* and *ADE* reporter genes, suggesting that *AtMPK3/6* C-terminus works as a trans-activation domain (tAD) in yeast.

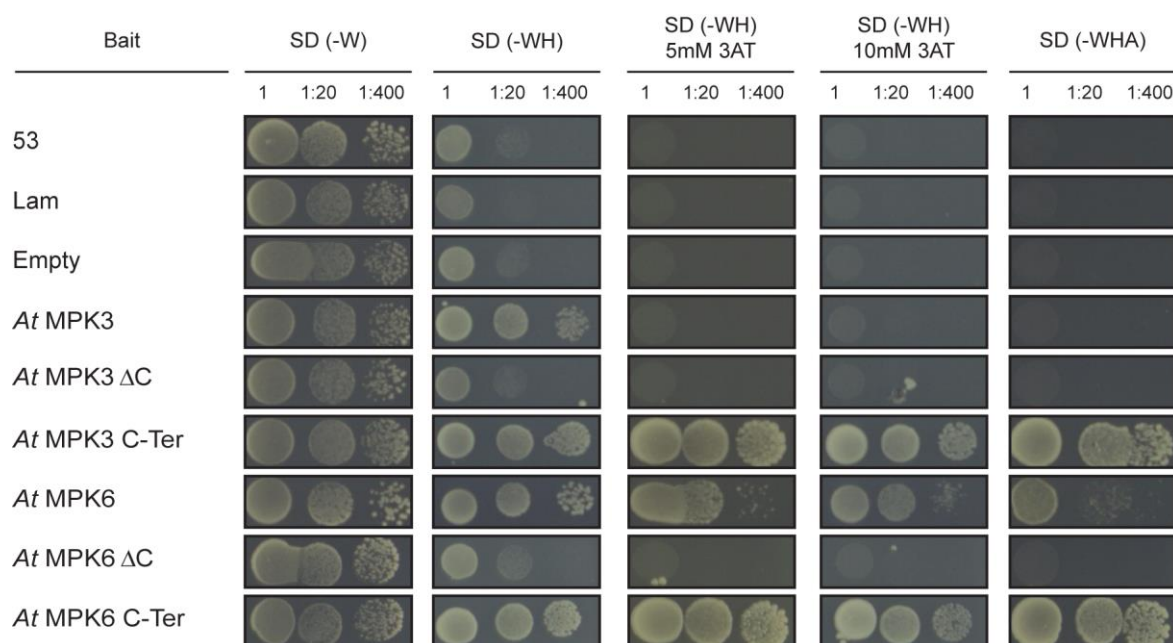


Figure 7: Baits containing *AtMPK3* and *AtMPK6* C-termini show autoactivity without a prey

Yeast transformation with the bait plasmids expressing the murine p53 (53), lamin (Lam), the empty vector, and the *AtMPK3/6* deletion constructs in the absence of the prey. Activation of reporter genes is indicated by yeast growth in selective media SD (-WLH) with 10mM 3AT, and SD (-WLHA). Dilutions were performed starting from an $OD_{600} = 1$. Pictures were taken 3 days after incubation at 30°C. Same results were obtained for the other two replicates.

MAPKs do not have DNA binding domains. Instead, they mediate transcription reprogramming by interaction with and phosphorylation of TFs, which target specific regions of the DNA for transcription. However, I found in yeast that when fused to the GAL4-DBD, *AtMPK3/6* C-termini induced the expression of reporter genes maybe through interacting with yeast transcriptional co-factors that mediate transcriptional activation. These observations led to an interesting hypothesis that when *AtMPK3/6* bind to a specific TF, MAPKs may activate transcription of genes whose promoter is bound by the TF through their C-terminal domain. As this does not require the full-length MAPK (i.e., kinase activity), this potential mechanism is different from the previously described mechanism in which the MAPKs phosphorylate CDKCs that in turn phosphorylate RNA pol II thereby activating transcription (Li et al., 2014).

Results

I found this MAPK C-terminus-mediated transcriptional activation interesting as this mechanism was not described before, and can link regulations of TFs and CDKCs by the MAPKs. In other words, TFs provide gene locus specificity, CDKCs activates transcription via phosphorylation of RNA pol II, and the MAPKs link them. Therefore, I focused on investigating the potential new role of *AtMPK3* and *AtMPK6* as transcriptional co-activators *in planta*.

2.2. *AtMPK3* and *AtMPK6* C-terminal domain induces transcription independently from their kinase activity *in planta*

2.2.1. *AtMPK3* and *AtMPK6* C-terminal domain present transcriptional activity *in planta*

Considering that *AtMPK3* and *AtMPK6* were able to activate three different reporters (*HIS3*, *MEL1*, and *ADE2*) in yeast and that the only common property is regulatory elements bound by GAL4 or LexA binding domain in their promoters, it is conceivable that activation of reporter genes was mediated by transcriptional activation. In addition, because Arabidopsis MAPKs mediated trans-activation in yeast, I expected that this trans-activation was caused by interactions with evolutionary conserved transcriptional machinery in eukaryotes. Therefore, I decided to investigate if *AtMPK3/6* transcriptional activation activity function was also present *in planta*. To measure the potential transcriptional activation activity of *AtMPK3/6* mediated by the C-terminal domain, I performed a reporter-effector transient expression based on luciferase reporter system. The reporter contained five consecutive GAL4 binding sites (BS) fused to the luciferase (*LUC2*) reporter gene. And the effector presented the GAL4-DBD fused to the different MAPKs constructs. Transformation efficiency is normalized by *Renilla* sp. luciferase under the control of the 35S promoter. With this setup, I could assess whether amino acid sequences fused to GAL4-DBD enhance or decrease the activity of the reporter gene *LUC2* by measuring relative luciferase activity (Figure 8A).

I used a known transcriptional activation domain, VP16 (Triezenberg et al., 1988; and Cousens et al., 1989), or a transcriptional repression domain, SRDX, (Hiratsu et al., 2004) as a positive or negative control, respectively. Because VP16 domain is one of the strongest transcriptional activation domain functioning in plants, *AtMYC2* TF, which has been previously described as a transcriptional activator in *A. thaliana* (Niu et al., 2011), was also included as an additional positive control to show the level of a conventional transcriptional

enhancement mediated by a TF. As for the MAPKs, the *At*MPK3 and *At*MPK6 full-length, ΔC, and C-terminal (C-ter) were included in the assay (Figure 8B). I additionally included *At*MPK3/6 P-def constructs to test if activation of the *At*MPK3 and *At*MPK6 influences their activity of trans-activation or not.

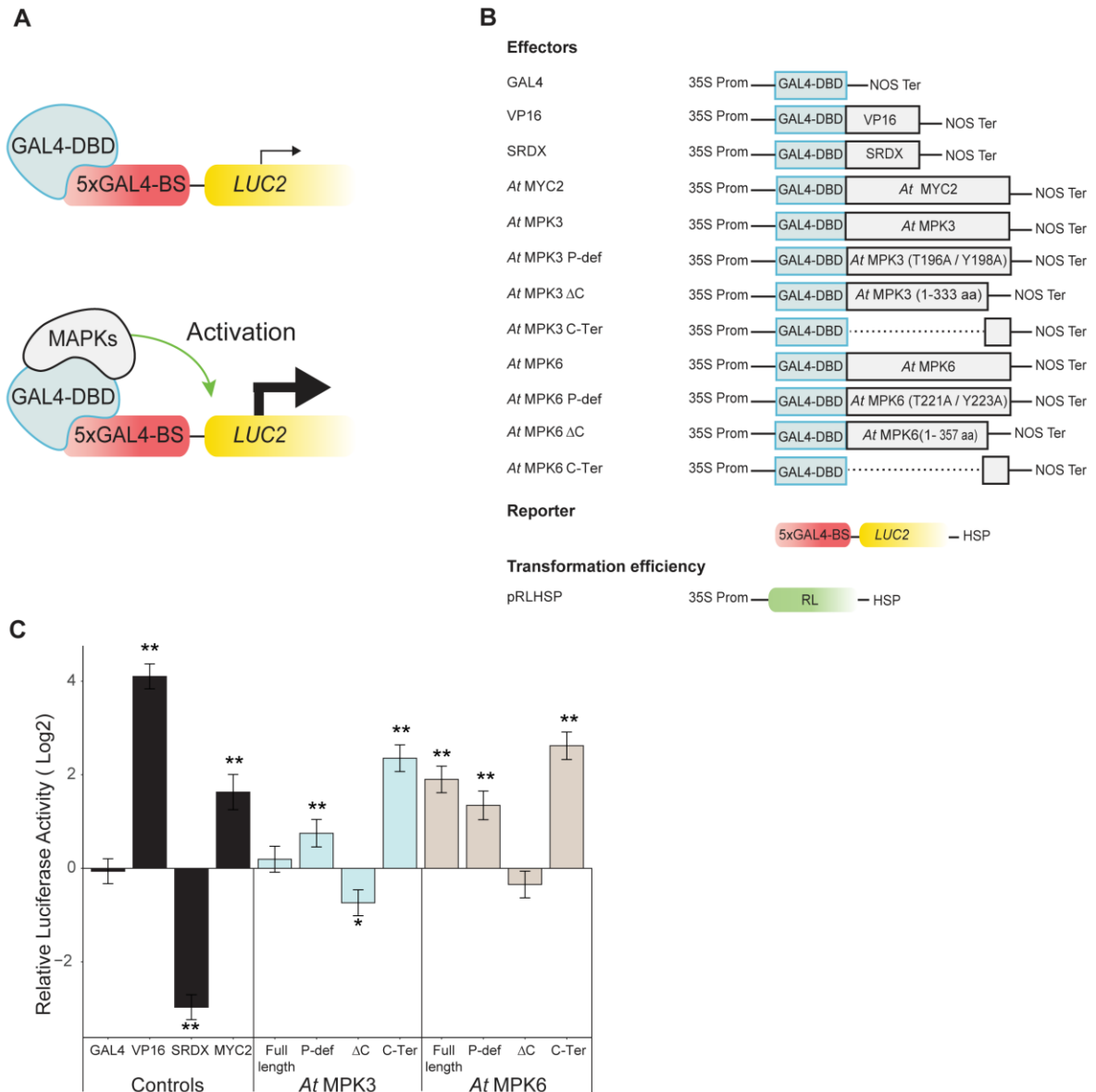


Figure 8: *At*MPK3 and *At*MPK6 C-terminus shows transcriptional activation activity in Arabidopsis

(A) Schematic representation for transcriptional activity assays *in planta*. MAPKs fused to GAL4 DBD (blue) may enhance transcription of luciferase gene driven by GAL4-binding promoter (red). (B) Schematic representation of the constructs used during the transient expression in *Arabidopsis* leaves via particle bombardment. The effectors contained GAL4-DBD or the different *At*MPK3/6 deletion constructs fused to the GAL4 DBD driven by 35S promoter. The reporter contained the firefly luciferase (*LUC2*) driven by five consecutive GAL4-Binding Sites (5xGAL4-BS). The pRLHSP encoding *Renilla* sp. luciferase under the 35S promoter used as transformation efficiency control. (C) Relative luciferase activity of *At*MPK3 and *At*MPK6 deletion constructs. For normalization, the values of GAL4-BD were set to 1. Bars represent relative luciferase

Results

activity means and \pm SE of 10 independent biological replicates with three replicates each. Data were \log_2 -transformed and analyzed by a mixed linear followed by a Student's t-test. Asterisks represent significant differences in comparison to GAL4-BD (*, $P < 0.05$; **, $P < 0.01$).

Transient expression assays performed in *Arabidopsis* leaves using particle bombardment (Figure 8C) showed an increase in luciferase activity for the *AtMPK6* full-length and *AtMPK6* P-def in comparison to *AtMPK6* Δ C, which showed a drastic reduction in luciferase activity. Furthermore, the *AtMPK6* C-terminus exhibited an enhancement in the luciferase activity, which was comparable or even higher to the known transcriptional activator *AtMYC2*. A similar trend was observed for *AtMPK3*, where the slight induction of luciferase activity generated by the full-length protein and P-def, was further reduced in the absence of the C-terminal domain (*AtMPK3* Δ C). Moreover, the *AtMPK3* C-terminal luciferase activity induction was similar to that mediated by *AtMPK6* C-terminal domain (Figure 8C). These results suggest that *AtMPK3/6* C-terminal domain is required and sufficient to induce transcriptional activation activity also *in planta*. Furthermore, considering the luciferase activity showed by *AtMPK3/6* P-def and *AtMPK3/6* C-terminus (Figure 8C), *AtMPK3/6* likely mediate transcriptional activation independent of their kinase activity. Considering that the luciferase activity of both *AtMPK3* and *AtMPK6* C-terminal domains was higher than that of *AtMYC2*, the newly identified function of MAPKs might be physiologically relevant in plants.

The data presented *in planta* was congruent with the data presented in yeast. Therefore, these results might suggest that when close to DNA, *AtMPK3/6* C-terminus activate transcription through an evolutionary conserved and kinase-independent mechanism.

2.2.2. Sequence-specific *AtMPK3* and *AtMPK6* C-termini activate transcription *in planta*

Considering that the *AtMPK3/6* C-terminus is the length of 37 or 38 amino acids (aa), respectively. While the data showing the MAPK C-terminus is necessary and sufficient for trans-activation suggest that the MAPK C-terminus-mediated transcriptional activation is sequence-specific, I was still concerned that the increased transcriptional activity mediated by *AtMPK3/6* C-terminus was a result of a short protein sequence fused to the GAL4-DBD and was not sequence-specific. Therefore, to confirm that MAPK-mediated transcriptional activity was sequence-specific, I generated new deletion constructs of *AtMPK3* and *AtMPK6* with a similar size of *AtMPK3/6* C-termini (Figure 9A). The new deletion constructs were *AtMPK3*

(58-89 aa), *AtMPK3* (137-173 aa), *AtMPK6* (162-199 aa), *AtMPK3* (271-307 aa), and *AtMPK6* (295-332 aa) (Supplementary Figure 3).

Considering that mesophyll protoplasts respond to physiological signals similar to mature leaves and that the method is more robust in terms of transformation efficiency compared to bombardment assay, the following transient assays were performed in *Arabidopsis* Col-0 protoplast system. Transient expression was done using the dual luciferase system described previously in Figure 8A. Results showed that only *AtMPK3/6* C-termini but not the other *AtMPK3/6* short peptides significantly induced relative luciferase activity (Figure 9B), indicating that the transcriptional activation activity exhibited by the C-terminal domain of *AtMPK3/6* is sequence-specific.

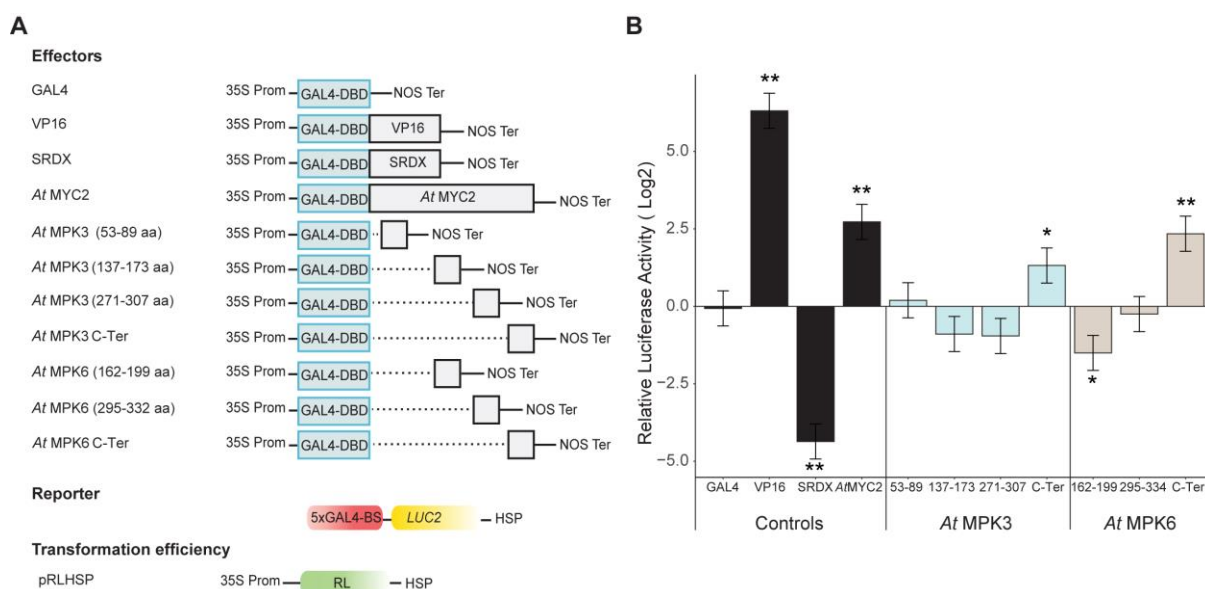


Figure 9: Transcriptional activation activity of *AtMPK3* and *AtMPK6* C-terminus is sequence specific

(A) Schematic representation of the constructs used during the transient expression assays in *Arabidopsis* mesophyll protoplasts. Effectors contained GAL4-DBD or the different *AtMPK3/6* deletion constructs fused to the GAL4-DBD driven by 35S promoter. The reporter contained the firefly luciferase (*LUC2*) driven by five consecutive GAL4-Binding Sites (5xGAL4-BS). The pRLHSP encoding *Renilla* sp. luciferase under the 35S promoter used as transformation efficiency control. (B) Relative luciferase activity of *AtMPK3* and *AtMPK6* short peptides deletion constructs. For normalization, the values of GAL4-BD were set to 1. Bars represent relative luciferase activity means and \pm SE of three independent biological replicates with three replicates each. Data were log₂-transformed and analyzed by a mixed linear followed by a Student's t-test. Asterisks represent significant differences in comparison to GAL4-BD (*, $P < 0.05$; **, $P < 0.01$).

Results

2.2.3. Transcriptional activation of *AtMPK3* and *AtMPK6* C-termini is independent of protein accumulation

After identifying that *AtMPK3/6* C-termini induce transcription in plants, raises the question of how do these MAPK C-terminal domains activate transcription? One possibility is that the *AtMPK3/6* C-terminus presents a protein stabilization motif, which allows them to enhance basal transcriptional activity mediated by GAL4-DBD. To test this possibility, I performed immunoblotting assays to detect protein accumulation of the *AtMPK3* deletion constructs using an α -GAL4-DBD antibody. Results showed that I was able to detect the accumulation of only GAL4-DBD control, VP16, and *AtMPK3* P-def, but not others. Immunoblotting using an α -MPK3 antibody, which would detect the full-length *AtMPK3* protein, showed that the *AtMPK3* full-length and *AtMPK3* P-def accumulate similarly. This result was inconsistent with immunoblotting results using the α -GAL4-DBD antibody (Supplementary Figure 4). Thus, the α -GAL4-DBD antibody did not properly work in my hands. Therefore, to monitor protein accumulation in the reporter-effector assays by immunoblotting, I re-cloned GAL4-DBD and *AtMPK3/6* deletion constructs into a vector with an HA-tag, which allowed me to detect fusion proteins with a well established α -HA antibody. As a result, the new effectors had the GAL4-DBD, the controls or MAPKs fragments, with three consecutive sequences of HA tag at their C-terminus (Figure 10A).

Reporter-effector assays showed that *AtMPK6* C-terminus had similar luciferase activity as seen in previous experiments. However, the luciferase activity of *AtMPK3* C-terminus was compromised (Figure 10B). Previous studies showed that addition of small tags like polyhistidine tag (His6-tag) altered the protein structure, activity, and kinetics (Panek et al., 2013; and Vologzhannikova et al., 2019). Moreover, the addition of c-MYC, FLAG, and HA tags to the enhanced green fluorescent protein (EGFP) showed alterations in protein structure, and reduction of fluorescence activity of EGFP (Shevtsova et al., 2006). These suggest that the HA tag negatively affected trans-activation activity of the *AtMPK3* C-terminus, which made the use of HA-tagged constructs unreasonable.

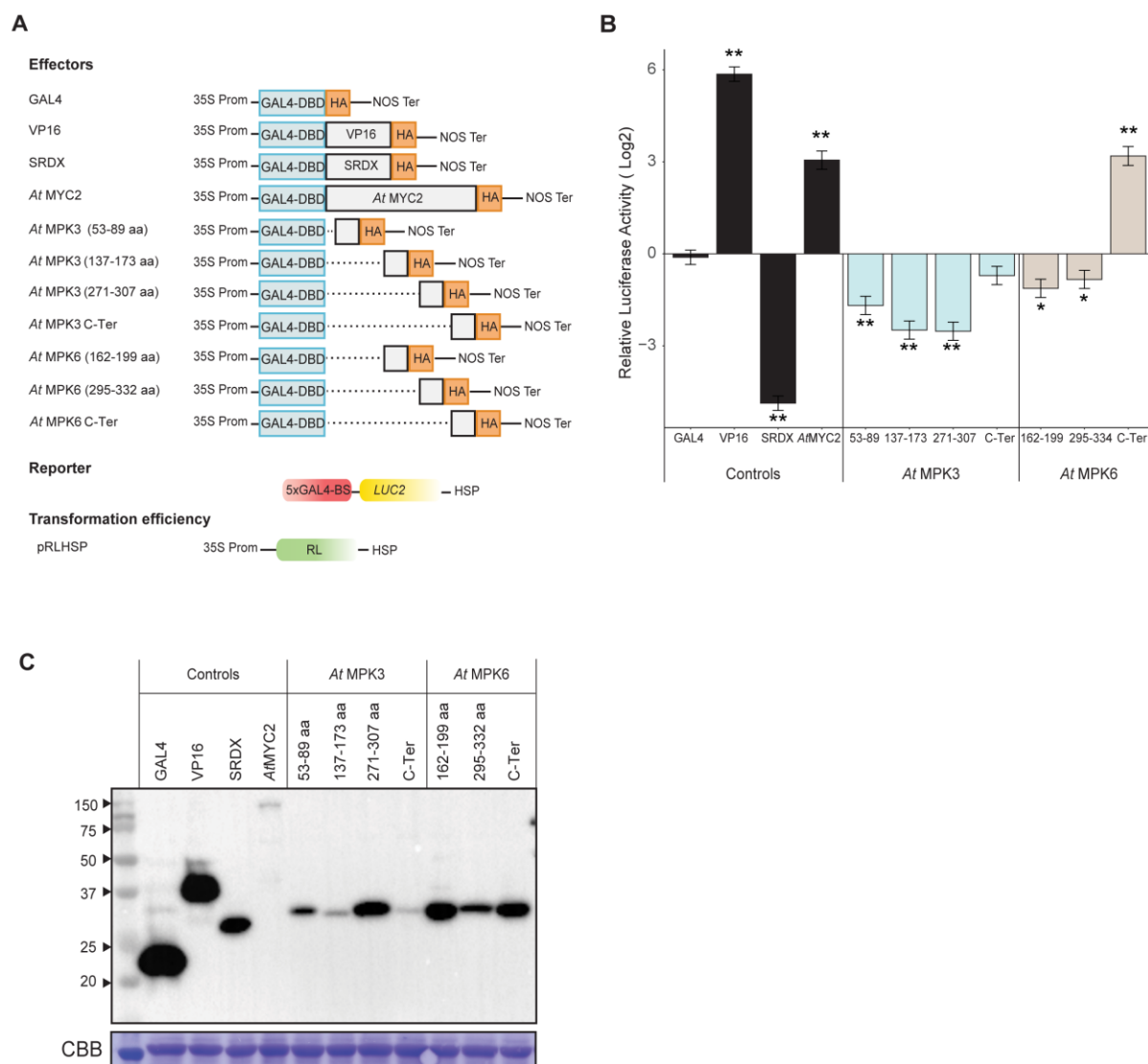


Figure 10: Protein expression does not explain transcriptional activation

(A) Schematic representation of the reporter-effector constructs used during the transient expression assays in *Arabidopsis mesophyll* protoplasts. Effectors contained the GAL4-DBD or the different *At*MPK3/6 deletion constructs fused to the GAL4-DBD and three consecutive sequenced of the HA tag, driven by the 35S promoter. The reporter contained the firefly luciferase (*LUC2*) driven by five consecutive GAL4-Binding Sites (5xGAL4-BS). The pRLHSP encoding *Renilla* sp. luciferase under the 35S promoter used as transformation efficiency control. (B) Relative luciferase activity of *At*MPK3 and *At*MPK6 short peptides deletion constructs tagged with HA. For normalization, the values of GAL4-BD were set to 1. Bars represent relative luciferase activity means and \pm SE of three independent biological replicates with three replicates each. Data were \log_2 -transformed and analyzed by a mixed linear followed by a Student's t-test. Asterisks represent significant differences in comparison to GAL4-BD (*, $P < 0.05$; **, $P < 0.01$). (C) WB shows protein accumulation levels of the effectors. For loading control, Coomassie Brilliant Blue (CBB) staining was implemented. Information of fragments sizes can be found in Supplementary Table 1.

Immunoblotting results showed that proteins were expressed according to the expected sizes (Supplementary Table 1). GAL4-DBD and VP16 protein exhibited a higher accumulation in comparison to the other two controls and the *At*MPK3 and *At*MPK6 deletion constructs.

Results

AtMYC2, *AtMPK3* (58-89 aa), *AtMPK3* (137-173 aa), and *AtMPK3* C-terminal, had a lower protein accumulation in comparison to the other samples (Figure 10C). Accumulation of *AtMPK6* C-terminus, which enhanced reporter gene expression, was similar to *AtMPK3* (271-307 aa), *AtMPK6* (162-199 aa), and *AtMPK6* (295-332 aa), which did not enhance reporter gene expression. Thus, enhanced protein accumulation was not the cause of the enhanced reporter gene expression mediated by the *AtMPK6* C-terminus, implying that the *AtMPK3/6* C-terminus activate transcription via interacting with other proteins, perhaps components of transcriptional complexes. Taken together, these data suggest that *AtMPK3/6* C-terminal domain-mediated transcriptional activation is sequence-specific and independent of protein stabilization and their kinase activity, which is likely conserved in eukaryotes.

I so far used an artificial system in which different parts of *AtMPK3* and *AtMPK6* were fused to the GAL4-DBD to detect trans-activation activity of the MAPK C-terminus. In natural conditions, it is possible that MAPKs interact with a DNA-binding TF, which is mimicry of MAPK fusions with a DNA-binding domain, thereby activating transcription of genes regulated by the TF. To test this hypothesis, I performed a promoter reporter assay in which the MAPKs and a TF that binds DNA and interacts with the MAPKs are expressed as different proteins. Previous studies showed that *AtWRKY33*, which is a phospho-target of *AtMPK3/6*, bind the W-boxes present in the *AtPROPEP2* and *AtPROPEP3* promoter regions (Mao et al., 2011; and Logemann et al., 2013). Therefore, I performed Arabidopsis protoplast assays using *AtMPK3* and *AtWRKY33* as effectors and the *AtPROPEP2* promoter-driven GUS reporter as the reporter. Additionally, I used a mutated *AtPROPEP2* promoter in which all W-boxes are mutated. To activate *AtMPK3* and subsequently *AtWRKY33*, I treated the samples with flg22. However, while flg22 treatment induced *AtPROPEP2* promoter activity dependent on the W-boxes, I did not detect positive effects of *AtMPK3* or *AtWRKY33* on the promoter activity. It may be possible that phosphorylation of overexpressed *AtMPK3* protein did not occur sufficiently due to the limitation of upstream kinases, I decided to artificially activate overexpressed *AtMPK3*. Therefore, I included *AtMKK4DD*, which phosphorylate *AtMPK3*, as an additional effector in some assays to test if activation of *AtMPK3* influences reporter activity. However, despite my efforts, I did not observe an enhancement of *AtWRKY33*-mediated transcriptional activation by *AtMPK3* in any tested conditions, implying that additional factors other than active *AtMPK3* and *AtWRKY33* are required (Supplementary Figure 5).

2.3. *AtMPK3* and *AtMPK6* C-terminal domain is evolutionary conserved across plant species

2.3.1. Angiosperms and non-plant kinases possess a conserved C-terminal domain

The Arabidopsis *AtMPK3* and *AtMPK6* C-terminal domain worked as tAD in both yeast and Arabidopsis, suggesting that this MAPK C-terminus function is evolutionary conserved. To investigate how conserved C-terminal regions of different eukaryotic MAPKs are, I analyzed a total of 60 full-length proteins from plants, mammals, and yeast. I included the *Saccharomyces cerevisiae* MAPKs *ScHOG1* and *ScFUS3* involved in stress response and proliferation (Saito and Tatebayashi, 2004; and Elion et al., 1993), and the mammal ERKs (Pagès et al., 1993). As for the plant MAPKs, I included 50 proteins from different angiosperms previously described by Ichimura et al., 2002.

Based on the consensus neighbor-joining (NJ) tree obtained, plant MAPKs are divided into four clades, named clades A-D (Figure 11A), consistently with Ichimura et al., 2002. The plant clades A, B, and C, and non-plant MAPKs (bootstrap 65) were separated from the plant clade D, suggesting that the clade D is a plant innovation. Moreover, I identified sequence similarity among MAPK C-terminal regions, by comparing the full-length and C-termini of the protein kinases used for the alignment with the full-length and C-terminal domain of *AtMPK3/6* (Figure 11B). This analysis evidenced that even though sequence similarity results showed that kinases from clade D were more similar to *AtMPK3/6* than non-plant kinases, they are evolutionary distant. This can be due to specific characteristics that protein kinases from clade D present. Clade D kinases have a TDY phosphorylation motif, different from MAPKs from clade ABC, which share a TEY phosphorylation motif, they possess an elongated C-terminal domain, and lack a CD domain required for upstream kinase (MAPKK) recognition (Ichimura et al., 2002). Additionally, little is known about the role of clade D kinases in stress response. Moreover, based on the consensus sequence and consensus match, I identified 21 residues conserved in half of the protein kinases, and nine highly conserved residues present in 75% of the MAPKs. Considering that C-terminal domains of MAPKs are widely conserved among angiosperms, mammals, and yeast kinases and that *AtMPK3/6* activated transcriptional activity in yeast and plant systems, MAPKs exert an evolutionarily conserved function. However, considering the protein differences that plant kinases from clade D possess, I excluded them from further analysis.

Results

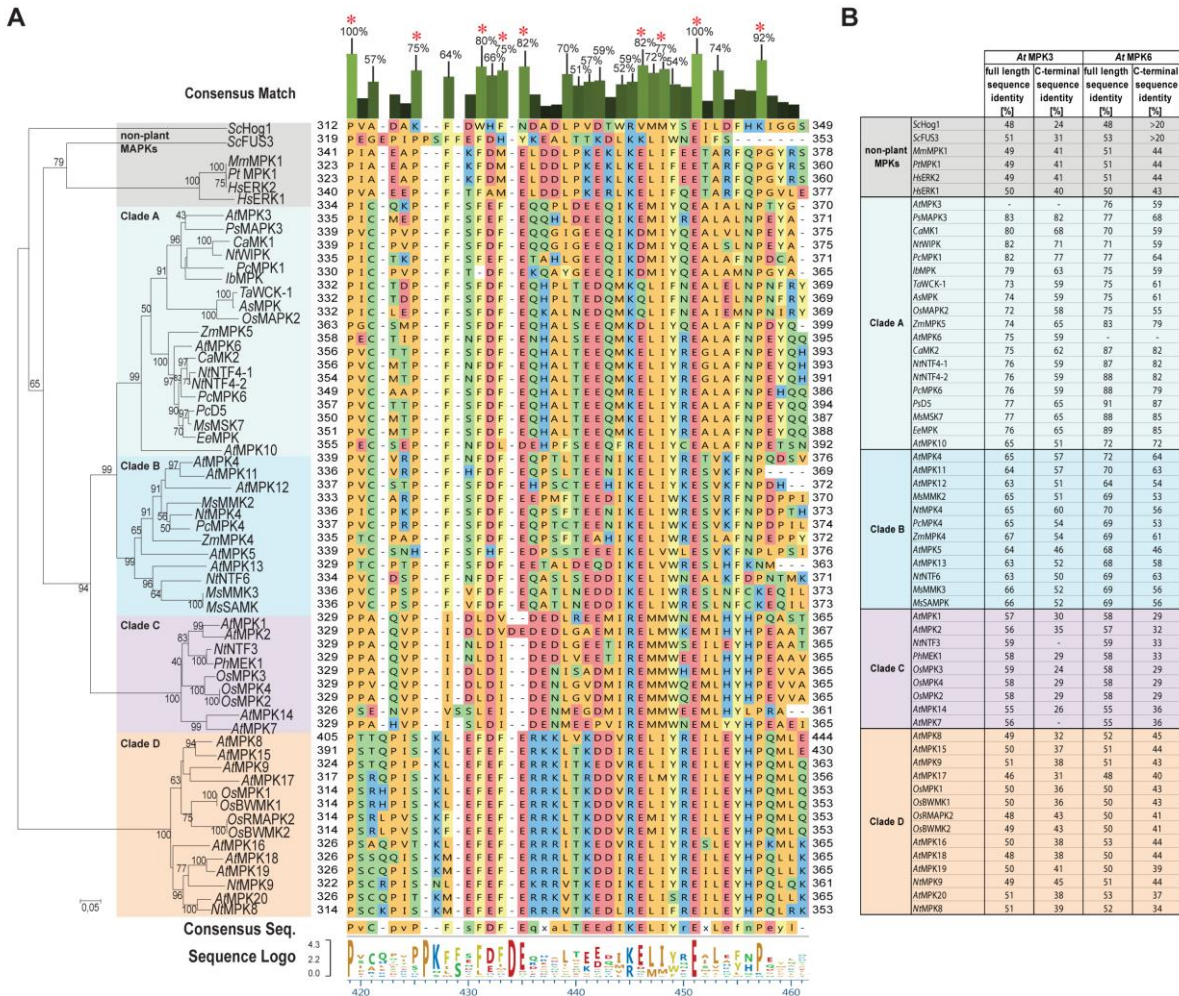


Figure 11: MAPKs phylogenetic tree and C-terminal protein profile reveal conserved residues

(A) Neighbor-joining (NJ) phylogenetic tree of MAPKs from plants, mammal, and fungi with a bootstrapping of 1000. Sequences alignment from total protein analysis, sequence logo, and consensus match, were obtained through MegaAlignPro. According to the consensus match, the C-terminal domain possessed 21 conserved residues present in more than 50% of the sequences along the different MAPKs. Asterisks (*) indicate conserved residues present in 75% of all species. (B) Percentage of protein identity of the different MAPKs compared with full length and C-terminal from *AtMPK3* and *AtMPK6*. In the phylogeny, the following abbreviations were used for the species. *As*: *Avena sativa*, *At*: *Arabidopsis thaliana*, *Ca*: *Capsicum annum*, *Ee*: *Euphorbia esula*, *Hs*: *Homo sapiens*, *Ib*: *Ipomoea batatas*, *Mm*: *Mus musculus*, *Ms*: *Medicago sativa*, *Nt*: *Nicotiana tabacum*, *Os*: *Oryza sativa*, *Pc*: *Petroselinum crispum*, *Ph*: *Petunia x hybrida*, *Ps*: *Pisum sativum*, *Pt*: *Pan troglodytes* *Sc*: *Saccharomyces cerevisiae*, *Ta*: *Triticum aestivum*; *Zm*: *Zea mays*.

2.3.2. MAPK C-terminal domains are conserved among the Viridiplantae clade

To further understand the evolutionary conservation of MAPK C-terminal domain, I included more MAPKs from the Viridiplantae clade for analysis. I searched for and selected the protein kinases through the software HMMER, based on the alignment and consensus sequence from proteins belonging to clades A, B, and C from Figure 11A. For selection, I used a threshold based on a 95% protein similarity and 75% protein identity in comparison to the

consensus sequence. As a result, 713 protein kinases from the Viridiplantae clade matched the threshold. These MAPKs included proteins from green algae, bryophytes, lycophytes, gymnosperms, and angiosperms.

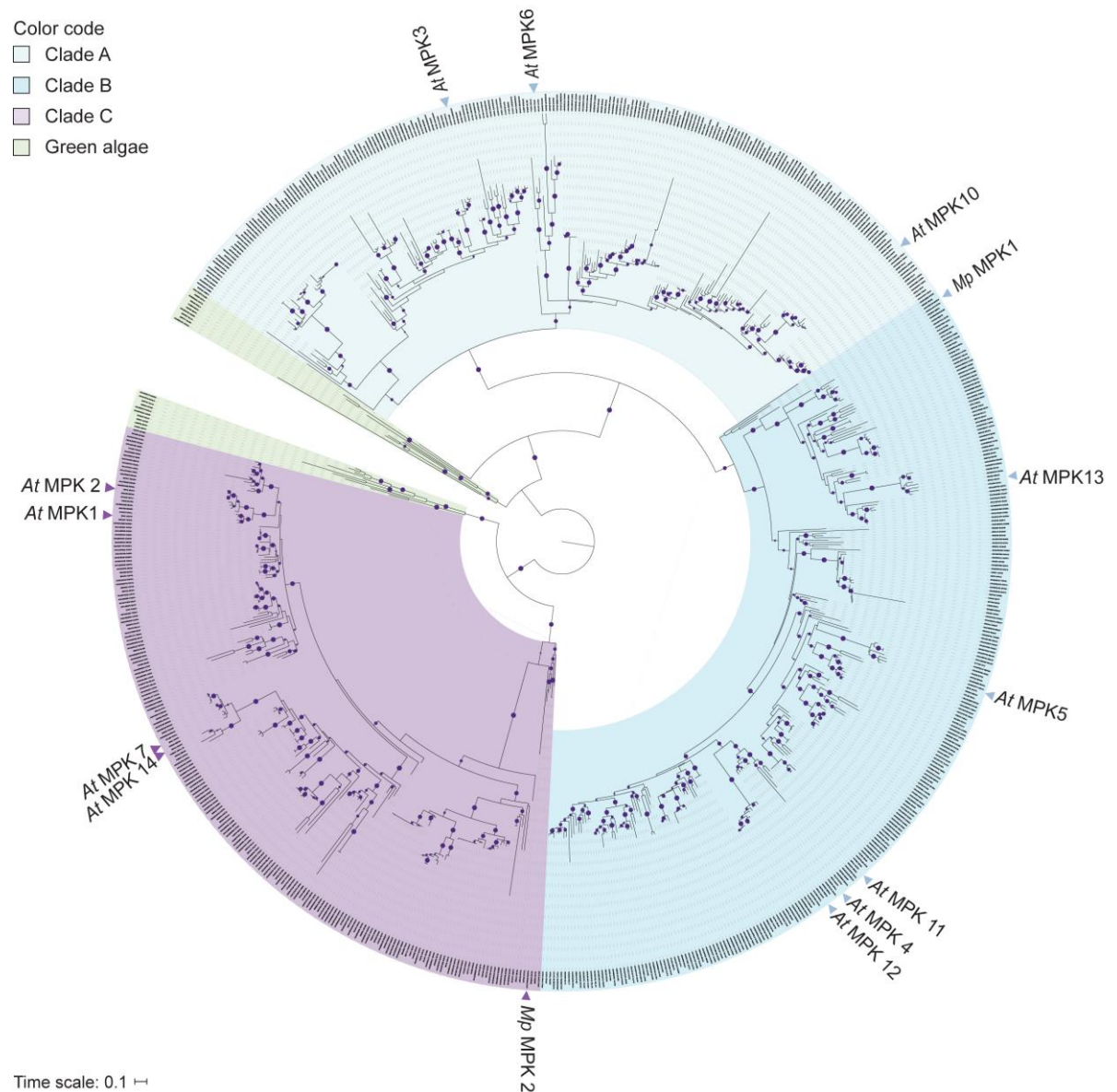


Figure 12: Phylogenetic analysis of 713 MAPKs from the Viridiplantae clade

Protein search was done with HMMER software, followed by alignment with T-Coffee. Maximum likelihood (ML) phylogenetic analysis was performed with PhyML software with the LG model and 1000 bootstrap for branch support. iTOL was used for tree visualization. Purple dots represent clades with a bootstrap support higher than 75. Colors represent the division of clades A-C and green algae. Labels and arrows indicate *A. thaliana* MAPKs (AtMPKs) and *M. polymorpha* MAPKs (MpMPKs) through the clades.

Results

Proteins were aligned by T-Coffee multiple sequence alignment software, which aligns protein sequences not only based on their sequence similarity but also based on conserved motifs. Phylogenetic analysis supported the clade division A-C previously presented (Figure 11A). Additionally, the presence of green algae proteins, as well as early-diverged land plants, like bryophytes, suggest that clade A and B diverged from an ancestral clade AB later in evolution (Figure 12). This result is congruent with Bowman et al., 2017, where they showed that bryophyte *Marchantia polymorpha* has only three MPKs *MpMPK1*, *MpMPK2* and *MpMPK3* belonging to clades AB, C, and D, respectively.

Considering that *AtMPK3* and *AtMPK6*, which belong to clade A, may have separated later in evolution, from the so-called clade AB. One can hypothesize that the tAD in the *AtMPK3* and *AtMPK6* C-terminal domain is a clade A function-specific trait. Alternatively, this trans-activation function of MAPK C-terminus is more evolutionarily ancient. Therefore, I tested *Arabidopsis* MAPKs belonging to clades A-C, the *M. polymorpha* *MpMPK1* and *MpMPK2*, animal, and yeast MAPKs for trans-activation activity.

2.3.3. MAPKs C-terminal domain transcriptional activation is conserved across kingdoms

I tested C-terminus of a total of 18 MAPKs from plant (*A. thaliana*, and *M. polymorpha*), mammals (*Homo sapiens*), and yeast (*S. cerevisiae*), for transcriptional activation activity. Phylogenetic tree shows the closely related MAPKs Clade A (*AtMPK3*, *AtMPK6*, *AtMPK10*) and clade B (*MpMPK1*, *AtMPK4*, *AtMPK11*, *AtMPK12*, *AtMPK5*, *AtMPK13*), the clade C (*MpMPK2*, *AtMPK1*, *AtMPK2*, *AtMPK17*, *AtMPK7*), and the non-plant kinases clade (*HsERK1*, *HsERK2*, *Hsp38*, and *ScFUS3*) (Figure 13A). Proteins were expressed transiently in *Arabidopsis* Col-0 protoplasts using the reporter-effector system described in previous sections (Figure 13B).

Results showed that all of MAPK C-terminal domains from *A. thaliana*, and *M. polymorpha* induced transcriptional activation, suggesting that the novel function identified for *AtMPK3* and *AtMPK6* C-terminal domain is conserved in plant MAPKs. Moreover, the non-plant MAPKs C-terminal domain also enhanced transcription (Figure 13C), suggesting that eukaryotic MAPK C-terminal domains work as tAD.

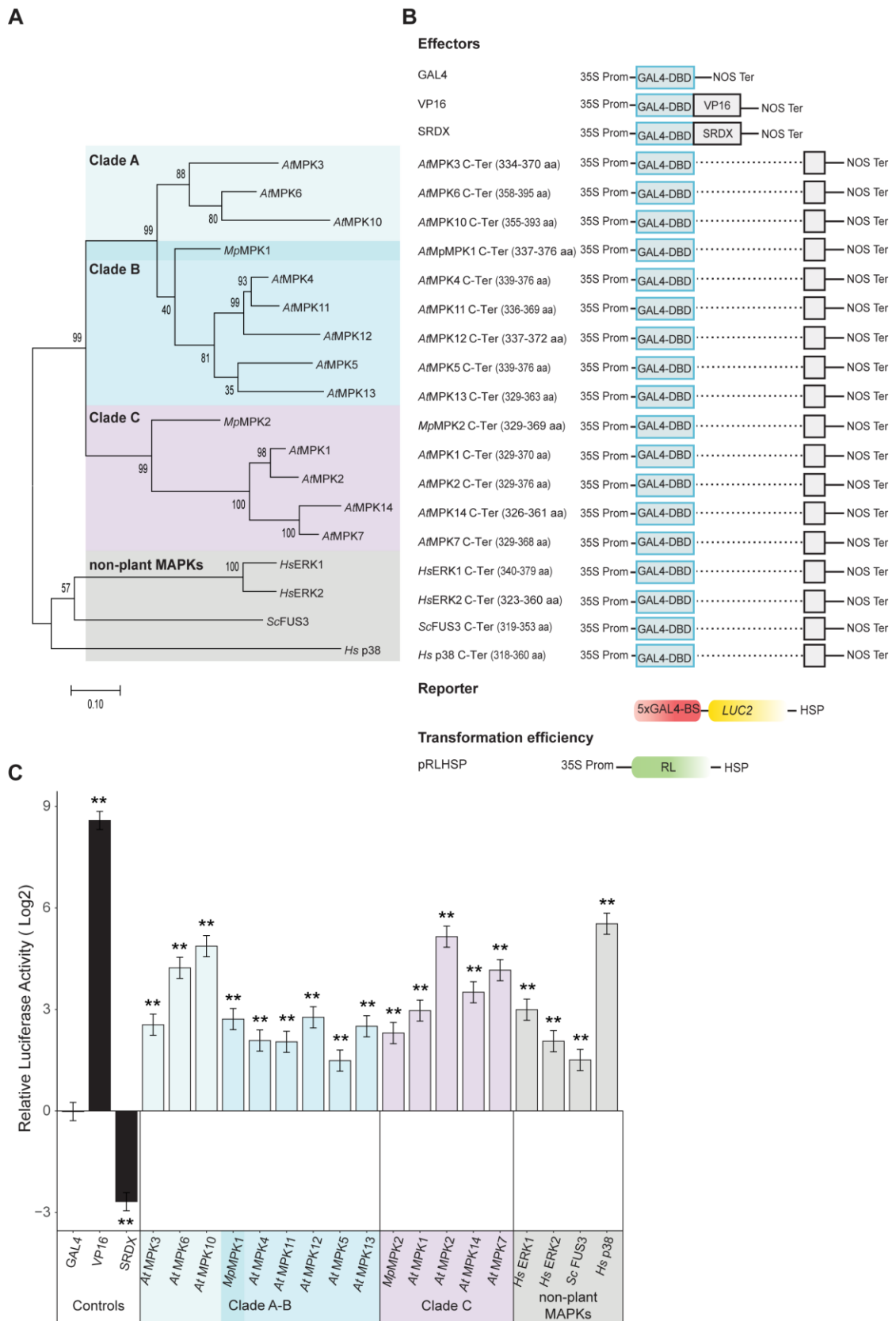


Figure 13: MAPK C-terminal domains across kingdoms induce transcriptional activity *in planta*

(A) Maximum likelihood (ML) phylogenetic tree from plant, mammal and fungi MAPKs was performed a bootstrapping of 1000. (B) Schematic representation of reporter-effector constructs used during the transient

Results

expression assays in *Arabidopsis* mesophyll protoplasts. Effectors contained the GAL4-DBD or the different AtMPK3/6 deletion constructs fused to the GAL4-DBD driven by the 35S promoter. The reporter contained the firefly luciferase (*LUC2*) driven by five consecutive GAL4-Binding Sites (5xGAL4-BS). The pRLHSP encoding *Renilla* sp. luciferase under the 35S promoter used as transformation efficiency control. (C) Relative luciferase activity of *A. thaliana* (*At*), *M. polymorpha* (*Mp*), *H. sapiens* (*Hs*) and *S. cerevisiae* (*Sc*) MAPKs C-terminal domain. For normalization, the values of GAL4-BD were set to 1. Bars represent relative luciferase activity means and \pm SE of three independent biological replicates with three replicates each. Data were \log_2 -transformed and analyzed by a mixed linear followed by a Student's t-test. Asterisks represent significant differences in comparison to GAL4-BD (**, $P < 0.01$).

To identify specific sequence motifs in the MAPK C-terminal regions associated with trans-activation, I aligned amino acid sequences of the MAPK C-terminal domains used in the assay. Results showed that 16 residues were present in more than 50% of the samples, and nine of them were present in 70% of the samples (Figure 14). According to the consensus sequence of the alignment, the conserved motif within the MAPKs C-terminal domain was P-(X₇₋₄)-P-F-(X₅₋₄)-E-(X₈₋₉)-(K/R)-E-L-(X₂)-E-(X₅₋₄)-P.

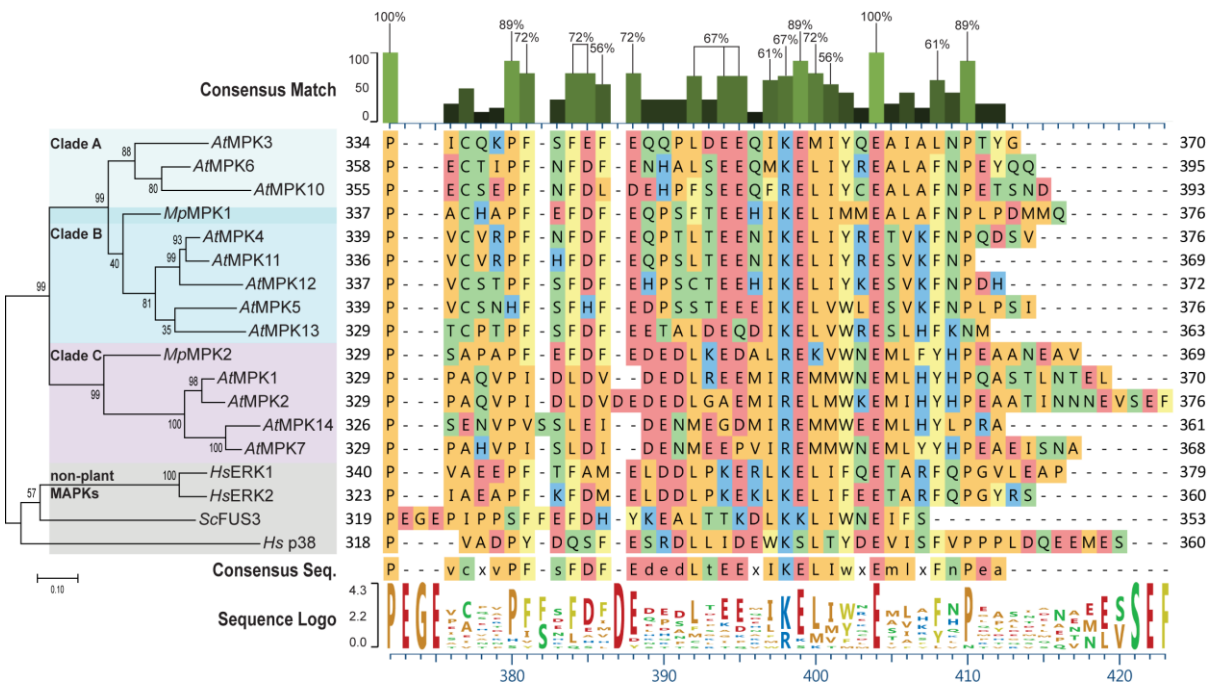


Figure 14: C-terminal MAPKs sequence analysis determined a potential conserved motif among eukaryotes

Maximum likelihood (ML) phylogenetic tree from C-terminal domain from *A. thaliana* (*At*), *M. polymorpha* (*Mp*), *H. sapiens* (*Hs*) and *S. cerevisiae* (*Sc*) MAPKs with a bootstrapping of 1000. Sequences alignment from protein analysis, sequence logo, and consensus match, were obtained through MegaAlignPro. Percentages indicate residue identity among eukaryotic MAPKs.

2.4. Physiological function of *AtMPK3* C-terminal domain in *A. thaliana*

Transient expression assays revealed that *AtMPK3* and *AtMPK6* C-terminal domain works as a tAD independent of their kinase activity. Moreover, this newly identified function of MAPKs C-terminal domain was conserved in MAPK C-terminus from different eukaryotes, suggesting that MAPKs could mediate transcriptional activation across kingdoms. To test the physiological significance of this finding, I attempted to complement *Atmpk3* and *Ampk6* mutants with the *AtMAPK3* Δ C, or *AtMAPK6* Δ C. Because *Atmpk3* and *Atmpk6* single mutants do not show a strong phenotype and *Atmpk3 Atmpk6* double mutant is embryo-lethal, I used for complementation the *Atmpk3 Atmpk6* (+/-) mutant plants, which present a normal development and seed production (Wang et al., 2007; Wang et al., 2008; and Beckers et al., 2009). I transformed *Atmpk3 Atmpk6* (+/-) mutant plants with a construct expressing the *AtMPK3* full-length, Δ C, or C-terminal domain under the native *AtMPK3* promoter. The full length *AtMPK3* driven by this promoter is known to complement *Atmpk3* phenotypes (Xu et al., 2014). Therefore, I expected to complement the developmental phenotype of *Atmpk3 Atmpk6* with the *AtMPK3* full-length and be able to evaluate if the *AtMPK3* C-terminal domain is required for development or immunity. I genotyped T1 generation plants which carried transgene (judged by BASTA resistance). If the locus is homozygous for *Atmpk6*, the transgene complemented the developmental phenotype of *Atmpk3 Atmpk6*. I tested 80 plants for the *AtMPK3prom::AtMPK3-GFP*, and 20 plants for *AtMPK3prom::AtMPK3 Δ C-GFP*, and 20 plants for *AtMPK3prom::AtMPK3C-term-GFP*, but I did not find *Atmpk6* mutants for any cases. I expected that at the T2 generation of *AtMPK3prom::AtMPK3-GFP* (genotype: *Atmpk3 Atmpk6* (+/-)), I would be able to obtain *Atmpk6* (-/-) genotypes in the presence of the transgene. Therefore I genotyped 20 plants per transgenic line which showed BASTA resistance, but I could not identify any *Atmpk6* (-/-) genotypes (Figure 15). Since I could not complement the developmental phenotype of *Atmpk3 Atmpk6* with the *AtMPK3* full-length or with the deletion constructs, it was not possible to determine, if the function of the *AtMPK3* C-terminal domain is physiologically relevant.

Results



















	T1			T2			
<i>At MPK3</i>	- / -	- / -	- / -	- / -	- / -	- / -	Background
<i>At MPK6</i>	+ / +	+ / -	- / -	+ / +	+ / -	- / -	
<i>At MPK3prom::AtMPK3-GFP</i>	29 	51 		12 	8 		Transformation Insert
<i>AtMPK3prom::AtMPK3 ΔC-GFP</i>	6 	14 		6 	14 		
<i>AtMPK3prom::AtMPK3 C-term-GFP</i>	6 	14 		5 	15 		

Figure 15: *AtMPK3prom::AtMPK3-GFP* did not complement the embryo-lethal phenotype in *Atmpk3 Atmpk6* double mutants.

Transgenic lines were generated through *Agrobacterium tumefaciens* transformation in the *Atmpk3 Atmpk6* (+/-) background, where only one allele of *AtMPK6* was expressed. *AtMPK3-GFP*, *AtMPK3 ΔC-GFP*, and *AtMPK3 C-term-GFP* domain did not complemented the *Atmpk3 Atmpk6* (-/-) phenotype.

3. Discussion

MAPK cascades are key regulatory components among eukaryotes. They translate extracellular stimuli into intracellular responses. In *Arabidopsis*, MAPKs are both important for development and immunity, indicating that they exert cellular functions as hubs in biological networks. *AtMPK3* and *AtMPK6* function as positive regulators of plant immunity and mediate transcriptional reprogramming through phosphorylation of several substrates including TFs. However, the molecular mechanisms of how the MAPKs regulate transcriptional reprogramming during immunity are not fully understood. In this study, I identified 12 new TFs that interact with *AtMPK3* and/or *AtMPK6* through a large-scale Y2H screen with a TF library containing ~ 1500 TFs from *Arabidopsis*. Moreover, I found that *AtMPK3* and *AtMPK6* C-terminal regions work as trans-activation domains, independently of their kinase activity. Furthermore, I found that this function is evolutionary conserved among other MAPKs in eukaryotes including *Arabidopsis*, *Marchantia polymorpha*, mammals, and yeast, suggesting that MAPKs possess a kinase-independent trans-activation function conserved across kingdoms.

3.1. Newly identified *AtMPK3* and *AtMPK6* interacting TFs

In *Arabidopsis*, MAPKs, *AtMPK3* and *AtMPK6*, mediate transcriptional reprogramming during plant immunity through phosphorylation of substrates including TFs. However, only a few TFs have been confirmed as phospho-targets of *AtMPK3/6*. These are *AtVIP1*, *AtMYB44*, *AtWRKY33*, *AtERF104*, and *AtERF6* (Djamei et al., 2007; Bethke et al., 2009; Mao et al., 2011; Nguyen et al., 2012a; ; Meng et al., 2013; and Persak and Pitzschke, 2013). A study showed that sustained *AtMPK3/6* activation alone triggers expression changes with more than four-fold of over 4500 genes (Tsuda et al., 2013), suggesting that there are numerous MAPK targets unidentified. To elucidate the role of *AtMPK3/6* in transcriptional reprogramming during plant immunity, several studies focused on identifying targets of these MAPKs (Popescu et al., 2009; Hoehenwarter et al., 2013; Lassowskat et al., 2014 ; Pecher et al., 2014; Latrasse et al., 2017; and Rayapuram et al., 2018). Here, I identified 12 novel TFs from four different families (Table 2). These TFs families are the VOZ, GATA, TCP, and WRKY, from which some of them are relevant for plant immunity (Tsuda and Somssich, 2015).

Discussion

These identified TFs broaden our understanding of MAPK-mediated transcriptional networks in plant immunity.

A. thaliana Vascular plant One Zinc finger protein (*AtVOZ1*) interacted with *AtMPK6* (Figure 6B). The VOZ TFs are zinc finger proteins that present a denominated Domain-B, which contains the DNA-BD and a dimerization domain of VOZ (Mitsuda et al., 2004). Moreover, *AtVOZ1* and *AtVOZ2* have been described as negative regulators of abiotic stress and positive regulators of immunity (Nakai et al., 2013; and Song et al., 2018). The *Atvoz1voz2* double knock-out mutant is susceptible against the fungal pathogen *Colletotrichum higginsianum* and the bacterial pathogen *P. syringae* DC3000 (*Pto* DC3000). Additionally, regulation of JA and SA-signaling pathway marker genes *AtPDF1.2* and *AtPRI* was compromised in *Atvoz1 Atvoz2* double mutants upon *C. higginsianum* infection (Nakai et al., 2013). These results suggest that *AtVOZ1* and *AtVOZ2* function redundantly in immune responses. Nevertheless, it remains unknown how *AtVOZ1* and *AtVOZ2* are regulated during plant immunity. Thus, my observation that *AtVOZ1* interacts with *AtMPK6* suggests that *AtMPK6* regulates the function of VOZ1 and VOZ2 thereby mediating transcriptional reprogramming during plant immunity.

The GATA-type zinc TFs *AtTIFY2A* and *AtTIFY2B* have a conserved ZIM domain (Reyes et al., 2004; and Shikata et al., 2004). These ZIM-like related TFs have been proposed as interactors of *AtMYC*-like TFs and Overexpressor of Cationic Peroxidase 3 (*AtOCP3*), both of which are involved in JA-signaling pathway (Arabidopsis Interactome Mapping Consortium, 2011; Ramírez et al., 2010; and Kazan and Manners, 2012). Yet, the function of *AtTIFY2A* and *AtTIFY2B* in immunity is unknown. However, considering that they interact with *AtMPK3* and *AtMPK6* (Figure 6D-6E) and that *AtMPK3* and *AtMPK6* are involved in JA responses genes (Bethke et al., 2009; and Meng et al., 2013), MAPK-mediated *AtTIFY2A/B* regulation may contribute to JA responses.

The plant-specific basic-helix-loop-helix (bHLH) TCP TFs are known for their importance in development and hormone signaling required for immunity (Martín-Trillo and Cubas, 2010; and Lopez et al., 2015). Here, I identified the *AtTCP8*, *AtTCP14*, *AtTCP15*, *AtTCP20*, and *AtTCP21* as interactors of *AtMPK3/6* (Figure 6F-6K). It has been reported that *AtTCP8*, *AtTCP14*, and *AtTCP15* are required for ETI, as the triple mutant of these TFs is more susceptible to *Pto* DC3000 expressing the effector gene *avrrips4*, which triggers ETI, compared to WT plants, but the triple mutant and WT plants are equally susceptible to *Pto* DC3000 which does not trigger ETI (Kim et al., 2014). Additionally, upon *P. syringae* pv. *maculicola* ES4326

(*Psm*.ES4326) infection, *AtTCP8* positively regulates the expression of the enzyme *ISOCHORISMATE SYNTHASE 1 (AtICS1)*, required for SA biosynthesis (Mauch et al., 2001; and Wang et al., 2015). Moreover, it is known that *AtTCP20* binds to the promoter of *LIPOXYGENASE 2 (AtLOX2)* and represses transcription of the JA biosynthesis precursor (Danisman et al., 2012; and Lopez et al., 2015). Therefore, it is possible that the MAPKs coordinate immune responses via regulating the activity of *AtTCPs*.

The WRKYs represent a plant-specific TF family. In Arabidopsis, there are over 70 WRKY TFs, and some of them work as positive or negative regulators of immunity, emphasizing the importance of studying their function within immune networks (Ülker and Somssich, 2004; Eulgem and Somssich, 2007; Rushton et al., 2010; Tsuda and Somssich, 2015; Birkenbihl et al., 2017; and Mine et al., 2018). Here, I reported that *AtMPK3/6* interacts with both *AtWRKY10* and *AtWRKY25*, and that *AtMPK6* interacts with *AtWRKY18* and *AtWRKY60* (Figure 6L-6P). Previous reports demonstrated the importance of *AtWRKY10* during endosperm development (Luo et al., 2005). Nevertheless, the role of *AtWRKY10* in immunity remains unknown. To determine the immune function of *AtWRKY10*, it would be necessary first to evaluate the susceptibility or resistance towards necrotrophic or hemibiotrophic pathogens in *Atwrky10* mutant plants, and then determine if *AtWRKY10* is downstream *AtMPK3/6* cascade. Different from *AtWRKY10*, *AtWRKY25* has been identified as a negative regulator of SA immune response towards *Psm* ES4326 downstream *AtMPK4* signaling cascade (Andreasson et al., 2005; and Zheng et al., 2007). Together with the results here presented, it is possible that during immunity *AtWRKY25* is also a downstream substrate of *AtMPK3/6*.

The *AtWRKY18*, *AtWRKY40*, and *AtWRKY60* TFs assemble a heterocomplex that mediates immunity by regulation of genes involved in the JA pathway. Additionally, in vitro assays showed, that *AtWRKY18* and *AtWRKY40* presented stronger DNA binding activities than *AtWRKY60* (Xu et al., 2006). This might reflect that upon an flg22 treatment, *AtWRKY18* and *AtWRKY40* bind to over 1000 genes, some of them involved in immunity (Birkenbihl et al., 2017). Considering that *AtMPK6* interacted with *AtWRKY18/60* but not with *AtWRKY40* in Y2H, it could be that *AtMPK6* influences the *AtWRKY18/40/60* heterocomplex via interaction specifically with *AtWRKY18/60*. In summary, my results provide a number of testable hypotheses for future investigation.

3.2. *AtMPK3* and *AtMPK6* C-terminal domain as trans-activation domain

A central concept in MAPK signaling is that MAPKs mediate intracellular signaling through phosphorylation of substrates, like TFs and enzymes. Phosphorylation of substrates leads to increased protein stabilization and enhanced DNA binding and/or transcription activity (Djamei et al., 2007; Joo et al., 2008; and Mao et al., 2011). Crystal structure analysis of *AtMPK6* revealed that *AtMPK6* has a similar structural topology with the human *HsERK2* and *Hsp38* kinases. Plant and mammalian MAPKs N-terminal and C-terminal domains interact in a way that forms a groove required for kinase function. This groove contains the ATP binding pocket required for substrate phosphorylation and a surface required for substrate recognition (Kornev et al., 2006; Roskoski, 2012; and Wang et al., 2016).

Functions independent from kinase activity have been described in yeast and animal MAPKs (Rodríguez and Crespo, 2011). It is known that *S. cerevisiae* *ScKss1* could interact and activate *ScSte12* TF by a mechanism independent of phosphorylation (Bardwell et al., 1998). Moreover, mammalian ERK kinases present several kinase-independent functions. ERKs directly interact with microtubules and actin fibers thereby regulating cytoskeletal dynamics during cell division and proliferation (Reszka et al., 1995; and Leinweber et al., 1999). Additionally, during meiosis, ERKs indirectly induce phosphorylation of topoisomerase II α (TOPO II α) independent of their kinase activity and phosphorylation status, resulting in chromatin reorganization (Shapiro et al., 1999). Moreover, ERK2 binds to the promoter regions at the sequence G/CAAAG/C and mediates transcription by forming a molecular complex with the upstream kinase (MEK) and transcriptional activator or repressors (Hu et al., 2009; and Rodríguez and Crespo, 2011). Nevertheless, kinase-independent function has not been identified in plant MAPKs. Here, I identified that *A. thaliana* MAPKs *AtMPK3* and *AtMPK6* when proximal to DNA, induce transcriptional activation in yeast and *in planta*. This function was present in full-length, phospho-deficient, and the C-terminal domain of both *AtMPK3/6* (Figure 8), demonstrating that these proteins induce transcription in a C-terminal domain-dependent manner in the absence of phosphorylation and kinase domain activity. Altogether, these results suggest that *AtMPK3* and *AtMPK6* can mediate intracellular signaling during plant immunity, independent from phosphorylation of substrates in plants.

A study using *Drosophila* S2 cells identified that short peptides present in different regions of TFs worked as trans-activation domains (tADs). These tADs assays were performed

in a GAL4-dependent system with *LUC2* as a reporter, similar to the one I used. They showed that tADs are diverse and lack clear sequence similarity, but have different sequence signatures, like glutamine-rich repeats, DBD-like structure, and overlap with a helix-loop-helix conformation (Arnold et al., 2018). According to the structure of *AtMPK6*, the end of the kinase present a helix-loop-helix conformation named the α I-L16- α L16, and the *AtMPK6* C-terminal domain described in this thesis is located at the loop-helix L16- α L16, also known as the L16 loop (Wang et al., 2016). The L16 loop is also present in animals, and it has been described to play an important role in basal kinase activity, MAPK activation, and structural conformation during active and inactive kinase status (Canagarajah et al., 1997; Diskin et al., 2007; and Nguyen et al., 2015). Studies in mammalian MAPKs *HsERK2* and *Hsp38* showed that structural conformation of inactive kinases was regulated by the formation of a salt bridge. The salt bridge is generated by the interaction between an arginine (R70^{*Hsp38*}, R84^{*AtMPK3*}, R109^{*AtMPK6*}) present in the kinase domain, and the conserved glutamic acid (E328^{*Hsp38*}, E354^{*AtMPK3*}, E369^{*AtMPK6*}) located at the L16 loop of the C-termini. Upon MAPKs activation by phosphorylation, the salt bridge is disrupted, releasing the C-terminus and opening a groove for interaction with downstream substrates (Kornev et al., 2006; Diskin et al., 2007; and Nguyen et al., 2015). This suggests that upon kinase activation, the MAPK C-terminal domain present at the L16 loop is loose and available for interaction with potential transcriptional cofactors. Furthermore, Arnold et al., 2018 showed that short peptides present in TFs have potential for transcriptional activation. Thus, embedded tAD in non-TF proteins could be an overlooked, physiologically relevant phenomenon, in particular for proteins that interact with TFs such as MAPKs.

Considering that the *AtMPK3/6* C-terminal domain induced transcription of multiple reporter genes in two different eukaryotic systems (i.e., in yeast, and *in planta*), MAPK C-terminal tails may work as tADs through interacting with basal transcriptional machinery components conserved among eukaryotes. In eukaryotes during transcription, RNA-Polymerase II (RNA-Pol II) is activated by phosphorylation of serine residues (Ser2, Ser5, and Ser7) present at the heptapeptide of the C-terminal domain (CTD) by cyclin-dependent kinases (CDKs) (Koiwa et al., 2004; Bataille et al., 2012; Hajheidari et al., 2013; and Li et al., 2014). Reports identified that in the yeast *Schizosaccharomyces pombe*, the MAPK *SpSty1*, which is involved in stress response, mediates phosphorylation of the *Sp*RNA-Pol II CTD through phosphorylation the CDK-like kinase *SpCDTK1* (Sukegawa et al., 2011). Moreover, in plants, *A.thaliana* MAPKs *AtMPK3/6* phosphorylate *AtCDKC1* and *AtCDKC2*, which leads to the

Discussion

activation of *At*RNA-Pol II via phosphorylation of serine residues (Ser2, Ser5, and Ser7) present at the CTD (Li et al., 2014). Considering this information, one can hypothesize that upon pathogen perception, active *At*MPK3 and *At*MPK6 mediate transcriptional reprogramming in a molecular complex that involve TFs, which provide locus specificity, CDKCs for recruitment of basal transcriptional machinery, and MAPK themselves. Once *At*MPK3/6 locate at the DNA via an interaction with a TF, they interact with and phosphorylate CDKCs, which in turn phosphorylate the RNA-Pol II CTD, thereby activating transcription of target gene. Considering that MAPK substrates generally contain multiple phosphorylation sites, MAPKs need to be re-activated after substrate phosphorylation or multiple active MAPKs are required. However, little is known about how MAPKs phosphorylate multiple sites. Interestingly, it is known that activation of animal kinase ERK2 promotes its homodimerization, which is essential for its nuclear localization (Khokhlatchev et al., 1998). Taking this information into account, one can suggest that upon activation, *At*MPK3 and *At*MPK6 homodimerize and translocate into the nucleus, where they interact with and phosphorylate both TFs and CDKCs for transcription of target genes. Nevertheless, considering the data presented in this thesis, one can propose a third mechanism of MAPK-mediated transcriptional reprogramming, which is not exclusive to the others. Considering the results obtained in yeast and *in planta*, the *At*MPK3/6 C-terminal domain works as a tAD. Upon pathogen perception, active *At*MPK3/6 may homodimerize as human ERKs and activate by phosphorylation both TFs and CDKCs. In addition to the phosphorylation-based mechanisms, the *At*MPK3/6 C-terminal domain works as a tADs by recruiting cofactors that mediate activation of transcription. Therefore, searching for the *At*MPK3/6 C-terminal domain-interacting proteins would be crucial to understand the mechanism by which the *At*MPK3/6 C-terminal domains exert transcriptional activation.

3.3. Evolutionary conserved trans-activation domain in MAPK C-terminal domains

The phylogeny based on green algae and land plants protein MAPKs from clades ABC gave a better resolution to the subdivision of clade AB into clade A and B. This result was congruent with previous studies based on the evolution of MAPKs in green algae and the early-diverged bryophyte *M. polymorpha*, where the species studied had at least one kinase belonging to the clade C and one kinase from the clade AB (Bowman et al., 2017; and Kalapos et al.,

2019). Additionally, these studies showed that green algae and *M. polymorpha* also possess a clade D kinase, supporting the hypothesis that clade D is a MAPK plant-specific clade (Bowman et al., 2017; and Kalapos et al., 2019). Considering that early-diverged species presented three MAPKs, one for each clade (clades AB, C, and D), but *A. thaliana* presents a total of 20 MAPKs, MAPKs specialization and diversification in flowering plants substantially occurred to provide fine regulation of complex biological processes (Ichimura et al., 2002; and Kalapos et al., 2019). I showed that MAPK C-terminal domains from *A.thaliana*, *M. polymorpha*, human, and yeast present a trans-activation activity *in planta*. Moreover, I confirmed that the C-terminal domain in *AtMPK3/6* was able to induce transcriptional activation in two different eukaryotic systems. Considering this information, one can suggest that eukaryotic MAPKs may possess a conserved tAD within the C-terminal domain that allows them to mediate activation of gene expression through conserved mechanisms among eukaryotes. Additionally, considering that this trans-activation activity was present in organisms from three different eukaryotic kingdoms, I hypothesize that this MAPK C-terminal function was derived from a common MAPK ancestor shared by fungi, plants, and animals. Furthermore, as animal kinase ERK5 has been reported to present a tAD at the extended, unconventional C-terminal domain (Kasler et al., 2000), having tAD at the C-terminus of MAPKs is a common theme. It would be interesting to determine if the trans-activation activity is also present in clade D kinases.

Sequence comparisons (Figure 14) revealed that there are conserved residues in the C-terminal regions of *A. thaliana*, *M. polymorpha*, animal, and yeast MAPKs. I was not able to identify the mechanism by which the C-terminus activates transcription, but I speculate that the secondary structure of the conserved L16 loop at the C-terminal (Canagarajah et al., 1997; Diskin et al., 2007; and Wang et al., 2016) is important for transcription activation. Evidence showed that the MAPK L16 loop participates in MAPK activation, structural conformation, and dimerization. Furthermore, it has been reported that alterations in the C-terminal domain causes enhanced kinase activity (Canagarajah et al., 1997; Diskin et al., 2007; and Nguyen et al., 2015). Enhancement of kinase activity by C-terminal modifications has also been reported for *Arabidopsis AtMPK6*, where mutation of phenylalanine residues into leucine (*AtMPK6*^{F364L}, *AtMPK6*^{F366L}, and *AtMPK6*^{F368L}) enhances kinase activity in comparison to WT *AtMPK6* (Wang et al., 2016). Therefore, the high sequence conservation at MAPK C-terminal regions can be attributed to multiple reasons, one of which can be a conserved trans-activation activity. Mutational analysis of the MAPK C-terminal domain at conserved residues may

Discussion

provide insights about how the MAPK C-terminus activates transcription. Candidates are the proline (P334^{AtMPK3}, P358^{AtMPK6}), the glutamic acid (E361^{AtMPK3}, E385^{AtMPK6}), or the phenylalanine residues (F340^{AtMPK3}, F364^{AtMPK6}), (F342^{AtMPK3}, F366^{AtMPK6}), (F344^{AtMPK3}, F368^{AtMPK6}).

3.4. Developmental phenotype of *Atmpk3 Atmpk6* double mutant was not complemented by *AtMPK3-GFP*

AtMPK3 and *AtMPK6* are involved in various signaling networks required for development and immunity (Bergmann et al., 2004; Wang et al., 2007; and Su et al., 2017). Both *AtMPK3* and *AtMPK6* have been identified as positive regulators of plant immunity. However, *Atmpk3* and *Atmpk6* single mutants did not present a strong immune phenotype (Beckers et al., 2009; and Su et al., 2017). Therefore, to evaluate the physiological function of the *AtMPK3/6* C-terminal domain, I required the *Atmpk3 Atmpk6* double mutant background. However, the *Atmpk3 Atmpk6* double mutant causes embryo lethality. Therefore I used the *Atmpk3 Atmpk6* (+/-), where developmental and seed production is not compromised (Wang et al., 2008).

When one allele of *AtMPK3* or *AtMPK6* is present in the *Atmpk3* (+/-) *mpk6* (-/-), or *Atmpk3* (-/-) *mpk6* (+/-) mutant backgrounds, the developmental phenotype is normal, and plants grow as WT. Nevertheless, *Atmpk3* (+/-) *mpk6* (-/-), is haplo-insufficient for ovule development, causing female sterility (Wang et al., 2008). This phenotype can be rescued through complementation with *AtMPK6* transgene, suggesting that female sterility is caused by a partial loss of function in of *AtMPK3* in an *Atmpk6* mutant background. Moreover, in response to wounding, the kinase activity of *AtMPK3* in *Atmpk3* (+/-) *mpk6* (-/-) background is compromised, suggesting interdependent kinase activity between *AtMPK3* and *AtMPK6* (Wang et al., 2008).

I transformed the *Atmpk3* (-/-) *Atmpk6* (+/-) plants with different transgenes of *AtMPK3*. I used the *AtMPK3-GFP*, *AtMPK3 ΔC-GFP*, and *AtMPK3 C-term-GFP* driven by the *AtMPK3* native promoter. Nevertheless, even full-length *AtMPK3prom::AtMPK3-GFP* failed to rescue the developmental embryo-lethal phenotype of *Atmpk3* (-/-) *Atmpk6* (-/-), and all obtained transgenic lines had one or two copies of *AtMPK6*. Considering that in the absence of *AtMPK6*, *AtMPK3* activity is compromised, the transgene *AtMPK3-GFP* was probably not sufficient to

rescue the embryo-lethal phenotype. Furthermore, considering that the transgenic lines were performed in *AtMPK3* transgenes tagged with green fluorescent protein (GFP), it is possible that the elongated GFP tag used had reduced *AtMPK3* activity, thereby the embryo-lethal phenotype was not rescued.

Without the complementation of *AtMPK3* full-length on *Atmpk3* (-/-) *Atmpk6* (-/-) background, it was not possible to evaluate the physiological function of the C-terminal domain in development or immunity. I wanted to complement *Atmpk3* (-/-) *Atmpk6* (+/-) mutant also with transgene sequences *AtMPK6-GFP*, *AtMPK6 ΔC-GFP*, and *AtMPK6 C-term-GFP* driven by the native promoter of *AtMPK6*. Nevertheless, I experienced cloning difficulties and could not obtain the *AtMPK6prom::AtMPK6-GFP* full-length and *AtMPK6prom::AtMPK6 ΔC-GFP*. I then generated only the transgenic lines with the *AtMPK6prom::AtMPK6 C-terminal-GFP* and obtained similar results as with the *AtMPK3prom::AtMPK3 C-term-GFP* transgenic lines (data not shown).

3.5. Concluding remarks and future perspectives

In plants, MAPKs *AtMPK3* and *AtMPK6* regulate immunity through phosphorylation of TFs and *AtCDKCs* thereby mediating transcriptional reprogramming (Meng and Zhang, 2013; Li et al., 2014; and Tsuda and Somssich, 2015). Nevertheless, transcriptional activation mediated by phosphorylation of *AtCDKCs* does not explain locus-specific regulations of gene expression. My study can potentially link these mechanisms through a molecular complex in which active MAPKs interacts with and phosphorylates TFs that target specific promoter regions, and recruit CDKCs through the MAPKs C-terminal domain. MAPKs then phosphorylate CDKCs that activate RNA-Pol II by phosphorylation. However, I could not detect an interaction between *AtMAPK3/6* C-terminal domain and *AtCDKC1/2* (data not shown). Thus, TF bound MAPK C-terminus may recruit another factor important for transcription at the locus. Studying this mechanism broadens the knowledge about MAPKs-mediated transcriptional reprogramming not only in plants, but also other eukaryotes as this mechanism is likely conserved in eukaryotes. This work provides the first evidence that plant MAPKs activates transcription through an evolutionarily conserved mechanism independent of their kinase activity across kingdoms.

Discussion

To understand the physiological function of these *AtMPK3* and *AtMPK6* C-terminal domains in immunity, one could transform the *AtMPK3/6* full-length, C-terminal deleted, and C-terminal domain expressed under their native promoter in the conditional *Atmpk3 Atmpk6* double mutant, *AtMPK3SR* and *AtMPK6SR* generated by Su et al., 2017. These transgenic plants behave like *Atmpk3 Atmpk6* double mutant plants in the presence of NA-PP1, which is a specific inhibitor of the modified MAPKs *AtMPK3SR* and *AtMPK6SR*. Thus, these transgenic lines will allow us to test the function of the *AtMPK3* and *AtMPK6* full-length, Δ C, and C-terminal domain in the presence of the inhibitor. MAPK functions in various biological processes such as development, pathogen resistance, and immune-related transcriptional reprogramming can be tested in a given tissue and time. Moreover, considering the importance of *AtMPK3/6* C-terminal domains, some pathogen effectors might bind and interfere with MAPK C-terminus.

4. Materials and Methods

4.1. Materials

4.1.1. Plant material and growth conditions

All transient expression assays were performed in *A. thaliana* accession Columbia-0 (Col-0) wild type (WT) plants. Seeds were stratified at 4°C in darkness for three days. Afterwards, seeds were sowed on moistured soil (Stender, Schermbeck Germany) and allowed to germinate under short day conditions (10 h light/ 14 h darkness, 23/20°C, 60% humidity) inside growth chambers. Posterior to germinations, seedlings were picked and transferred to 9 cm x 9 cm pots, and grown under the same conditions. Plants were sampled at a four-week stage for protoplasts assays, and five to six-week stage for particle bombardment assays.

4.1.2. Bacteria and Yeast material and growth conditions

To express the *At*MPKs, *Mp*MPKs, and non-plant MPKs for Y2H and transient expression assays *in planta*, numerous bacterial transformations were required. These transformations were performed in different bacteria and yeast genotypes depending on the assay (Table 3). *Escherichia coli* cells were grown in Luria-Bertani (LB) medium at 37°C for 16-20 h and with shaking at 190 rpm when grown in broth. *Agrobacterium tumefaciens* cells were grown in YEB medium at 28°C for two days, and in liquid culture at 220 rpm for 16-20 h. Yeast cells were grown in yeast extract-peptone-dextrose (YPD) media at 30°C for three days and with shaking at 220 rpm when grown in broth. Transformed *E. coli* and yeast cells were grown in selective media with antibiotics or nutrient deficiency, respectively, and according to the antibiotic resistance or reporter genes present on the plasmids.

Table 3: Bacteria and yeast strains used in this study

Organism	Strain	Resistance	Purpose
<i>Escherichia coli</i>	DH10B		Competent cells
	DB3.1		Competent cells
<i>Agrobacterium tumefaciens</i>	Gv3101 pMP90 RK	Rif / Gent / Kan	Competent cells
<i>Saccharomyces cerevisiae</i>	Y2H-GOLD		Competent cells
	L40		Competent cells

Materials and Methods

Table 4: Vectors used in this study

Vector name	Bacterial resistance	Purpose	Assay
pDONR207	Gent + Chlo	Generation of GATEWAY entry clones	
pDONR201	Kan	Generation of GATEWAY entry clones	
pENTR/D-TOPO	Kan	Generation of GATEWAY entry clones	
pGBKT7	Kan	Generation of GATEWAY destination vector containing GAL4-DBD at the N-terminal	Y2H
pBTM116	Amp	Generation of GATEWAY destination vector containing LexA-DBD at the N-terminal	Y2H
pGADT424	Amp	Generation of GATEWAY destination vector containing GAL4-AD at the N-terminal	Y2H
pGADT7-T	Amp	Y2H control, contains the Gal4 GAL4-AD and expresses <i>LEU2</i>	Y2H
pGBKT7-53	Kan	Y2H positive control, contains the GAL4-DBD expresses <i>TRP1</i>	Y2H
pGBKT7-Lam	Kan	Y2H negative control, contains the GAL4-DBD expresses <i>TRP1</i>	Y2H
p430T1.2	Amp	Generation of GATEWAY destination vector containing GAL4-DBD at the N-terminal	Dual luciferase transcriptional activation assay
pRLHSP	Amp	Transformation efficiency plasmid expressing <i>Renilla</i> luciferase under the 35S promoter	Dual luciferase transcriptional activation assay
pGAL_TATA_GL_HSP	Amp	Reporter plasmid with the GAL4-BS and luciferase (<i>LUC2</i>) from firefly	Dual luciferase transcriptional activation assay
pAM-PAT-HA	Amp	pAM-PAT GATEWAY compatible vector containing HA tag	Protein expression for dual luciferase activity assay
pE-SPYNE-GW	Amp	pE-SPYNE GATEWAY compatible vector containing the N-terminal YFP tag at the N-terminal	Biomolecular fluorescence complementation (BiFC) assays in <i>N. benthamiana</i>

pE-SPYCE-GW	Amp	pE-SPYNE GATEWAY compatible vector containing the C-terminal YFP tag at the N-terminal	Biomolecular fluorescence complementation (BiFC) assays in <i>N. benthamiana</i>
pXCSG-GFP	Amp	pXCSG GATEWAY compatible vector containing GFP tag under 35S promoter	Promoter activity assays with GUS reporter
pUC9 <i>promPropep2::GUS 2B</i>	Amp	<i>Arabidopsis thaliana</i> PROPEP2 promoter fused to GUS reporter gene (Logemann et al., 2013)	Promoter activity assays with GUS reporter
pUC9 <i>promPropep2::GUS 2B 5mut</i>	Amp	<i>Arabidopsis thaliana</i> mutated PROPEP2 promoter fused to GUS reporter gene (Logemann et al., 2013)	Promoter activity assays with GUS reporter
pTA7002 MKK4DD	Kan	<i>Arabidopsis thaliana</i> MKK4 T ₂₄₄ D and S ₂₃₀ D under the control of a steroid-inducible promoter (Dexamethasone) (Ren et al., 2002)	Promoter activity assays with GUS reporter
pXCG-GFP	Amp	Generation of transgenic lines under own promoter tagged with GFP vector contains BASTA resistance for selection in plants	Transgenic lines

Table 5: Vectors generated in this study

Name	Vector Backbone	Bacterial resistance	Purpose
pDONR207-MPK3 (1-370) pDONR207-MPK3 (1-185) pDONR207-MPK3 (1-241) pDONR207-MPK3 (1-333) pDONR207-MPK3 (186-241) pDONR207-MPK3 (186-333) pDONR207-MPK3 (186-370) pDONR207-MPK3 (334-370) pDONR207-MPK6 (1-395) pDONR207-MPK6 (1-197) pDONR207-MPK6 (1-264) pDONR207-MPK6 (1-357) pDONR207-MPK6 (198-264) pDONR207-MPK6 (198-357) pDONR207-MPK6(198-395) pDONR207-MPK6 (358-395)	pDONR207	Gent	Entry clones for transient assays in yeast and <i>in planta</i>
pGBKT7-GW-MPK3 (1-370) pGBKT7-GW-MPK3 (1-185) pGBKT7-GW.MPK3 (1-241)	pGBKT7	Kan	Destination vectors for Y2H assays for the

Materials and Methods

<p>pGBKT7-GW-MPK3 (1-333) pGBKT7-GW-MPK3 (186-241) pGBKT7-GW-MPK3 (186-333) pGBKT7-GW-MPK3 (186-370) pGBKT7-GW-MPK3 (334-370) pGBKT7-GW-MPK6 (1-395) pGBKT7-GW-MPK6 (1-197) pGBKT7-GW-MPK6 (1-264) pGBKT7-GW-MPK6 (1-357) pGBKT7-GW-MPK6 (198-264) pGBKT7-GW-MPK6 (198-357) pGBKT7-GW-MPK6(198-395) pGBKT7-GW-MPK6 (358-395)</p>			<p>GAL4 system Containing the GAL4-DBD at the N-terminal</p>
<p>pDEST-BTM116-MPK3 (1-370) pDEST-BTM116-MPK3 (1-185) pDEST-BTM116-MPK3 (1-241) pDEST-BTM116-MPK3 (1-333) pDEST-BTM116-MPK3 (186-241) pDEST-BTM116-MPK3 (186-333) pDEST-BTM116-MPK3 (186-370) pDEST-BTM116-MPK3 (334-370) pDEST-BTM116-MPK6 (1-395) pDEST-BTM116-MPK6 (1-197) pDEST-BTM116-MPK6 (1-264) pDEST-BTM116-MPK6 (1-357) pDEST-BTM116-MPK6 (198-264) pDEST-BTM116-MPK6 (198-357) pDEST-BTM116-MPK6(198-395) pDEST-BTM116-MPK6 (358-395)</p>	<p>pDEST-BTM116</p>	<p>Amp</p>	<p>Destination vectors for Y2H assays for the LexA system Containing the LexA-DBD at the N-terminal</p>
<p>pDONR201-MPK3 (T196A - Y198F) pDONR201 -MPK6 (T221A - Y223F)</p>	<p>pDONR201</p>	<p>Kan</p>	<p>Entry clones for transient assays <i>in planta</i>. Construct generated by Dr. Carolin Seyffert</p>
<p>pENTR -MYC2</p>	<p>pENTR/D-TOPO</p>	<p>Kan</p>	<p>Entry clones for transient assays <i>in planta</i>. Construct generated by Dr. Haitao Cui</p>
<p>pDONR207-MPK3 (53-89) pDONR207-MPK3 (137-173) pDONR207-MPK3 (271-301) pDONR207-MPK6 (162-199) pDONR207-MPK6 (358-395)</p>	<p>pDONR207</p>	<p>Gent</p>	<p>Entry clones for transient assays <i>in planta</i></p>
<p>p430T1.2-MYC2 p430T1.2-MPK3 (1-370) p430T1.2-MPK3 (T196A - Y198F) p430T1.2-MPK3 (1-333) p430T1.2-MPK3 (334-370) p430T1.2-MPK3 (53-89) p430T1.2-MPK3 (137-173) p430T1.2-MPK3 (271-301) p430T1.2-MPK6 (1-395) p430T1.2-MPK6 (T221A - Y223F) p430T1.2-MPK6 (1-357)</p>	<p>p430T1.2</p>	<p>Amp</p>	<p>Destination vectors for transient assays <i>in planta</i> containing the GAL4-DBD at the N-terminal</p>

p430T1.2-MPK6 (358-395) p430T1.2-MPK6 (162-199) p430T1.2-MPK6 (295-332)			
pDONR207 GAL4-BD pDONR207 GAL4-BD VP-16 pDONR207 GAL4-BD SRDX pDONR207 GAL4-BD MYC2 pDONR207 GAL4-BD MPK3 (53-89) pDONR207 GAL4-BD MPK3 (137-173) pDONR207 GAL4-BD MPK3 (271-301) pDONR207 GAL4-BD MPK3 (334-370) pDONR207 GAL4-BD MPK6 (162-199) pDONR207 GAL4-BD MPK6 (295-332) pDONR207 GAL4-BD MPK6 (358-395)	pDONR207	Gent	Entry clones for transient assays and protein expression <i>in planta</i>
pAM-PAT GAL4-BD HA pAM-PAT GAL4-BD VP-16 HA pAM-PAT GAL4-BD SRDX HA pAM-PAT GAL4-BD MYC2 HA pAM-PAT GAL4-BD MPK3 (53-89) HA pAM-PAT GAL4-BD MPK3 (137-173) HA pAM-PAT GAL4-BD MPK3 (271-301) HA pAM-PAT GAL4-BD MPK3 (334-370) HA pAM-PAT GAL4-BD MPK6 (162-199) HA pAM-PAT GAL4-BD MPK6 (259-332) HA pAM-PAT GAL4-BD MPK6 (358-395) HA	pAM-PAT-HA	Amp	Destination vectors for transient assays and protein expression <i>in planta</i>
pENTR MPK1C-ter pENTR MPK2C-ter pENTR MPK4C-ter pENTR MPK5C-ter pENTR MPK7C-ter pENTR MPK10 C-ter pENTR MPK11C-ter pENTR MPK12C-ter pENTR MPK13C-ter pENTR MPK14C-ter pENTR MpMPK1C-ter pENTR MpMPK2C-ter pENTR ERK1C-ter pENTR ERK2C-ter pENTR p38C-ter	pENTR/D-TOPO	Kan	Entry clones for transient assays expression <i>in planta</i> (Evolutionary Conserved MAPKs)

Materials and Methods

pENTR FUS3C-ter			
p430T1.2 MPK1C-ter p430T1.2 MPK2C-ter p430T1.2 MPK4C-ter p430T1.2 MPK5C-ter p430T1.2 MPK7C-ter p430T1.2 MPK10 C-ter p430T1.2 MPK11C-ter p430T1.2 MPK12C-ter p430T1.2 MPK13C-ter p430T1.2 MPK14C-ter p430T1.2 MpMPK1C-ter p430T1.2 MpMPK2C-ter p430T1.2 ERK1C-ter p430T1.2 ERK2C-ter p430T1.2 p38C-ter p430T1.2 FUS3C-ter	p430T1.2	Amp	Destination vectors for transient expression assays <i>in planta</i> containing the GAL4-BD at the N-terminal (Evolutionary Conserved MAPKs)
pE-SPYCE MPK3 (1-370) pE-SPYCE MPK3 (334-370) pE-SPYCE MPK6 (1-395) pE-SPYCE MPK6 (358-395)	pE-SPYCE	Amp	Biomolecular fluorescence complementation (BiFC) assays in <i>N. benthamiana</i>
pDONR 201 WRKY33 pXGSG WRKY33 GFP pAM-PAT MPK3 HA	pDONR201 pXCSG pAM-PAT-HA	Kan Amp Amp	Promoter activity assays with GUS reporter
pDONR207 <i>AtMPK3prom::AtMPK3-GFP</i> pDONR207 <i>AtMPK3prom::AtMPK3 ΔC-GFP</i> pDONR207 <i>AtMPK3prom::AtMPK3 C-term-GFP</i> pDONR207 <i>AtMPK6prom::AtMPK6 C-term-GFP</i>	pDONR207	Gent	Entry clones for transgenic lines
pXCG <i>AtMPK3prom::AtMPK3-GFP</i> pXCG <i>AtMPK3prom::AtMPK3 ΔC-GFP</i> pXCG <i>AtMPK3prom::AtMPK3 C-term-GFP</i> pXCG <i>AtMPK6prom::AtMPK6 C-term-GFP</i>	pXCG-GFP	Amp/Carb	Destination vectors for transgenic lines with BASTA resistance. Transformation in <i>A. tumefaciens</i>

4.1.3. Primer information

Primers used for amplification of planta and non-plant MAPKs coding sequence (CDS), promoter sequences of *AtMPK3* and *AtMPK6* and *AtWRKY33* are described in Table 6. In addition, primers for cloning confirmation via sequencing are described in Table 7.

Table 6: List of primers used in this study for PCR amplification

Insert	Sequence Forward	Sequence Reverse
MPK3(1-370)	GGGGACAAGTTTGTACAAAAAAGCAGGCT TCATGAACACCGGCGGTGGCCAATACACG	GGGGACCACTTTGTACAAGAAAGCTGGG TTCTAACCGTATGTTGGATTGAGTGCTAT
MPK3(1-185)	GGGGACAAGTTTGTACAAAAAAGCAGGCT TCATGAACACCGGCGGTGGCCAATACACG	GGGGACCACTTTGTACAAGAAAGCTGGG TTCAAAGACCGAAAATCACAAATCTTTA AATC
MPK3(1-241)	GGGGACAAGTTTGTACAAAAAAGCAGGCT TCATGAACACCGGCGGTGGCCAATACACG	GGGGACCACTTTGTACAAGAAAGCTGGG TTCAACCAGGGAACAAAGGCTTTCTATT CAT
MPK3(1-333)	GGGGACAAGTTTGTACAAAAAAGCAGGCT TCATGAACACCGGCGGTGGCCAATACACG	GGGGACCACTTTGTACAAGAAAGCTGGG TTCTCATCATTGCGGTCGTGCAATTTAGC AAG
MPK3(186-241)	GGGGACAAGTTTGTACAAAAAAGCAGGCT TCGCTAGACCTACTTCAGAGAATGATTTT	GGGGACCACTTTGTACAAGAAAGCTGGG TTCAACCAGGGAACAAAGGCTTTCTATT CAT
MPK3(186-333)	GGGGACAAGTTTGTACAAAAAAGCAGGCT TCGCTAGACCTACTTCAGAGAATGATTTT	GGGGACCACTTTGTACAAGAAAGCTGGG TTCTCATCATTGCGGTCGTGCAATTTAGC AAG
MPK3(186-370)	GGGGACAAGTTTGTACAAAAAAGCAGGCT TCGCTAGACCTACTTCAGAGAATGATTTT	GGGGACCACTTTGTACAAGAAAGCTGGG TTCTAACCGTATGTTGGATTGAGTGCTAT
MPK3(334-370)	GGGGACAAGTTTGTACAAAAAAGCAGGCT TCCAATCTGTCAAAAAGCCATTCTTTTT	GGGGACCACTTTGTACAAGAAAGCTGGG TTCTAACCGTATGTTGGATTGAGTGCTAT
MPK6(1-395)	GGGGACAAGTTTGTACAAAAAAGCAGGCT TCATGGACGGTGGTTCAGGTCAACCGGCG	GGGGACCACTTTGTACAAGAAAGCTGGG TTCTATTGCTGATATTCTGGATTGAAAGC
MPK6(1-197)	GGGGACAAGTTTGTACAAAAAAGCAGGCT TCATGGACGGTGGTTCAGGTCAACCGGCG	GGGGACCACTTTGTACAAGAAAGCTGGG TTTCAGTTCAGGAGGAGATTACTTGGTTT CAA
MPK6(1-264)	GGGGACAAGTTTGTACAAAAAAGCAGGCT TCATGGACGGTGGTTCAGGTCAACCGGCG	GGGGACCACTTTGTACAAGAAAGCTGGG TTTCAGAAGAGTGGCTTACGGTCCATTA ACTC
MPK6(1-357)	GGGGACAAGTTTGTACAAAAAAGCAGGCT TCATGGACGGTGGTTCAGGTCAACCGGCG	GGGGACCACTTTGTACAAGAAAGCTGGG TTCTCATCGTTATGTCGTGCAACGAGTT CAG
MPK6(198-264)	GGGGACAAGTTTGTACAAAAAAGCAGGCT TCGCAAACCTGCGACCTAAAAATCTGCGAT	GGGGACCACTTTGTACAAGAAAGCTGGG TTTCAGAAGAGTGGCTTACGGTCCATTA ACTC
MPK6(198-357)	GGGGACAAGTTTGTACAAAAAAGCAGGCT TCGCAAACCTGCGACCTAAAAATCTGCGAT	GGGGACCACTTTGTACAAGAAAGCTGGG TTCTCATCGTTATGTCGTGCAACGAGTT CAG
MPK6(198-395)	GGGGACAAGTTTGTACAAAAAAGCAGGCT TCGCAAACCTGCGACCTAAAAATCTGCGAT	GGGGACCACTTTGTACAAGAAAGCTGGG TTCTATTGCTGATATTCTGGATTGAAAGC

Materials and Methods

MPK6(358-395)	GGGGACAAGTTTGTACAAAAAAGCAGGCT TCCCAGATGTACAATACCTTTCAACTTT	GGGGACCACTTTGTACAAGAAAGCTGGG TTCTATTGCTGATATTCTGGATTGAAAGC
MPK3(53-89)	GGGGACAAGTTTGTACAAAAAAGCAGGCT TCTGCTCTGTGTTGGATACGGAG	GGGGACCACTTTGTACAAGAAAGCTGGG TCAAGAAGCTTGATCTCACGAAG
MPK3(137-173)	GGGGACAAGTTTGTACAAAAAAGCAGGCT TCTCAGAAGAACACTGTCAGTA	GGGGACCACTTTGTACAAGAAAGCTGGG TCGTTCAACAGAAGATTGCTCG
MPK3(271-301)	GGGGACAAGTTTGTACAAAAAAGCAGGCT TCGCGAAAAGATACATCCGGCAA	GGGGACCACTTTGTACAAGAAAGCTGGG TCAAACGTCAACATTCTGTCAAC
MPK6(162-199)	GGGGACAAGTTTGTACAAAAAAGCAGGCT TCTCCGAAGAACATTGCCAGTAT	GGGGACCACTTTGTACAAGAAAGCTGGG TCTGCGTTCAGGAGGAGATTACT
MPK6(358-395)	GGGGACAAGTTTGTACAAAAAAGCAGGCT TCGCAAAGCGATACATAAGACAG	GGGGACCACTTTGTACAAGAAAGCTGGG TCATCAAATGTTAACATCTTCTC
GAL4-BD	GGGGACAAGTTTGTACAAAAAAGCAGGCT TCATGAAGCTACTGTCTTCTATCGAA	GGGGACCACTTTGTACAAGAAAGCTGGG TTCGATACAGTCAACTGTCTTTG
GAL4-BD VP-16	GGGGACAAGTTTGTACAAAAAAGCAGGCT TCATGAAGCTACTGTCTTCTATCGAA	GGGGACCACTTTGTACAAGAAAGCTGGG TTCCACCGTACTCGTCAATTCC
GAL4-BD SRDX	GGGGACAAGTTTGTACAAAAAAGCAGGCT TCATGAAGCTACTGTCTTCTATCGAA	GGGGACCACTTTGTACAAGAAAGCTGGG TTAGCGAAACCCAAACGGAGTTC
GAL4-BD MYC2	GGGGACAAGTTTGTACAAAAAAGCAGGCT TCATGAAGCTACTGTCTTCTATCGAA	GGGGACCACTTTGTACAAGAAAGCTGGG TTACCGATTTTTGAAATCAAAC
GAL4-BD MPK3 (53-89)	GGGGACAAGTTTGTACAAAAAAGCAGGCT TCATGAAGCTACTGTCTTCTATCGAA	GGGGACCACTTTGTACAAGAAAGCTGGG TCAAGAAGCTTGATCTCACGAAG
GAL4-BD MPK3 (137-173)	GGGGACAAGTTTGTACAAAAAAGCAGGCT TCATGAAGCTACTGTCTTCTATCGAA	GGGGACCACTTTGTACAAGAAAGCTGGG TCGTTCAACAGAAGATTGCTCG
GAL4-BD MPK3 (271-301)	GGGGACAAGTTTGTACAAAAAAGCAGGCT TCATGAAGCTACTGTCTTCTATCGAA	GGGGACCACTTTGTACAAGAAAGCTGGG TCAAACGTCAACATTCTGTCAAC
GAL4-BD MPK3 (334-370)	GGGGACAAGTTTGTACAAAAAAGCAGGCT TCATGAAGCTACTGTCTTCTATCGAA	GGGGACCACTTTGTACAAGAAAGCTGGG TTCTAACCGTATGTTGGATTGAGTGCTAT
GAL4-BD MPK6 (162-199)	GGGGACAAGTTTGTACAAAAAAGCAGGCT TCATGAAGCTACTGTCTTCTATCGAA	GGGGACCACTTTGTACAAGAAAGCTGGG TCTGCGTTCAGGAGGAGATTACT
GAL4-BD MPK6 (295-332)	GGGGACAAGTTTGTACAAAAAAGCAGGCT TCATGAAGCTACTGTCTTCTATCGAA	GGGGACCACTTTGTACAAGAAAGCTGGG TCATCAAATGTTAACATCTTCTC
GAL4-BD MPK6 (358-395)	GGGGACAAGTTTGTACAAAAAAGCAGGCT TCATGAAGCTACTGTCTTCTATCGAA	GGGGACCACTTTGTACAAGAAAGCTGGG TCATCAAATGTTAACATCTTCTC

MPK1C-ter	CACCCCTCCTGCTCAAGTTCCTATCGATCT CGATGTAGATGAGGATTTGAGAGAGGAGA TGATAAGAGAAATGATGTGGA	GAGCTCAGTGTTTAAAGTTGAAGCTTGT GGATGGTAGTGAAGCATCTCATTCCACA TCATTCTCTATCATCTCCTCTC
MPK2C-ter	CACCCCTCCTGCTCAAGTTCCTATTGATCTC GATGTAGATGAAGACGAGGATTTGGGAGC AGAGATGATAAGAGAATTA	AAACTCAGAGACCTCATTGTTGTTTATGG TAGCAGCTTCTGGATGATAATGAATCATT TCCTCCACATTAATTCTCTTATCATCTCT GC
MPK4C-ter	CACCCCGGTATGTGTGAGGCCGTTCAATTT TGATTCGAGCAACCTACTTTGACAGAAGA GAACATTAAGGAGCTTATAT	CACTGAGTCTTGAGGATTGAACTTGACT GTTTCACGGTATATAAGCTCCTTAATGTT CTCTTCTGTCAAAGTAGGTTGCT
MPK5C-ter	CACCCCTGTTTGTTCACCAACCTTTCAGTTTC CATTTTGAGGATCCGTCTTCCACTGAAGAA GAGATAAAGGAGCTTGTGT	AATGCTCGGCAGAGGATTGAACTTCACA GATTCGAGCCACACAAGCTCCTTATCTC TTCTTCAGTGAAGACGGATCCT
MPK7C-ter	CACCCCGCTGCACATGTCCCAATCTCTCT GGACATAGATGAAAACATGGAGGAACCAG TGATAAGAGAGATGATGTGGA	GGCATTGAGATTCAGCTTCAGGGTGGT AATAAAGCATCTCATTCCACATCATCTCT CTTACTACTGGTTCTCCATGT
MPK10 C-ter	CACCCAGAGTGCTCAGAGCCTTCAATTT CGATTTAGATGAACATCCATTCTCTGAGGA GCAGTTTAGAGAGTTAATCT	ATCATTGCTGGTTTACAGGTTGAAAGCTA GGGCTTCACAGTAGATTAACCTCTCTAAA CTGCTCCTCAGAGAATGGATGTT
MPK11C-ter	CACCCCTGTGTGTGTGAGACCGTTCCATTT TGATTCGAGCAACCTTCATTGACGGAAGA GAACATCAAGGAGCTTATAT	AGGGTAAACTTGACTGATTACAGATAT ATAAGCTCCTTGATGTTCTCTCCGTCAA TGAAGGTTGCTCGAAATCAAAAT
MPK12C-ter	CACCCCGTCTGTTCGACTCCTTTAGCTTT GATTCGAACATCTTCTTGCACAGAAGAA CACATAAAGGAGCTTATCT	AAAGTGGTCAGGATTGAATTTGACAGAC TCCTTGTAGATAAGCTCCTTATGTGTTC TTCTGTGCAAGAAGGATGTTTCA
MPK13C-ter	CACCCCAACATGTCCTACTCCTTTAGCTTT GACTTTGAGGAGACAGCCTTAGATGAACA AGACATCAAGGAGCTTGTCT	CATATTCTTGAAGTGTAAGACTCTCTCC AGACAAGCTCCTTGATGTCTTGTTCATCT AAGGCTGTCTCTCAAAGTCAA
MPK14C-ter	CACCCCGTCGGAAAATGTTCCGGTCAGTAG TTTGAGATAGATGAGAACATGGAAGGAG ATATGATCAGGGAGATGATGT	AGCTCGGGGGAGGTAATGAAGCATCTCT TCCCACATCATCTCCCTGATCATATCTCC TTCCATGTTCTCATCTATCTCCA
MpMPK1C-ter	CACCCCGCTGCCACGCCCTTTTGTGATT TGATTTGAGCAGCCCTCGTTTACTGAGGA ACACATTAAGGAGCTGATTA	TTGCATCATGTCTGGTAGGGGATTGAAC GCAAGAGCTTCCATCATAATCAGCTCCTT AATGTGTTCTCAGTAAACGAGG
MpMPK2C-ter	CACCCCATCAGCGCCAGCACCGTTTGAATT CGATTTGAGGACGAGGATTTGAAGGAGG ACGCCTTGAGGGAGAAGGTGT	CACTGCCTCATTAGCTGCCTCCGGATGAT AAAACAGCATCTCATTCCACACCTTCTCC CTCAAGGCGTCTCCTTCAAAT
ERK1C-ter	CACCCAGTGCCGAGGAGCCCTTACCTT CGCCATGGAGCTGGATGACCTACCTAAGG AGCGGCTGAAGGAGCTCATCT	GGGGCCTCCAGCACTCCGGGCTGGAAG CGTGCTGTCTCCTGGAAGATGAGCTCCTT CAGCCGCTCCTTAGGTAGGTCAT
ERK2C-ter	CACCCCATCGCCGAAGCACCATTCAGTT CGACATGGAATTTGATGACTTGCCTAAGG AAAAGCTCAAAGAATAATTT	AGATCTGTATCCTGGCTGGAATCTAGCA GTCTCTTCAAAAATTAGTCTTTGAGCTT TTCTTAGGCAAGTCATCCAATT
p38C-ter	CACCCAGTGCCGATCCTTATGATCAGTC CTTTGAAAAGCAGGGACCTCTTATAGATGA GTGGAAAAGCCTGACCTATG	GGACTCCATCTCTTCTGGTCAAGGGGTG GTGGCACAAGCTGATGACTTCATCATA GGTCAGGCTTTTCCACTCATCTA
FUS3C-ter	CACCCCTGAAGCGAACCCATCCACCCA GCTTCTTCGAGTTTGTACTACTACAAGGAGG CACTAACGACGAAAGACCTCA	ACTAAATATTTCTGTTCCAAATGAGTTTCT TGAGGCTTTTCGTCGTTAGTGCCTCCTTG TAGTGATCAAACCTCGAAGAAGC
WRKY33	GGGGACAAGTTTGTACAAAAAAGCAGGCT TCATGGCTGCTTCTTTTCTTACAATG	GGGGACCACTTTGTACAAGAAAGCTGGG TTGGCATAAACGAATCGAAAAA

Materials and Methods

<i>MPK3prom</i> for fusion with MPK3 (1-370)	GGGGACAAGTTTGTACAAAAAAGCAGGCT TCGAATTCGATAGGCTAATGAGC	TTGGCCACCGCCGGTGTTCATTTCTCTCT CAATTGATCAAAG
MPK3 (1-370) for fusion with <i>MPK3prom</i>	CTTTGATCAATTGAGAGAGAAATGAACAC CGGCGGTGGCCAA	GGGGACCACTTTGTACAAGAAAGCTGGG TTCTAACCGTATGTTGGATTGAGTGCTAT
<i>MPK3prom</i> for fusion with MPK3 (1-333)	GGGGACAAGTTTGTACAAAAAAGCAGGCT TCGAATTCGATAGGCTAATGAGC	TTGGCCACCGCCGGTGTTCATTTCTCTCT CAATTGATCAAAG
MPK3 (1-333) for fusion with <i>MPK3prom</i>	CTTTGATCAATTGAGAGAGAAATGAACAC CGGCGGTGGCCAA	GGGGACCACTTTGTACAAGAAAGCTGGG TTCTCATCATTCGGGTCGTGCAATTTAGC AAG
<i>MPK3prom</i> for fusion with MPK3 (334-370)	GGGGACAAGTTTGTACAAAAAAGCAGGCT TCGAATTCGATAGGCTAATGAGC	TTGGCCACCGCCGGTGTTCATTTCTCTCT CAATTGATCAAAG
MPK3 (334-370) for fusion with <i>MPK3prom</i>	CTTTGATCAATTGAGAGAGAACCAATCTGT CAAAAGCCATTCTCTTTT	GGGGACCACTTTGTACAAGAAAGCTGGG TTCTAACCGTATGTTGGATTGAGTGCTAT
<i>MPK6prom</i> for fusion with MPK6 (1-395)	GGGGACAAGTTTGTACAAAAAAGCAGGCT TCGTCCGGTTACAGAGATCTCAC	TTGACCTGAACCACCGTCCATGACCGGT AAAGATGAAAGCTT
MPK6 (1-395) for fusion with <i>MPK6prom</i>	AAGCTTTCATCTTTACCGGTCATGGACGGT GGTTCAGGTCAA	GGGGACCACTTTGTACAAGAAAGCTGGG TTCTATTGCTGATATTCTGGATTGAAAGC
<i>MPK6prom</i> for fusion with MPK6 (1-357)	GGGGACAAGTTTGTACAAAAAAGCAGGCT TCGTCCGGTTACAGAGATCTCAC	TTGACCTGAACCACCGTCCATGACCGGT AAAGATGAAAGCTT
MPK6 (1-357) for fusion with <i>MPK6prom</i>	AAGCTTTCATCTTTACCGGTCATGGACGGT GGTTCAGGTCAA	GGGGACCACTTTGTACAAGAAAGCTGGG TTCTCATCGTTATGTCGTGCAACGAGTT CAG
<i>MPK6prom</i> for fusion with MPK6 (358-395)	GGGGACAAGTTTGTACAAAAAAGCAGGCT TCGTCCGGTTACAGAGATCTCAC	TTGACCTGAACCACCGTCCATGACCGGT AAAGATGAAAGCTT
MPK6 (358-395) for fusion with <i>MPK6prom</i>	AAGCTTTCATCTTTACCGGTCCAGAGTGT ACAATACCTTTCAACTTT	GGGGACCACTTTGTACAAGAAAGCTGGG TTCTATTGCTGATATTCTGGATTGAAAGC

Table 7: List of primers used for sequencing

Name	Primer	Purpose
SeLA SeLB	TCGCGTTAACGCTAGCATGGATCTC GTAACATCAGAGATTTTGAGACAC	Sequencing pDONR207
M13_F M13_R	CGTTGTAAAACGACGGCCAGT CAGGAAACAGCTATGACCATG	Sequencing pENRT/C-TOPO
35Spro_F NosTer_R	CGCACAATCCCACTATCCTT TGCGCGCTATATTTTGTTTTC	Sequencing p430T1.2
35Spro_F 35Ster_Rev	CGCACAATCCCACTATCCTT AGCGAAACCCTATAAGAA	Sequencing pAM-PAT-HA

4.1.4. Chemicals, and kits

Table 8: List of chemicals used during this study

Chemicals	Company
1,4-Dithiothreitol (DTT)	Roth(Karlsruhe; Germany)
3-Amino-1,2,4-triazole (3AT)	Sigma-Aldrich (Steinheim; Germany)
Adenine (A)	Sigma-Aldrich (Steinheim; Germany)
Ampicillin (Amp) 100 µg/ml	Duchefa Biochemie (Haarlem; Netherlands)
Anti-Rabbit IgG (A6154)	Sigma-Aldrich (Steinheim; Germany)
Bovine Serum Albumin (BSA)	Biomol (Hamburg; Germany)
Calcium Chloride Dihydrat	Roth(Karlsruhe; Germany)
Carbenicillin (Carb) 100 mg/l	Duchefa (Haarlem; Netherlands)
Cellulase Onozuka R-10 from <i>Trichoderma viride</i>	SERVA (Heidelberg; Germany)
Chloramphenicol (Chlo) 25 µg/ml	Sigma-Aldrich (Steinheim; Germany)
D-Mannitol	Sigma-Aldrich (Steinheim; Germany)
Gentamycin (Gent) 20 mg/l	Duchefa (Haarlem; Netherlands)
Glycine	Roth(Karlsruhe; Germany)
HA-tag (C29F4)	Cell Signaling
Histidine (H)	Sigma-Aldrich (Steinheim; Germany)
Kanamycin (Kan) 50 mg/l	Duchefa (Haarlem; Netherlands)
Leucine (L)	Sigma-Aldrich (Steinheim; Germany)
Macerozyme R-10 from <i>Rhizopus</i> sp.	SERVA (Heidelberg; Germany)
MES	Duchefa Biochemie (Haarlem; Netherlands)
MgCl ₂	Merck (Darmstadt; Germany)
Poly(ethylen glycol) 4000	Sigma-Aldrich (Steinheim; Germany)
Rifampicin (Rif) 40 mg/l	Sigma-Aldrich (Steinheim; Germany)
Sodium Chloride (NaCl)	Merck (Darmstadt; Germany)
Sperm Salmon	Invitrogen
Spermidine	Sigma-Aldrich (Steinheim; Germany)
TritonX	Sigma-Aldrich (Steinheim; Germany)
Tryptophan (W)	Sigma-Aldrich (Steinheim; Germany)
Tween 20	Sigma-Aldrich (Steinheim; Germany)
X-α-gal	Clontech

Table 9: Kits used in this study

Kit	Company
pENTER™/D-TOPO Cloning kit	Invitrogen
NucleoSpin Plasmid	Macherey-Nagel

Materials and Methods

NucleoSpin Gel and PCR Clean-up	Macherey-Nagel
NucleoBond PC500	Macherey-Nagel
GATEWAY LR clonase II	ThermoFisher Scientific
GATEWAY BP clonase II	ThermoFisher Scientific
Dual-Luciferase Reporter Assay System	Promega

4.1.5. Media, buffers and solutions

Table 10: Media used for bacteria and yeast growth

Media	Components
Luria-Bertani (LB) pH 7.0 For liquid medium do not add agar	1% (w/v) trypton 1% (w/v) NaCl 0.5% (w/v) yeast extract 1.5% (w/v) agar Autoclave and add the Antibiotics
SD (Minimal Synthetic Defined) pH 5.8 For liquid medium do not add agar	0.67% (w/v) Yeast nitrogen base without amino acids 0.06% (w/v) -Ade/-His/-Trp/-Leu DO supplement 0.002% (w/v) Amino Acid (-Ade/-His/-Trp/-Leu) 2% (w/v) bacto agar Autoclave and add 2% (w/v) Glucose If necessary add after autoclave X- α -gal (0.001% (v/v) form the stock) 3AT for the concentration required
YPD (A) pH 6.5 For liquid medium do not add agar	2% (w/v) peptone 1% (w/v) yeast extract 0.003% (w/v) Adenine hemisulfate 2% (w/v) bacto agar Autoclave and add 2% (w/v) Glucose
YEB For liquid medium do not add agar	5 g/l beef extract 1 g/l yeast extract 5 g/l peptone 5 g/l sucrose 0.5 g/l MgCl ₂ 1.5% (w/v) Agar Autoclave

Table 11: Solutions and buffers used in this study

Solution and buffers	Components	Protocol
Glucose (D-glucose monohydrate)	40% (w/v) Glucose Solubilized in H ₂ O (sterile) Vacuum Filter (Micropore 0.22 µm) and store at 4°C	Y2H
TE Buffer (pH 8.0)	10 mM Tris-HCl (pH 8.0, 25°C) 1 mM EDTA (pH 8.0) Autoclave	
10X TE Buffer (pH 7.5)	0.1 M Tris-HCl (pH 7.5, 25°C) 10 mM EDTA (pH 8.0) Autoclave	
10X LiAc	1M LiAc (adjust to pH 6.8 by CH ₃ COOH) Autoclave	
PEG 4000	50% (w/v) PEG 4000 Solubilized in H ₂ O Autoclave	
1.1X TE/LiAc Solution	1.1 ml 10X TE 1.1 ml 10X LiAc 8.2 ml H ₂ O (sterile)	
PEG/LiAc Solution	8 ml 50% PEG 4000 1 ml 10X LiAc 1 ml 10X TE buffer	
3-Amino-1,2,4-triazole (3AT)	1 M 3AT Solubilized in H ₂ O (sterile) Vacuum Filter (Micropore 0.22 µm) and stored at 4°C in the dark	
X-α-gal (Clontech)	200% (w/v) X-α-gal Solubilized in dimethylformamide (DMF) Stored at 4°C in the dark in a glass bottle	
60 mg/ml Gold/Tungsten particles	60 mg of Gold/Tungsten particles (Bio- Rad) Wash twice with 1 ml of 100% EtOH Resuspend in 1 ml 50% Glycerol	
2.5 M CaCl ₂	2.5 M CaCl ₂ dissolved in Milli-Q water	
0.1 M Spermidine	0.1 M Spermidine (Sigma) dissolved in Milli-Q water	
Enzyme solution for Protoplasts digestion	1.5% (w/v) Cellulase Onozuka R-10 from <i>Trichoderma viride</i> 0.4% (w/v) Macerozyme R-10 from <i>Rhizopus</i> sp. 0.4 M Mannitol 20 mM KCl 20 mM MES pH 5.7 Warm solution at 55°C for 10 min, and cool at room temperature 10 mM CaCl ₂ 0.1% BSA	Protoplasts Preparation

Materials and Methods

W5 solution (Protoplasts)	2 mM MES pH 5.7 154 mM NaCl 125 mM CaCl ₂ 5 mM KCL	
MMG solution (Protoplasts)	4 mM MES pH 5.7 0.4 M Mannitol 15 mM MgCl ₂	
PEG-calcium transfection (Protoplasts)	40% (w/v) PEG4000 0.2 M Mannitol 100 mM CaCl ₂	
PLB (Protein extraction for Dual Luciferase assay-Promega)	25 mM Tris-phosphate pH 7.8 2 mM DTT 2 mM 1,2-diaminocyclohexane-N,N,N',N'-tetraacetic acid 10% Glycerol 1% Triton	Protein Extraction
Laemmli buffer (4x) (Protein extraction for WB)	4.4 ml H ₂ O 1 ml Stacking gel buffer 0.5 M Tris-HCl pH 6.8 0.7 ml 100% Glycerol 1.6 ml 10% SDS 1.186 g DTT (154 mg/ml) Spatula tip bromophenol blue	
Separating gel buffer	1.5 M Tris-HCl (pH 6.8) 0.3% (w/v) SDS	WB
Stacking gel buffer	0.5 M Tris-HCl (pH 6.8) 0.3% (w/v) SDS	
SDS-PAGE running buffer	192 mM Glycin 25 mM Tris-HCl (pH 8.3) 0.1% (w/v) SDS	
TBS-T	20 mM Tris-HCl (pH 7.6) 137 mM NaCl 0.05% (v/v) Tween-20	
Transfer (blotting) buffer	25 mM Tris-HCl (pH 8.0) 192 mM Glycin 0.1% (v/v) SDS 20% (w/v) Methanol	
Coomassie staining solution	2.5 g Coomassie Brilliant Blue R250 100 ml Acetic Acid 400 ml Methanol 500 ml H ₂ O MilliQ	
Coomassie destaining solution	450 ml H ₂ O MilliQ 450 ml Methanol 100 ml Acetic Acid	

4.2. Methods

4.2.1. Cloning of MAPKs for Y2H and transient assays *in planta*

The deletion constructs of *AtMPK3* and *AtMPK6* used for Y2H and transient assays in protoplasts mentioned from Figure 3 to Figure 10, were amplified with specific primers (Table 6) that contained the attB1 (primer forward), and attB2 (primer reverse) sequences for GATEWAY cloning. PCR amplification was performed with PrimeSTAR HS DNA Polymerase (TAKARA BIO INC) for a final volume of 20 μ l per reaction as described in Table 12.

Table 12: PrimeSTAR HS Takara master mix

Compound	Volume
5X PrimeSTAR Buffer	4 μ l
dNTPs Mixture (2.5 mM each)	2 μ l
0.2 μ M Primer Forward	2 μ l
0.2 μ M Primer Reverse	2 μ l
Prime STAR HS DNA Polymerase (2.5 U/ μ l)	0.2 μ l
Template	<200 ng
Sterilized distilled water	up to 20 μ l

Two different PCR programs were used to optimize the reaction according to the expected fragment size (Table 13). Fragments <500 base pairs (bp) had an increase in the annealing temperature and elongation time in comparison with the program used for fragments >500 bp of length.

Table 13: PCR Program for *AtMPK3* and *AtMPK6* deletion constructs

Program for <500 bp			Program for >500 bp		
Initial denaturation	98°C	2 min	Initial denaturation	98°C	2 min
Denaturation	98°C	10 s	Denaturation	98°C	10 s
Annealing	60°C	20 s	Annealing	55°C	20 s
Extension	72°C	20 s	Extension	72°C	80 s
Final Extension	72°C	3 min	Final Extension	72°C	3 min

35 cycles

The PCR product was loaded on 1% agarose gel and ran electrophoresis at 120 V for 35 min for fragment size confirmation. The bands with the correct fragments were excised and

Materials and Methods

cleaned with the NucleoSpin® Gel and PCR kit (Macherey-Nagel). The sixteen different MPK fragments obtained from PCR amplification were cloned into the entry vector pDONR207 with BP Clonase II enzyme from Invitrogen. The reaction mix was performed as recommended by the company and incubated for a period of two hours at room temperature (RT). Subsequently, 1 µl of proteinase K was added and incubated for 10 min at 37°C to terminate the reaction.

A total of 50 µl of *E. coli* DH10B chemical competent cells were transformed with 2.5 µl of the cloning reaction. Cells remained in ice with the cloning reaction for 10 min. Afterwards, heat-shock treatment of 42°C for 40 s was performed, and the cells were immediately placed on ice for 2 min. The heat-shock generates pores in the cell membrane making it amenable to the entrance of exogenous plasmids, immediate incubation in ice allows the cell recovery and closing of the pores at the membrane surface. Then 500 µl of LB medium without antibiotics was added and cells were incubated at 37°C for one hour to allow the cells to replicate. Finally, 100 µl of the culture was plated in LB medium with Gent (20 mg/l) for selection and incubated at 37°C overnight. Positive clones were confirmed through plasmid sequencing. For plasmid isolation, positive colonies from each transformation were selected and grown in LB broth at 37°C overnight while shaking at 190 rpm. Then, the cells were harvested and plasmids were isolated with the NucleoSpin Plasmid kit (Macherey-Nagel). Afterwards, they were sequenced with SeLA and SeLB primers (Table 7). Results were analyzed through BioEdit for sequence alignment and SeqBuilder from DNASTAR Lasergen 8 software.

Entry vectors were then cloned into the destination vectors pGBKT7 (GAL4-DBD), pDEST-pBTM116 (LexA-DBD), and p430T1.2 with the LR Clonase II enzyme from Invitrogen as prescribed by the manufacturer. Incubation and termination of the enzyme activity were performed with Proteinase K. *E. coli* (DH10B) transformations were performed as described previously. An aliquot of 100 µl of each transformation reaction was plated on LB medium with antibiotics for selection and incubated at 37°C overnight. Cells that were transformed with pGBKT7 were grown in LB with Kan (50 µg/ml) and the ones with pDEST-pBTM116 and p403T1.2 in LB with Amp (100 µg/ml). Positive colonies were picked and grown in LB broth with the respective antibiotics overnight, followed by plasmid isolation and sequencing for confirmation with primers 35Spro_F and NosTer_R (Table 7). Results were analyzed through BioEdit for sequence alignment and SeqBuilder from DNASTAR Lasergen 8 software.

Protein accumulation assays (Figure 10) required the generation of new entry vectors containing the GAL4-DBD-MPKs sequences. To attain this, fragments were amplified with the forward primer containing the attB1 sequence followed by 24 bp of the GAL4-DBD, and a reverse primer containing 21 bp from VP-16, SRDX, MYC2, and *AtMPKs*, and the attB2 sequence (Table 6). PCR amplification was performed with PrimeSTAR HS DNA Polymerase (TAKARA BIO INC) as described before (Table 12), following the PCR program for fragments bigger than 500 bp (Table 13). Subsequently, 20 μ l of PCR product was loaded on a 1% agarose gel for fragment confirmation. Electrophoresis was conducted as described before. Bands with the correct fragment size were excised and cleaned with the NucleoSpin® Gel and PCR kit (Macherey-Nagel). PCR fragments were cloned into the pDONR207 with the BP clonase followed by an LR reaction into the pAM-PAT-HA vector, as described before. Finally, positive clones were confirmed by sequencing with primers 35Spro_F and 35Ster_Rev (Table 7).

The C-terminal sequences of MAPKs from *A. thaliana*, *M. polymorpha*, human, and yeast used for the evolutionarily conserved function assays (Figure 13), were synthesized by oligo-amplification (Table 6). Forward primers contained the 5'- CACC sequence required for pENRT/D-TOPO cloning. For amplification, the PrimeSTAR HS DNA Polymerase (TAKARA BIO INC) was used in the absence of a DNA template (Table 14). The PCR program for fragments <500bp was used (Table 13).

Table 14: PrimeSTAR HS Takara master mix for oligo-amplification

Compound	Volume
5X PrimeSTAR Buffer	4 μ l
dNTPs Mixture (2.5 mM each)	2 μ l
0.2 μ M Primer Forward	3 μ l
0.2 μ M Primer Reverse	3 μ l
Prime STAR HS DNA Polymerase (2.5 U/ μ l)	0.2 μ l
Sterilized distilled water	7.8 μ l

The PCR product was loaded on a 1.8% agarose gel for fragment size confirmation. Electrophoresis was performed at 120 V for 35 min and bands with the correct fragments were excised and cleaned with the NucleoSpin® Gel and PCR kit (Macherey-Nagel). Subsequently, PCR fragments were cloned into the pENTR/D-TOPO following the protocol recommended by the pENTR/D-TOPO cloning kit (Invitrogen). Afterwards, *E. coli* DH10B chemical competent cells were transformed with 5 μ l of the reaction and grown in LB with Kan for

Materials and Methods

selection. Clones were confirmed by sequencing with primers M13_F and M13_R (Table 7) and subsequently transformed into the p403T1.2 vector with the LR clonase as described previously. Finally, positive clones were confirmed by sequencing with primers 35Spro_F and NosTer_R (Table 7).

4.2.2. Y2H assays for *AtMPK3* and *AtMPK6* interactors

Y2H was used for the identification of physical interaction between *A. thaliana* TFs and *AtMPK3* and *AtMPK6*, using a suitable and efficient large-scale screening method against a transcription factor (TF) library composed of ~1500 TF (Mitsuda et al., 2010b). Y2H assays were performed using the GAL4 and LexA systems. The MAPKs *AtMPK3* and *AtMPK6* were expressed in the bait, which contained the GAL4-DBD or LexA-DBD, and the TFs in the prey with the AD. Two yeast strains were used to test the different *AtMPK3* and *AtMPK6* constructs under both Y2H systems, the Y2HGold strain was implemented for the GAL4 system, and L40 for the LexA system.

Yeast competent cells were freshly prepared for each Y2H assay as described in the Yeast Protocol Handbook from Clontech. Yeast strains (Y2HGold and L40) were grown independently on YPD (A) agar for three days at 30°C. Subsequently, one colony was selected and incubated in 10 ml YPD (A) liquid medium at 30°C shaking (220 rpm) overnight. Cells were transferred to an Erlenmeyer flask of 250 ml with 50 ml of YPD (A) liquid medium and the concentration was adjusted to an $OD_{600} = 0.2$. The culture was grown for 5 h under the same conditions as before until reaching an $OD_{600} = (0.4-0.6)$. Afterwards, cells were transferred to a falcon tube and centrifuged for 5 min at 700 g at RT. The pellet was harvested and washed with 30 ml of sterilized distilled water, and centrifuged under the same conditions. Subsequently, the pellet was resuspended in 1.5 ml of freshly prepared 1.1X TE/LiAc and transferred to 2 ml Eppendorf tubes. Cells were collected (centrifuged at 10,000 rpm for 15 s) and resuspended in a final volume of 600 μ l of 1.1X TE/LiAc. From this time on, cells were suitable for transformation and kept on ice.

Transformation mix for yeast (Table 15) was prepared under sterile conditions in a 2 ml Eppendorf tube and kept on ice before adding the competent cells. The salmon sperm DNA (ssDNA) carrier from Invitrogen was denatured at 99°C-100°C for 5 min and immediately transferred to an ice bath. Since plasmid concentration was crucial for transformation efficiency and reproducibility, different concentrations for the bait and prey (50 ng/ μ l, 100 ng/ μ l, 300

ng/ μ l) were tested to determine and standardized the method for yeast transformation. A plasmid DNA concentration of 300 ng/ μ l was found to be optimal and was used for bait and prey.

Table 15: Y2H transformation mix

Component	Volume
Bait vector [300 ng/ μ l]	1 μ l
Prey vector [300 ng/ μ l]	1 μ l
ssDNA carrier [10 μ g/ μ l]	5 μ l
PEG/LiAc	500 μ l

An aliquot of 50 μ l yeast competent cells were added and gently mixed by tapping, followed by incubation for 30 min at 30°C shaking (200 rpm). Afterwards, 20 μ l of 100% Dimethyl sulfoxide (DMSO) was supplied and cells were incubated again for water bath at 42°C for 15 min. Subsequently, cells were harvested (10,000 rpm for 30 s), resuspended in 500 μ l of YPD (A) liquid medium and incubated for 30 min at 30°C with 220 rpm shaking. Finally, cells were collected using the same conditions as before, resuspended in 150 μ l sterilized distilled water and plated on selective medium. For co-transformation (BD and AD plasmids) transformants grew in SD (-WL) and for single transformations (BD plasmid) in SD (-W). Positive clones were obtained three days after incubation at 30°C. One colony per transformation was selected and transferred to 5 ml of liquid SD (-WL) or SD (-W). Cells were incubated at 30°C while shaking at 220 rpm overnight. Subsequently, yeast cultures were adjusted to an $OD_{600} = 1.0$ in a final volume of 1 ml sterilized distilled water. Finally, 20 μ l of three different dilutions 1, 1:20 and 1:400 were plotted on selective media (Table 16). Results were taken after three days of incubation at 30°C.

Table 16: Selective media used for co-transformations or single transformations in yeast

Co-transformations (Bait-Prey)	Transformations (Bait)
SD (-WL) Growth control	SD (-W) Growth control
SD (-WLH) with 3AT [0 mM, 1 mM, 5 mM, 10 mM]	SD (-WH) with 3AT [0 mM, 5 mM, 10 mM]
SD (-WLH) supplemented with X- α -gal	SD (-WHA)
SD (-WLHA)	

Materials and Methods

4.2.3. Biomolecular fluorescence complementation (BiFC) assays in *N. benthamiana*

The pDONRs with the *AtMPK3* and *AtMPK6* full-length and C-terminal domain were transformed into the pE-SPYCE vector containing the C-terminal YFP, with the LR clonase as described previously. Afterwards, the plasmids were transformed into *E.coli* DH10B cells as described before, and positive clones were confirmed by sequencing with primers 35Spro_F and NosTer_R (Table 7). The pE-SPYCE vectors containing the *AtMPK3/6* fragments, and the empty vector of the pE-SPYNE expressing the N-terminal YFP, were cloned into *A. tumefaciens* (Gv3101 pMP90) electrocompetent cells. For transformation, 50 μ l of competent cells and 1 μ g/ μ l of plasmid DNA were used. Cells remained in ice for 5 min, and then were electroporated for 5 min at 2500 V; 25 μ F and 400 Ω in a 1mm electroporation cuvette. Cells were recovered in 1ml YEB without antibiotics and incubated at 28°C for a period of 2 h while shaking at 200 rpm. Afterwards, 50 μ l of the cells were plated on YEB medium with antibiotics and incubated for 48 h at 28°C.

For transient expression on *N. benthamiana* one colony of *A. tumefaciens* expressing the pE-SPYNE and pE-SPYCE with *AtMPK3/6* constructs were grown in 5 ml selective YEB media overnight (28°C; 200 rpm). Afterwards, 2 ml of liquid culture was centrifuged 5 min at 8000 rpm (4°C). Harvested bacteria were washed twice with 1 ml infiltration buffer (10 mM MES; 10 mM MgCl₂; 150 μ M Acetosyringone; pH 5.7) and diluted to a final concentration of OD₆₀₀ = 0.5. Bacteria suspension was incubated for 3 h at RT and infiltrated with a needle-less syringe into *N. benthamiana* leaves. Plants were kept under normal light conditions for 2 days at RT. Leaf disks of 8 mm in diameter were cut for biomolecular fluorescence complementation assays. Samples were analyzed with a confocal scanhead LSM700 laser-scanning microscope (Carl Zeiss MicroImaging, Jena, Germany). Fluorophores were excited with an argon laser. YFP was excited at 514 nm and emission detected at 530-600 nm. As for chlorophyll autofluorescence, excitation was done with 405 nm and collected with 647-745 nm. Images were captured and analyzed with the ZEN 2011 software from Carl Zeiss.

4.2.4. Particle bombardment transient assay in *Arabidopsis* leaves

For particle preparation, the DNA solution containing the effector (1.2 μ g), reporter (1.6 μ g), and transformation efficiency plasmid (0.4 μ g) from the reporter-effector system (Figure 8A), was placed on a 1.5 ml Eppendorf. Subsequently, 22 μ l of the 60 mg/ml

gold/tungsten solution, 22 μl of 2.5 M CaCl_2 , and 8.6 μl of freshly made 0.1 M spermidine were added (Table 11). Afterwards, samples were vortexed for 15 min in a vortex attached with a multi-tube holder. Samples were spun down, and the supernatant was discarded. Then, 200 μl of 70% EtOH were added, and particles were resuspended by applying 10 pulses with a duration of 10 s each in the Sonic Dismembrator Model100 (Fisher Scientific). Subsequently, DNA-coated particles were harvested and resuspended in 30 μl of 100% EtOH. Samples were vortexed, and 10 μl aliquot was placed into a macrocarrier (Bio-Rad), which was rinsed with 95% EtOH and allowed to dry at RT. The rest of the DNA-coated samples were used for replicates two and three.

Concomitantly, one leaf from *Arabidopsis* Col-0 six-week-old plants was detached from the rosette and placed on top of a filter paper in a Petri dish. The filter paper was previously humidified and kept closed before bombardment. The PDS-1000/He Biolistic equipment from DUPONT was used during these trials. The 1,100 psi rupture discs and the stopping screen (Bio-Rad) were assembled into the holders facing the macrocarrier, which in turn faced the Col-0 leaf. After the DNA-coated particles were delivered into the leaf, the vacuum present in the equipment was released rapidly, and plant material was covered with the lid of the petri dish. Leaf samples were stored at RT in dark conditions overnight. Finally, the plant material was collected for protein extraction and dual luciferase measurements.

4.2.5. Transient expression assays in *Arabidopsis* mesophyll protoplast

Arabidopsis Col-0 mesophyll protoplasts were prepared as previously reported by Yoo et al., 2007. Leaves from four-week-old plants were detached from the rosette and cut in stripes of 0.5-1 mm and placed in a beaker with the enzyme solution (Table 11). For sample preparation, 20 to 24 leaves digested in 10 ml of enzyme solution were used to generate $1-2 \times 10^4$ protoplasts. Subsequently, samples were vacuum-infiltrated for 15 min, to guarantee uniform absorption of the enzymatic solution. Digestion of the cell wall was performed for two hours at RT while shaking at 40 rpm. Afterwards, the enzyme solution containing the protoplasts was filtered through a 75- μm nylon mesh into a 50 ml Falcon tube. Protoplasts were harvested using the Eppendorf 5810R centrifuge at 100 (rcf) for 2 min at RT, with a soft acceleration and deceleration. The supernatant was discarded, and protoplasts were washed in 20 ml W5 solution (Table 11) twice and incubated in ice for 30 min. Finally, protoplasts were

Materials and Methods

harvested using the same centrifugation parameters as before and resuspended in 2×10^5 /ml of MMg solution (Table 11).

During the incubation in ice, 7.46 μ g of the effector, 11.2 μ g of the reporter, and 2.8 μ g of the transformation efficiency plasmid were prepared in a 2 ml Eppendorf tube. Subsequently, 200 μ l of protoplast suspension on MMg were added. Before adding the 220 μ l of 40% PEG-Calcium solution (Table 11), the reaction was mixed gently to avoid settling of the protoplasts on the bottom upon PEG addition. Samples were incubated at RT for 15 min and then washed with 1 ml of W5 solution. Finally, samples were harvested by centrifugation (100 rcf for 2 min), resuspended in 1 ml of W5 solution and kept under light for 16 h. Next day, samples were harvested for protein extraction and subsequent dual luciferase assays.

4.2.6. Dual luciferase assays

Samples from transient expression assays through particle bombardment and protoplast were used for dual luciferase measurements. Proteins were extracted in the passive lysis buffer (PLB) supplied by the dual luciferase kit from Promega. For particle bombardment samples, leaf material was frozen on liquid nitrogen and crushed with metallic balls for 6 min in a paint shaker. Afterwards, 300 μ l of PLB was added to each sample and vortexed vigorously. For protoplast assays, after harvesting by centrifugation (100 rcf for 2 min) samples were resuspended in 100 μ l of PLB and vortexed vigorously. From this moment forward, samples were kept on ice. Subsequently, samples from both particle bombardment and protoplasts were centrifuged at 14,000 rpm for 15 min at 4°C. The supernatant was transferred to a new 1.5 ml Eppendorf and used for luciferase measurements.

Luciferase assays were performed on a Centro XS³ LB960 Microplate Luminometer (BERTHOLD) and on microplates (96 wells) from PerkinElmer. The Promega Luciferase Assay Reagent II (LARII) and the Stop & Glo reagent were used for detection of Firefly, and *Renilla* sp. luciferase, respectively. An aliquot of 10 μ l from each protein sample was loaded into the microplate, and subsequently, 50 μ l of the LARII was added to each well with an interval of 5 s between wells. The first measurement was done at a wavelength range of 340-630 nm, for firefly luciferase during 5 s on each well. Afterwards, 50 μ l of the Stop & Glo reagent was added to each well to stop the firefly luciferase reaction thus provided substrates for the *Renilla* luciferase reaction. The second measurement was read at the same wavelength as for the firefly luciferase, and for a period of 5 s on each well.

4.2.7. *At*MPK3/6 short peptides protein accumulation

*At*MPK protein accumulation was detected for *At*MPK3 constructs and the short peptide sequences from both *At*MPK3 and *At*MPK6 (Figure 9B, and Supplementary Figure 4). After protoplasts transfection, samples were harvested at 100 rcf for 2 min and resuspended in 100 μ l of Laemmli buffer (Table 11) for protein extraction. Afterwards, proteins were extracted by a centrifugation 4,000 rpm for 15 min at 4°C. Proteins were separated by SDS-PAGE for 1.5 hr at 120 V. Protein accumulation was detected via immunoblotting with the α -GAL4-DBD, α -MPK3, and α -HA antibody (Table 17) as a first antibody, and α -Mouse IgG, and α -Rabbit as the secondary (Table 17). Finally, West Femto Chemiluminescent reagent (Thermo Fisher Scientific) was added and homogeneously distributed throughout the membrane. Luminescence was detected on a ChemiDoc MPK imaging system (Rio-Rad).

Table 17: Antibodies used for immunoblotting

First antibody	Solution	Second antibody	Solution
α -GAL4-DBD (Abcam)	1 μ g/ml in TBST with 2.5% milk	α -Mouse IgG HRP (Amersham life science)	1:10000 diluted in TBST with 2.5% milk
α -MPK3 (Sigma-Aldrich)	1:2000 diluted in TBST with 2.5% milk	α -Rabbit IgG (Sigma-Aldrich)	1:10000 diluted in TBST with 2.5% milk
α -HA (Cell Signaling Technology)	1:5000 diluted in TBST with 2.5% milk	α -Rabbit IgG (Sigma-Aldrich)	1:10000 diluted in TBST with 2.5% milk

4.2.8. Promoter activity assays with GUS reporter

*At*WRKY33 coding sequence (CDS) was amplified with primers containing the attB1 and attB2 sites for GATEWAY cloning (Table 6). Cloning of *At*WRKY33 fragment into the entry vector pDONR201, and destination vector pXCSG was performed as described in section 4.2.1. The pDONR207 with the *At*MPK3 full-length was transformed into the pAM-PAT vector containing the HA tag, with the LR clonase as described previously. Afterwards, the plasmids were transformed into *E.coli* DH10B cells as described before. Positive clones were confirmed by sequencing with primers 35Spro_F and NosTer_R (Table 7).

Promoter activity assays were performed transiently in protoplasts from Arabidopsis Col-0, and transgenic lines *At*PROPEP2 *prom*-GUS, and *At*PROPEP2 *prom* (*mut*)-GUS.

Materials and Methods

Protoplast preparation was performed as described previously on section 4.2.5. Sample treatment was performed with 100 nM flg22 (EZBiolab Inc - Westfield, USA) or 2 μ M DEX depending on the trial. Promoter activity assays with GUS reporter were performed as described by (Logemann et al., 2013).

4.2.9. Phylogenetic analysis

Phylogenetic analyses for MAPKs on Figure 10A, Figure 12, and Figure 13 were generated using the alignment program MEGA5 2.2. The sequences from plant and non-plant MAPKs were obtained from the NCBI database and aligned by ClustalW. The consensus neighbor-joining (NJ) and maximum likelihood (ML) trees were performed with 1000 bootstrap. Sequences were analyzed using the program MegAlignPro to obtain the sequence logo and consensus match for the protein profile. Sequence homology analyses (Figure 11B) were performed using *AtMPK3* and *AtMPK6* full length and C-terminal sequences in the protein BLAST device from NCBI.

The search of the MAPKs belonging to the Viridiplantae clade was performed via HMMER. To perform the search, the plant MAPK alignment obtained from Figure 10A was used as a reference, and the program searched for protein sequences that matched this profile using Markov Models. The threshold search was adjusted to 95% similarity and 75% identity. The 713 protein sequences obtained were aligned by T-Coffee. Maximum likelihood phylogeny was obtained with Seaview program, using PhyML with the LG model (Le and Gascuel, 2008) with a 1000 bootstrap for branch support. Finally, the online tool iTOL (iTOL.embl.de) was used for visualization.

4.2.10. Transformation of *A. thaliana Atmpk3 Atmpk6* double mutant by floral dipping

To generate the *AtMPK3/6* full-length, Δ C, and C-terminal constructs under the *AtMPK3/6* promoter I first amplified the promoter sequence and coding sequences with specific primers (Table 6). PCR amplification was performed using PrimeSTAR HS DNA Polymerase (TAKARA BIO INC) as described previously (Table 12), and the PCR program was performed as recommended by the manufacturer. Afterwards, PCR product was loaded on 1% agarose gel and ran electrophoresis at 120 V for 35 min for fragment size confirmation.

The bands with the correct fragments were excised and cleaned with the NucleoSpin® Gel and PCR kit (Macherey-Nagel). Subsequently, the promoter sequence was fused to the coding sequence for each kinase fragment. Fusion PCR was performed with PrimeSTAR HS DNA Polymerase (TAKARA BIO INC). Components for PCR reaction and PCR program are described in Table 18.

Table 18: Fusion PCR components and program for *AtMPK3/6* promoter and coding sequences

PCR reaction mix	Volume	PCR program			
5X PrimeSTAR Buffer	10 µl	Initial denaturation	98°C	2 min	5 cycles and 35 cycles
dNTPs Mixture (2.5 mM each)	4 µl	Denaturation	98°C	10 s	
Promoter sequence (25 ng/µl)	2 µl	Annealing	60°C	20 s	
CDS <i>AtMPK3/6</i> fragments (25 ng/µl)	2 µl	Extension	72°C	20 s	
Prime STAR HS DNA Polymerase (2.5 U/µl)	1 µl	Final Extension	72°C	3 min	
Sterilized distilled water	41 µl	After the first 5 cycles, add 2 µl of forward and reverse (0.2 µM). Then run for 35 cycles more.			

Afterwards, the PCR products were confirmed by electrophoresis, which was run as described previously. Fragments with the correct size were excised and cleaned with the NucleoSpin® Gel and PCR kit (Macherey-Nagel). The fused promoter-coding sequences were cloned into the pDONR207 with BP Clonase II enzyme from Invitrogen and transformed into the *E. coli* DH10B chemical competent cells as described in section 4.2.1. Positive clones were confirmed by sequencing with SeLA and SeLB primers (Table 7). Entry vectors were then cloned into the destination vector pXCG-GFP with the LR Clonase II enzyme from Invitrogen, and transformed in *E. coli* DH10B cells as described previously. Then vectors were transformed in *A. tumefaciens* (Gv3101 pMP90) electrocompetent cells as described in section 4.2.3.

A positive *A. tumefaciens* colony was selected and grown in broth YEB medium at 28°C for 16-20 h and with shaking at 200 rpm. An aliquot of 100 µl culture was plated on selective YEB (Rif, Gent, Kan, and Carb,) medium at 28°C for 24 h. Afterwards, bacteria lawn was resuspended in 30 ml transfection solution (5% sucrose, 0.03% Silwet L-77) and transferred to a 50ml falcon tube. Bacteria suspension was diluted in 100 ml transfection solution until an $OD_{600} = 0.8$ was reached. *A. thaliana Atmpk3 Atmpk6* (+/-) inflorescences were dipped twice in the bacteria solution for ~2 min. Plants were then covered with a plastic bag and placed in

Materials and Methods

the dark overnight. Afterwards, plants were transferred to the greenhouse, where they grew under long day conditions.

Transgenic plants were judged by BASTA resistance and genotyped to identify the *Atmpk6* (-/-) mutants. Genotype was performed using Whatman FTA cards and the recommended primer combination from the *Atmpk6* mutant line (SALK_073907). The primers SALK_073907_LP2, and SALK_073907_RP2 were used to identified WT *AtMPK6*, and the LBE, and SALK_073907_RP2 for *Atmpk6* mutant. PCR reaction and genotype program used are described in Table 19.

Table 19: PCR components and program for *Atmpk6* genotyping

PCR reaction mix	Volume	PCR program		
10x PCR buffer	2 μ l	Initial denaturation	95°C	5 min
dNTP mix (10 mM)	0.3 μ l	Denaturation	95°C	30 s
Primer 1 (100 mM)	0.05 μ l	Annealing	55°C	30 s
Primer 2 (100 mM)	0.05 μ l	Extension	72°C	1 s
BSA (10 mg/ml)	0.5 μ l	Final Extension	72°C	5 min
Tween-20 (10%)	8 μ l		4°C	∞
Homemade Taq polymerase	1 μ l			
Sterilized distilled water	8.1 μ l			

5. References

- Andreasson, E., and Ellis, B. (2010). Convergence and specificity in the Arabidopsis MAPK nexus. *Trends Plant Sci.* *15*, 106–113.
- Andreasson, E., Jenkins, T., Brodersen, P., Thorgrimsen, S., Petersen, N.H.T., Zhu, S., Qiu, J.-L., Micheelsen, P., Rocher, A., Petersen, M., et al. (2005). The MAP kinase substrate MKS1 is a regulator of plant defense responses. *EMBO J.* *24*, 2579–2589.
- Arabidopsis Interactome Mapping Consortium (2011). Evidence for Network Evolution in an Arabidopsis Interactome Map. *Science* *333*, 601–607.
- Arnold, C.D., Nemčko, F., Woodfin, A.R., Wienerroither, S., Vlasova, A., Schleiffer, A., Pagani, M., Rath, M., and Stark, A. (2018). A high-throughput method to identify trans-activation domains within transcription factor sequences. *EMBO J.* *37*, e98896.
- Asai, T., Tena, G., Plotnikova, J., Willmann, M.R., Chiu, W.-L., Gomez-Gomez, L., Boller, T., Ausubel, F.M., and Sheen, J. (2002). MAP kinase signalling cascade in Arabidopsis innate immunity. *Nature* *415*, 977–983.
- Bardwell, L., Cook, J.G., Voora, D., Baggott, D.M., Martinez, A.R., and Thorner, J. (1998). Repression of yeast Ste12 transcription factor by direct binding of unphosphorylated Kss1 MAPK and its regulation by the Ste7 MEK. *Genes Dev.* *12*, 2887–2898.
- Bataille, A.R., Jeronimo, C., Jacques, P.-É., Laramée, L., Fortin, M.-È., Forest, A., Bergeron, M., Hanes, S.D., and Robert, F. (2012). A universal RNA polymerase II CTD cycle is orchestrated by complex interplays between kinase, phosphatase, and isomerase enzymes along genes. *Mol. Cell* *45*, 158–170.
- Beckers, G.J.M., Jaskiewicz, M., Liu, Y., Underwood, W.R., He, S.Y., Zhang, S., and Conrath, U. (2009). Mitogen-Activated Protein Kinases 3 and 6 Are Required for Full Priming of Stress Responses in Arabidopsis thaliana. *Plant Cell* *21*, 944–953.
- Berens, M.L., Berry, H.M., Mine, A., Argueso, C.T., and Tsuda, K. (2017). Evolution of Hormone Signaling Networks in Plant Defense. *Annu. Rev. Phytopathol.* *55*, 401–425.
- Bergmann, D.C., Lukowitz, W., and Somerville, C.R. (2004). Stomatal Development and Pattern Controlled by a MAPKK Kinase. *Science* *304*, 1494–1497.
- Bethke, G., Unthan, T., Uhrig, J.F., Pöschl, Y., Gust, A.A., Scheel, D., and Lee, J. (2009). Flg22 regulates the release of an ethylene response factor substrate from MAP kinase 6 in Arabidopsis thaliana via ethylene signaling. *Proc. Natl. Acad. Sci. U. S. A.* *106*, 8067–8072.
- Bethke, G., Pecher, P., Eschen-Lippold, L., Tsuda, K., Katagiri, F., Glazebrook, J., Scheel, D., and Lee, J. (2011). Activation of the Arabidopsis thaliana Mitogen-Activated Protein Kinase MPK11 by the Flagellin-Derived Elicitor Peptide, flg22. *Mol. Plant. Microbe Interact.* *25*, 471–480.
- Bhattacharyya, R.P., Reményi, A., Good, M.C., Bashor, C.J., Falick, A.M., and Lim, W.A. (2006). The Ste5 scaffold allosterically modulates signaling output of the yeast mating pathway. *Science* *311*, 822–826.
- Bi, G., Zhou, Z., Wang, W., Li, L., Rao, S., Wu, Y., Zhang, X., Menke, F.L.H., Chen, S., and Zhou, J.-M. (2018). Receptor-Like Cytoplasmic Kinases Directly Link Diverse Pattern

References

- Recognition Receptors to the Activation of Mitogen-Activated Protein Kinase Cascades in Arabidopsis. *Plant Cell* 30, 1543–1561.
- Bigeard, J., and Hirt, H. (2018). Nuclear Signaling of Plant MAPKs. *Front. Plant Sci.* 9.
- Birkenbihl, R.P., Kracher, B., Roccaro, M., and Somssich, I.E. (2017). Induced Genome-Wide Binding of Three Arabidopsis WRKY Transcription Factors during Early MAMP-Triggered Immunity. *Plant Cell* 29, 20–38.
- Blackwell, E., Kim, H.-J.N., and Stone, D.E. (2007). The pheromone-induced nuclear accumulation of the Fus3 MAPK in yeast depends on its phosphorylation state and on Dig1 and Dig2. *BMC Cell Biol.* 8, 44.
- Bowman, J.L., Kohchi, T., Yamato, K.T., Jenkins, J., Shu, S., Ishizaki, K., Yamaoka, S., Nishihama, R., Nakamura, Y., Berger, F., et al. (2017). Insights into Land Plant Evolution Garnered from the *Marchantia polymorpha* Genome. *Cell* 171, 287-304.e15.
- Brennan, D.F., Dar, A.C., Hertz, N.T., Chao, W.C.H., Burlingame, A.L., Shokat, K.M., and Barford, D. (2011). A Raf-induced allosteric transition of KSR stimulates phosphorylation of MEK. *Nature* 472, 366–369.
- Brent, R., and Ptashne, M. (1985). A eukaryotic transcriptional activator bearing the DNA specificity of a prokaryotic repressor. *Cell* 43, 729–736.
- Buscà, R., Pouysségur, J., and Lenormand, P. (2016). ERK1 and ERK2 Map Kinases: Specific Roles or Functional Redundancy? *Front. Cell Dev. Biol.* 4.
- Canagarajah, B.J., Khokhlatchev, A., Cobb, M.H., and Goldsmith, E.J. (1997). Activation Mechanism of the MAP Kinase ERK2 by Dual Phosphorylation. *Cell* 90, 859–869.
- Cao, Y., Liang, Y., Tanaka, K., Nguyen, C.T., Jedrzejczak, R.P., Joachimiak, A., and Stacey, G. (2014). The kinase LYK5 is a major chitin receptor in Arabidopsis and forms a chitin-induced complex with related kinase CERK1. *ELife* 3.
- Cargnello, M., and Roux, P.P. (2011). Activation and Function of the MAPKs and Their Substrates, the MAPK-Activated Protein Kinases. *Microbiol. Mol. Biol. Rev.* 75, 50–83.
- Chen, R.E., and Thorner, J. (2007). Function and Regulation in MAPK Signaling Pathways. *Biochim. Biophys. Acta* 1773, 1311–1340.
- Chen, R.H., Sarnecki, C., and Blenis, J. (1992). Nuclear localization and regulation of erk- and rsk-encoded protein kinases. *Mol. Cell. Biol.* 12, 915–927.
- Cheng, Z., Li, J.-F., Niu, Y., Zhang, X.-C., Woody, O.Z., Xiong, Y., Djonović, S., Millet, Y., Bush, J., McConkey, B.J., et al. (2015). Pathogen-secreted proteases activate a novel plant immune pathway. *Nature* 521, 213–216.
- Chezem, W.R., Memon, A., Li, F.-S., Weng, J.-K., and Clay, N.K. (2017). SG2-Type R2R3-MYB Transcription Factor MYB15 Controls Defense-Induced Lignification and Basal Immunity in Arabidopsis. *Plant Cell* 29, 1907–1926.
- Chinchilla, D., Zipfel, C., Robatzek, S., Kemmerling, B., Nürnberger, T., Jones, J.D.G., Felix, G., and Boller, T. (2007). A flagellin-induced complex of the receptor FLS2 and BAK1 initiates plant defence. *Nature* 448, 497–500.
- Chisholm, S.T., Coaker, G., Day, B., and Staskawicz, B.J. (2006). Host-Microbe Interactions: Shaping the Evolution of the Plant Immune Response. *Cell* 124, 803–814.
- Choi, K.Y., Satterberg, B., Lyons, D.M., and Elion, E.A. (1994). Ste5 tethers multiple protein kinases in the MAP kinase cascade required for mating in *S. cerevisiae*. *Cell* 78, 499–512.

- Colcombet, J., and Hirt, H. (2008). Arabidopsis MAPKs: a complex signalling network involved in multiple biological processes. *Biochem. J.* *413*, 217.
- Cousens, D.J., Greaves, R., Goding, C.R., and O'Hare, P. (1989). The C-terminal 79 amino acids of the herpes simplex virus regulatory protein, Vmw65, efficiently activate transcription in yeast and mammalian cells in chimeric DNA-binding proteins. *EMBO J.* *8*, 2337–2342.
- Couto, D., and Zipfel, C. (2016). Regulation of pattern recognition receptor signalling in plants. *Nat. Rev. Immunol.* *16*, 537–552.
- Cui, H., Tsuda, K., and Parker, J.E. (2015). Effector-Triggered Immunity: From Pathogen Perception to Robust Defense. *Annu. Rev. Plant Biol.* *66*, 487–511.
- Danisman, S., Wal, F. van der, Dhondt, S., Waites, R., Folter, S. de, Bimbo, A., Dijk, A.D. van, Muino, J.M., Cutri, L., Dornelas, M.C., et al. (2012). Arabidopsis Class I and Class II TCP Transcription Factors Regulate Jasmonic Acid Metabolism and Leaf Development Antagonistically. *Plant Physiol.* *159*, 1511–1523.
- Ding, B., and Wang, G.-L. (2015). Chromatin versus pathogens: the function of epigenetics in plant immunity. *Front. Plant Sci.* *6*.
- Dinh, T.T., Girke, T., Liu, X., Yant, L., Schmid, M., and Chen, X. (2012). The floral homeotic protein APETALA2 recognizes and acts through an AT-rich sequence element. *Development* *139*, 1978–1986.
- Diskin, R., Lebendiker, M., Engelberg, D., and Livnah, O. (2007). Structures of p38 α Active Mutants Reveal Conformational Changes in L16 Loop that Induce Autophosphorylation and Activation. *J. Mol. Biol.* *365*, 66–76.
- Djamei, A., Pitzschke, A., Nakagami, H., Rajh, I., and Hirt, H. (2007). Trojan Horse Strategy in Agrobacterium Transformation: Abusing MAPK Defense Signaling. *Science* *318*, 453–456.
- Dodds, P.N., and Rathjen, J.P. (2010). Plant immunity: towards an integrated view of plant-pathogen interactions. *Nat. Rev. Genet.* *11*, 539–548.
- Dubos, C., Stracke, R., Grotewold, E., Weisshaar, B., Martin, C., and Lepiniec, L. (2010). MYB transcription factors in Arabidopsis. *Trends Plant Sci.* *15*, 573–581.
- Elion, E.A., Satterberg, B., and Kranz, J.E. (1993). FUS3 phosphorylates multiple components of the mating signal transduction cascade: evidence for STE12 and FAR1. *Mol. Biol. Cell* *4*, 495–510.
- Eulgem, T., and Somssich, I.E. (2007). Networks of WRKY transcription factors in defense signaling. *Curr. Opin. Plant Biol.* *10*, 366–371.
- Eulgem, T., Rushton, P.J., Robatzek, S., and Somssich, I.E. (2000). The WRKY superfamily of plant transcription factors. *Trends Plant Sci.* *5*, 199–206.
- Galán, J.E., and Collmer, A. (1999). Type III secretion machines: bacterial devices for protein delivery into host cells. *Science* *284*, 1322–1328.
- Glazebrook, J. (2005). Contrasting Mechanisms of Defense Against Biotrophic and Necrotrophic Pathogens. *Annu. Rev. Phytopathol.* *43*, 205–227.
- Gómez-Gómez, L., and Boller, T. (2000). FLS2: an LRR receptor-like kinase involved in the perception of the bacterial elicitor flagellin in Arabidopsis. *Mol. Cell* *5*, 1003–1011.
- Good, M., Tang, G., Singleton, J., Reményi, A., and Lim, W.A. (2009). The Ste5 scaffold directs mating signaling by catalytically unlocking the Fus3 MAP kinase for activation. *Cell* *136*, 1085–1097.

References

- Good, M.C., Zalatan, J.G., and Lim, W.A. (2011). Scaffold Proteins: Hubs for Controlling the Flow of Cellular Information. *Science* 332, 680–686.
- Hajheidari, M., Farrona, S., Huettel, B., Koncz, Z., and Koncz, C. (2012). CDKF;1 and CDKD Protein Kinases Regulate Phosphorylation of Serine Residues in the C-Terminal Domain of Arabidopsis RNA Polymerase II. *Plant Cell* 24, 1626–1642.
- Hajheidari, M., Koncz, C., and Eick, D. (2013). Emerging roles for RNA polymerase II CTD in Arabidopsis. *Trends Plant Sci.* 18, 633–643.
- Harlen, K.M., Trotta, K.L., Smith, E.E., Mosaheb, M.M., Fuchs, S.M., and Churchman, L.S. (2016). Comprehensive RNA Polymerase II Interactomes Reveal Distinct and Varied Roles for Each Phospho-CTD Residue. *Cell Rep.* 15, 2147–2158.
- Hiratsu, K., Mitsuda, N., Matsui, K., and Ohme-Takagi, M. (2004). Identification of the minimal repression domain of SUPERMAN shows that the DLELRL hexapeptide is both necessary and sufficient for repression of transcription in Arabidopsis. *Biochem. Biophys. Res. Commun.* 321, 172–178.
- Hoehenwarter, W., Thomas, M., Nukarinen, E., Egelhofer, V., Röhrig, H., Weckwerth, W., Conrath, U., and Beckers, G.J.M. (2013). Identification of Novel *in vivo* MAP Kinase Substrates in Arabidopsis thaliana Through Use of Tandem Metal Oxide Affinity Chromatography. *Mol. Cell. Proteomics* 12, 369–380.
- Hu, S., Xie, Z., Onishi, A., Yu, X., Jiang, L., Lin, J., Rho, H., Woodard, C., Wang, H., Jeong, J.-S., et al. (2009). Profiling the Human Protein-DNA Interactome Reveals ERK2 as a Transcriptional Repressor of Interferon Signaling. *Cell* 139, 610–622.
- Ichimura, K., Tena, G., Sheen, J., Henry, Y., Champion, A., Kreis, M., Zhang, S., Hirt, H., Wilson, C., Heberle-Bors, E., et al. (2002). Mitogen-activated protein kinase cascades in plants: a new nomenclature. *Trends Plant Sci.* 7, 301–308.
- Imperial, R., Toor, O.M., Hussain, A., Subramanian, J., and Masood, A. (2019). Comprehensive pancancer genomic analysis reveals (RTK)-RAS-RAF-MEK as a key dysregulated pathway in cancer: Its clinical implications. *Semin. Cancer Biol.* 54, 14–28.
- Inouye, C., Dhillon, N., and Thorner, J. (1997). Ste5 RING-H2 domain: role in Ste4-promoted oligomerization for yeast pheromone signaling. *Science* 278, 103–106.
- Jakoby, M., Weisshaar, B., Dröge-Laser, W., Vicente-Carbajosa, J., Tiedemann, J., Kroj, T., and Parcy, F. (2002). bZIP transcription factors in Arabidopsis. *Trends Plant Sci.* 7, 106–111.
- Jones, J.D.G., and Dangl, J.L. (2006). The plant immune system. *Nature* 444, 323–329.
- Joo, S., Liu, Y., Lueth, A., and Zhang, S. (2008). MAPK phosphorylation-induced stabilization of ACS6 protein is mediated by the non-catalytic C-terminal domain, which also contains the cis-determinant for rapid degradation by the 26S proteasome pathway. *Plant J.* 54, 129–140.
- Kagaya, Y., Ohmiya, K., and Hattori, T. (1999). RAV1, a novel DNA-binding protein, binds to bipartite recognition sequence through two distinct DNA-binding domains uniquely found in higher plants. *Nucleic Acids Res.* 27, 470–478.
- Kalapos, B., Hlavová, M., Nádai, T.V., Galiba, G., Bišová, K., and Dóczi, R. (2019). Early Evolution of the Mitogen-Activated Protein Kinase Family in the Plant Kingdom. *Sci. Rep.* 9, 4094.
- Kasler, H.G., Victoria, J., Duramad, O., and Winoto, A. (2000). ERK5 is a novel type of mitogen-activated protein kinase containing a transcriptional activation domain. *Mol. Cell. Biol.* 20, 8382–8389.

- Kazan, K., and Manners, J.M. (2012). JAZ repressors and the orchestration of phytohormone crosstalk. *Trends Plant Sci.* 17, 22–31.
- Khokhlatchev, A.V., Canagarajah, B., Wilsbacher, J., Robinson, M., Atkinson, M., Goldsmith, E., and Cobb, M.H. (1998). Phosphorylation of the MAP Kinase ERK2 Promotes Its Homodimerization and Nuclear Translocation. *Cell* 93, 605–615.
- Kim, S.H., Son, G.H., Bhattacharjee, S., Kim, H.J., Nam, J.C., Nguyen, P.D.T., Hong, J.C., and Gassmann, W. (2014). The Arabidopsis immune adaptor SRFR1 interacts with TCP transcription factors that redundantly contribute to effector-triggered immunity. *Plant J.* 78, 978–989.
- Klein, S., Reuveni, H., and Levitzki, A. (2000). Signal transduction by a nondissociable heterotrimeric yeast G protein. *Proc. Natl. Acad. Sci. U. S. A.* 97, 3219–3223.
- Koiwa, H., Barb, A.W., Xiong, L., Li, F., McCully, M.G., Lee, B., Sokolchik, I., Zhu, J., Gong, Z., Reddy, M., et al. (2002). C-terminal domain phosphatase-like family members (AtCPLs) differentially regulate Arabidopsis thaliana abiotic stress signaling, growth, and development. *Proc. Natl. Acad. Sci.* 99, 10893–10898.
- Koiwa, H., Hausmann, S., Bang, W.Y., Ueda, A., Kondo, N., Hiraguri, A., Fukuhara, T., Bahk, J.D., Yun, D.-J., Bressan, R.A., et al. (2004). Arabidopsis C-terminal domain phosphatase-like 1 and 2 are essential Ser-5-specific C-terminal domain phosphatases. *Proc. Natl. Acad. Sci.* 101, 14539–14544.
- Kong, Q., Qu, N., Gao, M., Zhang, Z., Ding, X., Yang, F., Li, Y., Dong, O.X., Chen, S., Li, X., et al. (2012). The MEKK1-MKK1/MKK2-MPK4 Kinase Cascade Negatively Regulates Immunity Mediated by a Mitogen-Activated Protein Kinase Kinase Kinase in Arabidopsis. *Plant Cell* 24, 2225–2236.
- Kornev, A.P., Haste, N.M., Taylor, S.S., and Eyck, L.F.T. (2006). Surface comparison of active and inactive protein kinases identifies a conserved activation mechanism. *Proc. Natl. Acad. Sci.* 103, 17783–17788.
- Kutschera, A., Dawid, C., Gisch, N., Schmid, C., Raasch, L., Gerster, T., Schäffer, M., Smakowska-Luzan, E., Belkhadir, Y., Vlot, A.C., et al. (2019). Bacterial medium-chain 3-hydroxy fatty acid metabolites trigger immunity in Arabidopsis plants. *Science* 364, 178–181.
- Lampard, G.R., Lukowitz, W., Ellis, B.E., and Bergmann, D.C. (2009). Novel and expanded roles for MAPK signaling in Arabidopsis stomatal cell fate revealed by cell type-specific manipulations. *Plant Cell* 21, 3506–3517.
- Lassowskat, I., Böttcher, C., Eschen-Lippold, L., Scheel, D., and Lee, J. (2014). Sustained mitogen-activated protein kinase activation reprograms defense metabolism and phosphoprotein profile in Arabidopsis thaliana. *Front. Plant Sci.* 5.
- Latrasse, D., Jégu, T., Li, H., Zelicourt, A. de, Raynaud, C., Legras, S., Gust, A., Samajova, O., Veluchamy, A., Rayapuram, N., et al. (2017). MAPK-triggered chromatin reprogramming by histone deacetylase in plant innate immunity. *Genome Biol.* 18, 131.
- Le, S.Q., and Gascuel, O. (2008). An Improved General Amino Acid Replacement Matrix. *Mol. Biol. Evol.* 25, 1307–1320.
- Leinweber, B.D., Leavis, P.C., Grabarek, Z., Wang, C.L., and Morgan, K.G. (1999). Extracellular regulated kinase (ERK) interaction with actin and the calponin homology (CH) domain of actin-binding proteins. *Biochem. J.* 344, 117–123.

References

- Le Roux, C., Huet, G., Jauneau, A., Camborde, L., Trémousaygue, D., Kraut, A., Zhou, B., Levaillant, M., Adachi, H., Yoshioka, H., et al. (2015). A Receptor Pair with an Integrated Decoy Converts Pathogen Disabling of Transcription Factors to Immunity. *Cell* *161*, 1074–1088.
- Li, F., Cheng, C., Cui, F., de Oliveira, M.V.V., Yu, X., Meng, X., Intorne, A.C., Babilonia, K., Li, M., Li, B., et al. (2014). Modulation of RNA polymerase II phosphorylation downstream of pathogen perception orchestrates plant immunity. *Cell Host Microbe* *16*, 748–758.
- Li, G., Meng, X., Wang, R., Mao, G., Han, L., Liu, Y., and Zhang, S. (2012). Dual-Level Regulation of ACC Synthase Activity by MPK3/MPK6 Cascade and Its Downstream WRKY Transcription Factor during Ethylene Induction in Arabidopsis. *PLOS Genet.* *8*, e1002767.
- Li, J., Brader, G., and Palva, E.T. (2004). The WRKY70 Transcription Factor: A Node of Convergence for Jasmonate-Mediated and Salicylate-Mediated Signals in Plant Defense. *Plant Cell* *16*, 319–331.
- Libault, M., Wan, J., Czechowski, T., Udvardi, M., and Stacey, G. (2007). Identification of 118 Arabidopsis Transcription Factor and 30 Ubiquitin-Ligase Genes Responding to Chitin, a Plant-Defense Elicitor. *Mol. Plant. Microbe Interact.* *20*, 900–911.
- Licausi, F., Ohme-Takagi, M., and Perata, P. (2013). APETALA2/Ethylene Responsive Factor (AP2/ERF) transcription factors: mediators of stress responses and developmental programs. *New Phytol.* *199*, 639–649.
- Liu, Y., and Zhang, S. (2004). Phosphorylation of 1-Aminocyclopropane-1-Carboxylic Acid Synthase by MPK6, a Stress-Responsive Mitogen-Activated Protein Kinase, Induces Ethylene Biosynthesis in Arabidopsis. *Plant Cell* *16*, 3386–3399.
- Logemann, E., Birkenbihl, R.P., Rawat, V., Schneeberger, K., Schmelzer, E., and Somssich, I.E. (2013). Functional dissection of the PROPEP2 and PROPEP3 promoters reveals the importance of WRKY factors in mediating microbe-associated molecular pattern-induced expression. *New Phytol.* *198*, 1165–1177.
- Lopez, J.A., Sun, Y., Blair, P.B., and Mukhtar, M.S. (2015). TCP three-way handshake: linking developmental processes with plant immunity. *Trends Plant Sci.* *20*, 238–245.
- Lu, D., Wu, S., Gao, X., Zhang, Y., Shan, L., and He, P. (2010). A receptor-like cytoplasmic kinase, BIK1, associates with a flagellin receptor complex to initiate plant innate immunity. *Proc. Natl. Acad. Sci.* *107*, 496–501.
- Luger, K., Mäder, A.W., Richmond, R.K., Sargent, D.F., and Richmond, T.J. (1997). Crystal structure of the nucleosome core particle at 2.8 Å resolution. *Nature* *389*, 251–260.
- Luo, M., Dennis, E.S., Berger, F., Peacock, W.J., and Chaudhury, A. (2005). MINISEED3 (MINI3), a WRKY family gene, and HAIKU2 (IKU2), a leucine-rich repeat (LRR) KINASE gene, are regulators of seed size in Arabidopsis. *Proc. Natl. Acad. Sci. U. S. A.* *102*, 17531–17536.
- Mackey, D., Belkhadir, Y., Alonso, J.M., Ecker, J.R., and Dangl, J.L. (2003). Arabidopsis RIN4 Is a Target of the Type III Virulence Effector AvrRpt2 and Modulates RPS2-Mediated Resistance. *Cell* *112*, 379–389.
- Mao, G., Meng, X., Liu, Y., Zheng, Z., Chen, Z., and Zhang, S. (2011). Phosphorylation of a WRKY transcription factor by two pathogen-responsive MAPKs drives phytoalexin biosynthesis in Arabidopsis. *Plant Cell* *23*, 1639–1653.

- Martín-Trillo, M., and Cubas, P. (2010). TCP genes: a family snapshot ten years later. *Trends Plant Sci.* *15*, 31–39.
- Mauch, F., Mauch-Mani, B., Gaille, C., Kull, B., Haas, D., and Reimmann, C. (2001). Manipulation of salicylate content in *Arabidopsis thaliana* by the expression of an engineered bacterial salicylate synthase. *Plant J. Cell Mol. Biol.* *25*, 67–77.
- McCubrey, J.A., Steelman, L.S., Bäsecke, J., and Martelli, A.M. (2015). Raf/MEK/ERK Signaling. In *Targeted Therapy of Acute Myeloid Leukemia*, M. Andreeff, ed. (New York, NY: Springer New York), pp. 275–305.
- McKay, M.M., Ritt, D.A., and Morrison, D.K. (2009). Signaling dynamics of the KSR1 scaffold complex. *Proc. Natl. Acad. Sci. U. S. A.* *106*, 11022–11027.
- Meng, X., and Zhang, S. (2013). MAPK cascades in plant disease resistance signaling. *Annu. Rev. Phytopathol.* *51*, 245–266.
- Meng, X., Wang, H., He, Y., Liu, Y., Walker, J.C., Torii, K.U., and Zhang, S. (2012). A MAPK Cascade Downstream of ERECTA Receptor-Like Protein Kinase Regulates Arabidopsis Inflorescence Architecture by Promoting Localized Cell Proliferation. *Plant Cell* *24*, 4948–4960.
- Meng, X., Xu, J., He, Y., Yang, K.-Y., Mordorski, B., Liu, Y., and Zhang, S. (2013). Phosphorylation of an ERF Transcription Factor by Arabidopsis MPK3/MPK6 Regulates Plant Defense Gene Induction and Fungal Resistance. *Plant Cell Online* tpc.112.109074.
- Mine, A., Berens, M.L., Nobori, T., Anver, S., Fukumoto, K., Winkelmüller, T.M., Takeda, A., Becker, D., and Tsuda, K. (2017a). Pathogen exploitation of an abscisic acid- and jasmonate-inducible MAPK phosphatase and its interception by Arabidopsis immunity. *Proc. Natl. Acad. Sci. U. S. A.* *114*, 7456–7461.
- Mine, A., Nobori, T., Salazar-Rondon, M.C., Winkelmüller, T.M., Anver, S., Becker, D., and Tsuda, K. (2017b). An incoherent feed-forward loop mediates robustness and tunability in a plant immune network. *EMBO Rep.* *18*, 464–476.
- Mine, A., Seyfferth, C., Kracher, B., Berens, M.L., Becker, D., and Tsuda, K. (2018). The Defense Phytohormone Signaling Network Enables Rapid, High-Amplitude Transcriptional Reprogramming during Effector-Triggered Immunity. *Plant Cell* *30*, 1199–1219.
- Mitsuda, N., Hisabori, T., Takeyasu, K., and Sato, M.H. (2004). VOZ; isolation and characterization of novel vascular plant transcription factors with a one-zinc finger from *Arabidopsis thaliana*. *Plant Cell Physiol.* *45*, 845–854.
- Mitsuda, N., Ikeda, M., Takada, S., Takiguchi, Y., Kondou, Y., Yoshizumi, T., Fujita, M., Shinozaki, K., Matsui, M., and Ohme-Takagi, M. (2010a). Efficient Yeast One-/Two-Hybrid Screening Using a Library Composed Only of Transcription Factors in *Arabidopsis thaliana*. *Plant Cell Physiol.* *51*, 2145–2151.
- Mitsuda, N., Ikeda, M., Takada, S., Takiguchi, Y., Kondou, Y., Yoshizumi, T., Fujita, M., Shinozaki, K., Matsui, M., and Ohme-Takagi, M. (2010b). Efficient Yeast One-/Two-Hybrid Screening Using a Library Composed Only of Transcription Factors in *Arabidopsis thaliana*. *Plant Cell Physiol.* *51*, 2145–2151.
- Miya, A., Albert, P., Shinya, T., Desaki, Y., Ichimura, K., Shirasu, K., Narusaka, Y., Kawakami, N., Kaku, H., and Shibuya, N. (2007). CERK1, a LysM receptor kinase, is essential for chitin elicitor signaling in *Arabidopsis*. *Proc. Natl. Acad. Sci.* *104*, 19613–19618.

References

- Morimoto, H., Kondoh, K., Nishimoto, S., Terasawa, K., and Nishida, E. (2007). Activation of a C-terminal Transcriptional Activation Domain of ERK5 by Autophosphorylation. *J. Biol. Chem.* *282*, 35449–35456.
- Müller, J., Ory, S., Copeland, T., Piwnica-Worms, H., and Morrison, D.K. (2001). C-TAK1 regulates Ras signaling by phosphorylating the MAPK scaffold, KSR1. *Mol. Cell* *8*, 983–993.
- Nakai, Y., Nakahira, Y., Sumida, H., Takebayashi, K., Nagasawa, Y., Yamasaki, K., Akiyama, M., Ohme-Takagi, M., Fujiwara, S., Shiina, T., et al. (2013). Vascular plant one-zinc-finger protein 1/2 transcription factors regulate abiotic and biotic stress responses in Arabidopsis. *Plant J.* *73*, 761–775.
- Nakano, T., Suzuki, K., Fujimura, T., and Shinshi, H. (2006). Genome-Wide Analysis of the ERF Gene Family in Arabidopsis and Rice. *Plant Physiol.* *140*, 411–432.
- Nguyen, T., Ruan, Z., Oruganty, K., and Kannan, N. (2015). Co-Conserved MAPK Features Couple D-Domain Docking Groove to Distal Allosteric Sites via the C-Terminal Flanking Tail. *PLoS ONE* *10*, e0119636.
- Nguyen, X.C., Hoang, M.H.T., Kim, H.S., Lee, K., Liu, X.-M., Kim, S.H., Bahk, S., Park, H.C., and Chung, W.S. (2012a). Phosphorylation of the transcriptional regulator MYB44 by mitogen activated protein kinase regulates Arabidopsis seed germination. *Biochem. Biophys. Res. Commun.* *423*, 703–708.
- Nguyen, X.C., Kim, S.H., Lee, K., Kim, K.E., Liu, X.-M., Han, H.J., Hoang, M.H.T., Lee, S.-W., Hong, J.C., Moon, Y.-H., et al. (2012b). Identification of a C2H2-type zinc finger transcription factor (ZAT10) from Arabidopsis as a substrate of MAP kinase. *Plant Cell Rep.* *31*, 737–745.
- Niu, Y., Figueroa, P., and Browse, J. (2011). Characterization of JAZ-interacting bHLH transcription factors that regulate jasmonate responses in Arabidopsis. *J. Exp. Bot.* *62*, 2143–2154.
- Nühse, T.S., Peck, S.C., Hirt, H., and Boller, T. (2000). Microbial Elicitors Induce Activation and Dual Phosphorylation of the Arabidopsis thaliana MAPK 6. *J. Biol. Chem.* *275*, 7521–7526.
- Ohme-Takagi, M., and Shinshi, H. (1995). Ethylene-inducible DNA binding proteins that interact with an ethylene-responsive element. *Plant Cell* *7*, 173–182.
- Ohme-Takagi, M., Suzuki, K., and Shinshi, H. (2000). Regulation of ethylene-induced transcription of defense genes. *Plant Cell Physiol.* *41*, 1187–1192.
- Ory, S., Zhou, M., Conrads, T.P., Veenstra, T.D., and Morrison, D.K. (2003). Protein Phosphatase 2A Positively Regulates Ras Signaling by Dephosphorylating KSR1 and Raf-1 on Critical 14-3-3 Binding Sites. *Curr. Biol.* *13*, 1356–1364.
- Pagès, G., Lenormand, P., L'Allemain, G., Chambard, J.C., Meloche, S., and Pouysségur, J. (1993). Mitogen-activated protein kinases p42mapk and p44mapk are required for fibroblast proliferation. *Proc. Natl. Acad. Sci.* *90*, 8319–8323.
- Pandey, S.P., and Somssich, I.E. (2009). The Role of WRKY Transcription Factors in Plant Immunity. *Plant Physiol.* *150*, 1648–1655.
- Panek, A., Pietrow, O., Filipkowski, P., and Synowiecki, J. (2013). Effects of the polyhistidine tag on kinetics and other properties of trehalose synthase from *Deinococcus geothermalis*. *Acta Biochim. Pol.* *60*.

- Pecher, P., Eschen-Lippold, L., Herklotz, S., Kuhle, K., Naumann, K., Bethke, G., Uhrig, J., Weyhe, M., Scheel, D., and Lee, J. (2014). The *Arabidopsis thaliana* mitogen-activated protein kinases MPK3 and MPK6 target a subclass of ‘VQ-motif’-containing proteins to regulate immune responses. *New Phytol.* *203*, 592–606.
- Peng, Y., van Wersch, R., and Zhang, Y. (2017). Convergent and Divergent Signaling in PAMP-Triggered Immunity and Effector-Triggered Immunity. *Mol. Plant. Microbe Interact.* *31*, 403–409.
- Persak, H., and Pitzschke, A. (2013). Tight Interconnection and Multi-Level Control of *Arabidopsis* MYB44 in MAPK Cascade Signalling. *PLOS ONE* *8*, e57547.
- Petersen, M., Brodersen, P., Naested, H., Andreasson, E., Lindhart, U., Johansen, B., Nielsen, H.B., Lacy, M., Austin, M.J., Parker, J.E., et al. (2000). *Arabidopsis* map kinase 4 negatively regulates systemic acquired resistance. *Cell* *103*, 1111–1120.
- Pieterse, C.M.J., Leon-Reyes, A., Van der Ent, S., and Van Wees, S.C.M. (2009). Networking by small-molecule hormones in plant immunity. *Nat. Chem. Biol.* *5*, 308–316.
- Pitzschke, A. (2015). Modes of MAPK substrate recognition and control. *Trends Plant Sci.* *0*.
- Pitzschke, A., Djamei, A., Teige, M., and Hirt, H. (2009). VIP1 response elements mediate mitogen-activated protein kinase 3-induced stress gene expression. *Proc. Natl. Acad. Sci.* *106*, 18414–18419.
- Popescu, S.C., Popescu, G.V., Bachan, S., Zhang, Z., Gerstein, M., Snyder, M., and Dinesh-Kumar, S.P. (2009). MAPK target networks in *Arabidopsis thaliana* revealed using functional protein microarrays. *Genes Dev.* *23*, 80–92.
- Pryciak, P.M., and Huntress, F.A. (1998). Membrane recruitment of the kinase cascade scaffold protein Ste5 by the Gbetagamma complex underlies activation of the yeast pheromone response pathway. *Genes Dev.* *12*, 2684–2697.
- Qiu, J.-L., Fiil, B.K., Petersen, K., Nielsen, H.B., Botanga, C.J., Thorgrimsen, S., Palma, K., Suarez-Rodriguez, M.C., Sandbech-Clausen, S., Lichota, J., et al. (2008). *Arabidopsis* MAP kinase 4 regulates gene expression through transcription factor release in the nucleus. *EMBO J.* *27*, 2214–2221.
- Ramírez, V., Ent, S.V. der, García-Andrade, J., Coego, A., Pieterse, C.M., and Vera, P. (2010). OCP3 is an important modulator of NPR1-mediated jasmonic acid-dependent induced defenses in *Arabidopsis*. *BMC Plant Biol.* *10*, 199.
- Ranf, S., Gisch, N., Schäffer, M., Illig, T., Westphal, L., Knirel, Y.A., Sánchez-Carballo, P.M., Zähringer, U., Hüchelhoven, R., Lee, J., et al. (2015). A lectin S-domain receptor kinase mediates lipopolysaccharide sensing in *Arabidopsis thaliana*. *Nat. Immunol.* *16*, 426–433.
- Rayapuram, N., Bigeard, J., Alhoraibi, H., Bonhomme, L., Hesse, A.-M., Vinh, J., Hirt, H., and Pflieger, D. (2018). Quantitative Phosphoproteomic Analysis Reveals Shared and Specific Targets of *Arabidopsis* Mitogen-Activated Protein Kinases (MAPKs) MPK3, MPK4, and MPK6. *Mol. Cell. Proteomics* *17*, 61–80.
- Reményi, A., Good, M.C., Bhattacharyya, R.P., and Lim, W.A. (2005). The role of docking interactions in mediating signaling input, output, and discrimination in the yeast MAPK network. *Mol. Cell* *20*, 951–962.
- Ren, D., Yang, H., and Zhang, S. (2002). Cell Death Mediated by MAPK Is Associated with Hydrogen Peroxide Production in *Arabidopsis*. *J. Biol. Chem.* *277*, 559–565.

References

- Ren, D., Liu, Y., Yang, K.-Y., Han, L., Mao, G., Glazebrook, J., and Zhang, S. (2008). A fungal-responsive MAPK cascade regulates phytoalexin biosynthesis in Arabidopsis. *Proc. Natl. Acad. Sci.* *105*, 5638–5643.
- Reszka, A.A., Seger, R., Diltz, C.D., Krebs, E.G., and Fischer, E.H. (1995). Association of mitogen-activated protein kinase with the microtubule cytoskeleton. *Proc. Natl. Acad. Sci. U. S. A.* *92*, 8881–8885.
- Reyes, J.C., Muro-Pastor, M.I., and Florencio, F.J. (2004). The GATA Family of Transcription Factors in Arabidopsis and Rice. *Plant Physiol.* *134*, 1718–1732.
- Rodríguez, J., and Crespo, P. (2011). Working Without Kinase Activity: Phosphotransfer-Independent Functions of Extracellular Signal-Regulated Kinases. *Sci. Signal.* *4*, re3–re3.
- Roskoski, R. (2012). ERK1/2 MAP kinases: Structure, function, and regulation. *Pharmacol. Res.* *66*, 105–143.
- Rushton, P.J., Somssich, I.E., Ringler, P., and Shen, Q.J. (2010). WRKY transcription factors. *Trends Plant Sci.* *15*, 247–258.
- Saito, H., and Tatebayashi, K. (2004). Regulation of the Osmoregulatory HOG MAPK Cascade in Yeast. *J. Biochem. (Tokyo)* *136*, 267–272.
- Sakamoto, H., Maruyama, K., Sakuma, Y., Meshi, T., Iwabuchi, M., Shinozaki, K., and Yamaguchi-Shinozaki, K. (2004). Arabidopsis Cys2/His2-Type Zinc-Finger Proteins Function as Transcription Repressors under Drought, Cold, and High-Salinity Stress Conditions. *Plant Physiol.* *136*, 2734–2746.
- Schuhegger, R., Nafisi, M., Mansourova, M., Petersen, B.L., Olsen, C.E., Svatoš, A., Halkier, B.A., and Glawischnig, E. (2006). CYP71B15 (PAD3) Catalyzes the Final Step in Camalexin Biosynthesis. *Plant Physiol.* *141*, 1248–1254.
- Shapiro, P.S., Whalen, A.M., Tolwinski, N.S., Wilsbacher, J., Froelich-Ammon, S.J., Garcia, M., Osheroff, N., and Ahn, N.G. (1999). Extracellular Signal-Regulated Kinase Activates Topoisomerase II α through a Mechanism Independent of Phosphorylation. *Mol. Cell. Biol.* *19*, 3551–3560.
- Shevtsova, Z., Malik, J.M.I., Michel, U., Schöll, U., Bähr, M., and Kügler, S. (2006). Evaluation of epitope tags for protein detection after *in vivo* CNS gene transfer. *Eur. J. Neurosci.* *23*, 1961–1969.
- Shikata, M., Matsuda, Y., Ando, K., Nishii, A., Takemura, M., Yokota, A., and Kohchi, T. (2004). Characterization of Arabidopsis ZIM, a member of a novel plant-specific GATA factor gene family. *J. Exp. Bot.* *55*, 631–639.
- Shim, J.S., Jung, C., Lee, S., Min, K., Lee, Y.-W., Choi, Y., Lee, J.S., Song, J.T., Kim, J.-K., and Choi, Y.D. (2013). AtMYB44 regulates WRKY70 expression and modulates antagonistic interaction between salicylic acid and jasmonic acid signaling. *Plant J. Cell Mol. Biol.* *73*, 483–495.
- Shimotohno, A., Umeda-Hara, C., Bisova, K., Uchimiya, H., and Umeda, M. (2004). The Plant-Specific Kinase CDKF;1 Is Involved in Activating Phosphorylation of Cyclin-Dependent Kinase-Activating Kinases in Arabidopsis. *Plant Cell* *16*, 2954–2966.
- Shlyueva, D., Stampfel, G., and Stark, A. (2014). Transcriptional enhancers: from properties to genome-wide predictions. *Nat. Rev. Genet.* *15*, 272–286.
- Smith, N.C., and Matthews, J.M. (2016). Mechanisms of DNA-binding specificity and functional gene regulation by transcription factors. *Curr. Opin. Struct. Biol.* *38*, 68–74.

- Song, C., Lee, J., Kim, T., Hong, J.C., and Lim, C.O. (2018). VOZ1, a transcriptional repressor of DREB2C, mediates heat stress responses in Arabidopsis. *Planta* 247, 1439–1448.
- Sörensson, C., Lenman, M., Veide-Vilg, J., Schopper, S., Ljungdahl, T., Grøtli, M., Tamás, M.J., Peck, S.C., and Andreasson, E. (2012). Determination of primary sequence specificity of *Arabidopsis* MAPKs MPK3 and MPK6 leads to identification of new substrates. *Biochem. J.* 446, 271–278.
- Spitz, F., and Furlong, E.E.M. (2012). Transcription factors: from enhancer binding to developmental control. *Nat. Rev. Genet.* 13, 613–626.
- Stockinger, E.J., Gilmour, S.J., and Thomashow, M.F. (1997). Arabidopsis thaliana CBF1 encodes an AP2 domain-containing transcriptional activator that binds to the C-repeat/DRE, a cis-acting DNA regulatory element that stimulates transcription in response to low temperature and water deficit. *Proc. Natl. Acad. Sci.* 94, 1035–1040.
- Su, J., Xu, J., and Zhang, S. (2015). RACK1, scaffolding a heterotrimeric G protein and a MAPK cascade. *Trends Plant Sci.* 20, 405–407.
- Su, J., Zhang, M., Zhang, L., Sun, T., Liu, Y., Lukowitz, W., Xu, J., and Zhang, S. (2017). Regulation of Stomatal Immunity by Interdependent Functions of a Pathogen-responsive MPK3/MPK6 Cascade and Abscisic Acid. *Plant Cell* tpc.00577.2016.
- Suarez-Rodriguez, M.C., Adams-Phillips, L., Liu, Y., Wang, H., Su, S.-H., Jester, P.J., Zhang, S., Bent, A.F., and Krysan, P.J. (2007). MEKK1 Is Required for flg22-Induced MPK4 Activation in Arabidopsis Plants. *Plant Physiol.* 143, 661–669.
- Sukegawa, Y., Yamashita, A., and Yamamoto, M. (2011). The Fission Yeast Stress-Responsive MAPK Pathway Promotes Meiosis via the Phosphorylation of Pol II CTD in Response to Environmental and Feedback Cues. *PLoS Genet* 7, e1002387.
- Sun, T., Nitta, Y., Zhang, Q., Wu, D., Tian, H., Lee, J.S., and Zhang, Y. (2018). Antagonistic interactions between two MAP kinase cascades in plant development and immune signaling. *EMBO Rep.* 19, e45324.
- Taj, G., Agarwal, P., Grant, M., and Kumar, A. (2010). MAPK machinery in plants. *Plant Signal. Behav.* 5, 1370–1378.
- Takken, F.L., and Govere, A. (2012). How to build a pathogen detector: structural basis of NB-LRR function. *Curr. Opin. Plant Biol.* 15, 375–384.
- Tena, G., Boudsocq, M., and Sheen, J. (2011). Protein kinase signaling networks in plant innate immunity. *Curr. Opin. Plant Biol.* 14, 519–529.
- Therrien, M., Michaud, N.R., Rubin, G.M., and Morrison, D.K. (1996). KSR modulates signal propagation within the MAPK cascade. *Genes Dev.* 10, 2684–2695.
- Triezenberg, S.J., Kingsbury, R.C., and McKnight, S.L. (1988). Functional dissection of VP16, the trans-activator of herpes simplex virus immediate early gene expression. *Genes Dev.* 2, 718–729.
- Tsuda, K., and Somssich, I.E. (2015). Transcriptional networks in plant immunity. *New Phytol.* 206, 932–947.
- Tsuda, K., Sato, M., Stoddard, T., Glazebrook, J., and Katagiri, F. (2009). Network Properties of Robust Immunity in Plants. *PLoS Genet* 5, e1000772.
- Tsuda, K., Mine, A., Bethke, G., Igarashi, D., Botanga, C.J., Tsuda, Y., Glazebrook, J., Sato, M., and Katagiri, F. (2013). Dual regulation of gene expression mediated by extended MAPK

References

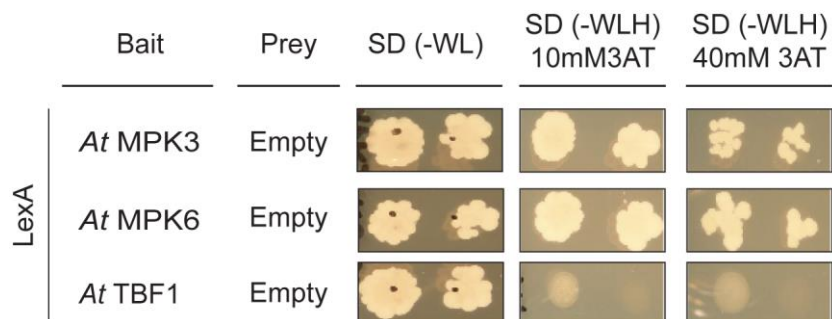
- activation and salicylic acid contributes to robust innate immunity in *Arabidopsis thaliana*. *PLoS Genet.* 9, e1004015.
- Ülker, B., and Somssich, I.E. (2004). WRKY transcription factors: from DNA binding towards biological function. *Curr. Opin. Plant Biol.* 7, 491–498.
- Vailleau, F., Daniel, X., Tronchet, M., Montillet, J.-L., Triantaphylidès, C., and Roby, D. (2002). A R2R3-MYB gene, AtMYB30, acts as a positive regulator of the hypersensitive cell death program in plants in response to pathogen attack. *Proc. Natl. Acad. Sci.* 99, 10179–10184.
- Vidhyasekaran, P. (2014). *PAMP Signals in Plant Innate Immunity - Signal Perception and Transduction* (Springer Berlin Heidelberg).
- Vologzhannikova, A.A., Khorn, P.A., Kazakov, A.S., Permyakov, E.A., Uversky, V.N., and Permyakov, S.E. (2019). Effects of his-tags on physical properties of parvalbumins. *Cell Calcium* 77, 1–7.
- Wang, B., Qin, X., Wu, J., Deng, H., Li, Y., Yang, H., Chen, Z., Liu, G., and Ren, D. (2016). Analysis of crystal structure of *Arabidopsis* MPK6 and generation of its mutants with higher activity. *Sci. Rep.* 6, 25646.
- Wang, H., Ngwenyama, N., Liu, Y., Walker, J.C., and Zhang, S. (2007). Stomatal Development and Patterning Are Regulated by Environmentally Responsive Mitogen-Activated Protein Kinases in *Arabidopsis*. *Plant Cell* 19, 63–73.
- Wang, H., Liu, Y., Bruffett, K., Lee, J., Hause, G., Walker, J.C., and Zhang, S. (2008). Haplo-Insufficiency of MPK3 in MPK6 Mutant Background Uncovers a Novel Function of These Two MAPKs in *Arabidopsis* Ovule Development. *Plant Cell* 20, 602–613.
- Wang, K.L.-C., Li, H., and Ecker, J.R. (2002). Ethylene Biosynthesis and Signaling Networks. *Plant Cell* 14, S131–S151.
- Wang, X., Gao, J., Zhu, Z., Dong, X., Wang, X., Ren, G., Zhou, X., and Kuai, B. (2015). TCP transcription factors are critical for the coordinated regulation of ISOCHORISMATE SYNTHASE 1 expression in *Arabidopsis thaliana*. *Plant J.* 82, 151–162.
- Wang, Y., Li, J., Hou, S., Wang, X., Li, Y., Ren, D., Chen, S., Tang, X., and Zhou, J.-M. (2010). A *Pseudomonas syringae* ADP-ribosyltransferase inhibits *Arabidopsis* mitogen-activated protein kinase kinases. *Plant Cell* 22, 2033–2044.
- Weber, B., Zicola, J., Oka, R., and Stam, M. (2016). Plant Enhancers: A Call for Discovery. *Trends Plant Sci.* 21, 974–987.
- Weirauch, M.T., and Hughes, T.R. (2011). A Catalogue of Eukaryotic Transcription Factor Types, Their Evolutionary Origin, and Species Distribution. In *A Handbook of Transcription Factors*, T.R. Hughes, ed. (Dordrecht: Springer Netherlands), pp. 25–73.
- Willmann, R., Lajunen, H.M., Erbs, G., Newman, M.-A., Kolb, D., Tsuda, K., Katagiri, F., Fliegmann, J., Bono, J.-J., Cullimore, J.V., et al. (2011). *Arabidopsis* lysin-motif proteins LYM1 LYM3 CERK1 mediate bacterial peptidoglycan sensing and immunity to bacterial infection. *Proc. Natl. Acad. Sci. U. S. A.* 108, 19824–19829.
- Witzel, F., Maddison, L.E., and Blüthgen, N. (2012). How scaffolds shape MAPK signaling: what we know and opportunities for systems approaches. *Front. Physiol.* 3.
- Xing, D., Zhao, H., Xu, R., and Li, Q.Q. (2008). *Arabidopsis* PCFS4, a homologue of yeast polyadenylation factor Pcf11p, regulates FCA alternative processing and promotes flowering time. *Plant J.* 54, 899–910.

- Xu, J., Xie, J., Yan, C., Zou, X., Ren, D., and Zhang, S. (2014). A chemical genetic approach demonstrates that MPK3/MPK6 activation and NADPH oxidase-mediated oxidative burst are two independent signaling events in plant immunity. *Plant J. Cell Mol. Biol.* *77*, 222–234.
- Xu, X., Chen, C., Fan, B., and Chen, Z. (2006). Physical and Functional Interactions between Pathogen-Induced Arabidopsis WRKY18, WRKY40, and WRKY60 Transcription Factors. *Plant Cell* *18*, 1310–1326.
- Yablonski, D., Marbach, I., and Levitzki, A. (1996). Dimerization of Ste5, a mitogen-activated protein kinase cascade scaffold protein, is required for signal transduction. *Proc. Natl. Acad. Sci.* *93*, 13864–13869.
- Yamada, K., Yamaguchi, K., Shirakawa, T., Nakagami, H., Mine, A., Ishikawa, K., Fujiwara, M., Narusaka, M., Narusaka, Y., Ichimura, K., et al. (2016). The *Arabidopsis* CERK1-associated kinase PBL27 connects chitin perception to MAPK activation. *EMBO J.* *35*, 2468–2483.
- Yang, S., and Liu, G. (2017). Targeting the Ras/Raf/MEK/ERK pathway in hepatocellular carcinoma (Review). *Oncol. Lett.* *13*, 1041–1047.
- Yanhui, C., Xiaoyuan, Y., Kun, H., Meihua, L., Jigang, L., Zhaofeng, G., Zhiqiang, L., Yunfei, Z., Xiaoxiao, W., Xiaoming, Q., et al. (2006). The MYB Transcription Factor Superfamily of Arabidopsis: Expression Analysis and Phylogenetic Comparison with the Rice MYB Family. *Plant Mol. Biol.* *60*, 107–124.
- Yoo, S.-D., Cho, Y.-H., and Sheen, J. (2007). Arabidopsis mesophyll protoplasts: a versatile cell system for transient gene expression analysis. *Nat. Protoc.* *2*, 1565–1572.
- Yu, W., Fantl, W.J., Harrowe, G., and Williams, L.T. (1998). Regulation of the MAP kinase pathway by mammalian Ksr through direct interaction with MEK and ERK. *Curr. Biol.* *8*, 56–64.
- Zhang, J., Shao, F., Li, Y., Cui, H., Chen, L., Li, H., Zou, Y., Long, C., Lan, L., Chai, J., et al. (2007). A *Pseudomonas syringae* Effector Inactivates MAPKs to Suppress PAMP-Induced Immunity in Plants. *Cell Host Microbe* *1*, 175–185.
- Zhang, M., Su, J., Zhang, Y., Xu, J., and Zhang, S. (2018). Conveying endogenous and exogenous signals: MAPK cascades in plant growth and defense. *Curr. Opin. Plant Biol.* *45*, 1–10.
- Zhang, Z., Wu, Y., Gao, M., Zhang, J., Kong, Q., Liu, Y., Ba, H., Zhou, J., and Zhang, Y. (2012). Disruption of PAMP-Induced MAP Kinase Cascade by a *Pseudomonas syringae* Effector Activates Plant Immunity Mediated by the NB-LRR Protein SUMM2. *Cell Host Microbe* *11*, 253–263.
- Zhang, Z., Liu, Y., Huang, H., Gao, M., Wu, D., Kong, Q., and Zhang, Y. (2017). The NLR protein SUMM2 senses the disruption of an immune signaling MAP kinase cascade via CRCK3. *EMBO Rep.* *18*, 292–302.
- Zheng, Z., Mosher, S.L., Fan, B., Klessig, D.F., and Chen, Z. (2007). Functional analysis of Arabidopsis WRKY25 transcription factor in plant defense against *Pseudomonas syringae*. *BMC Plant Biol.* *7*, 2.
- Zhou, C., Zhang, L., Duan, J., Miki, B., and Wu, K. (2005). HISTONE DEACETYLASE19 Is Involved in Jasmonic Acid and Ethylene Signaling of Pathogen Response in Arabidopsis. *Plant Cell* *17*, 1196–1204.

References

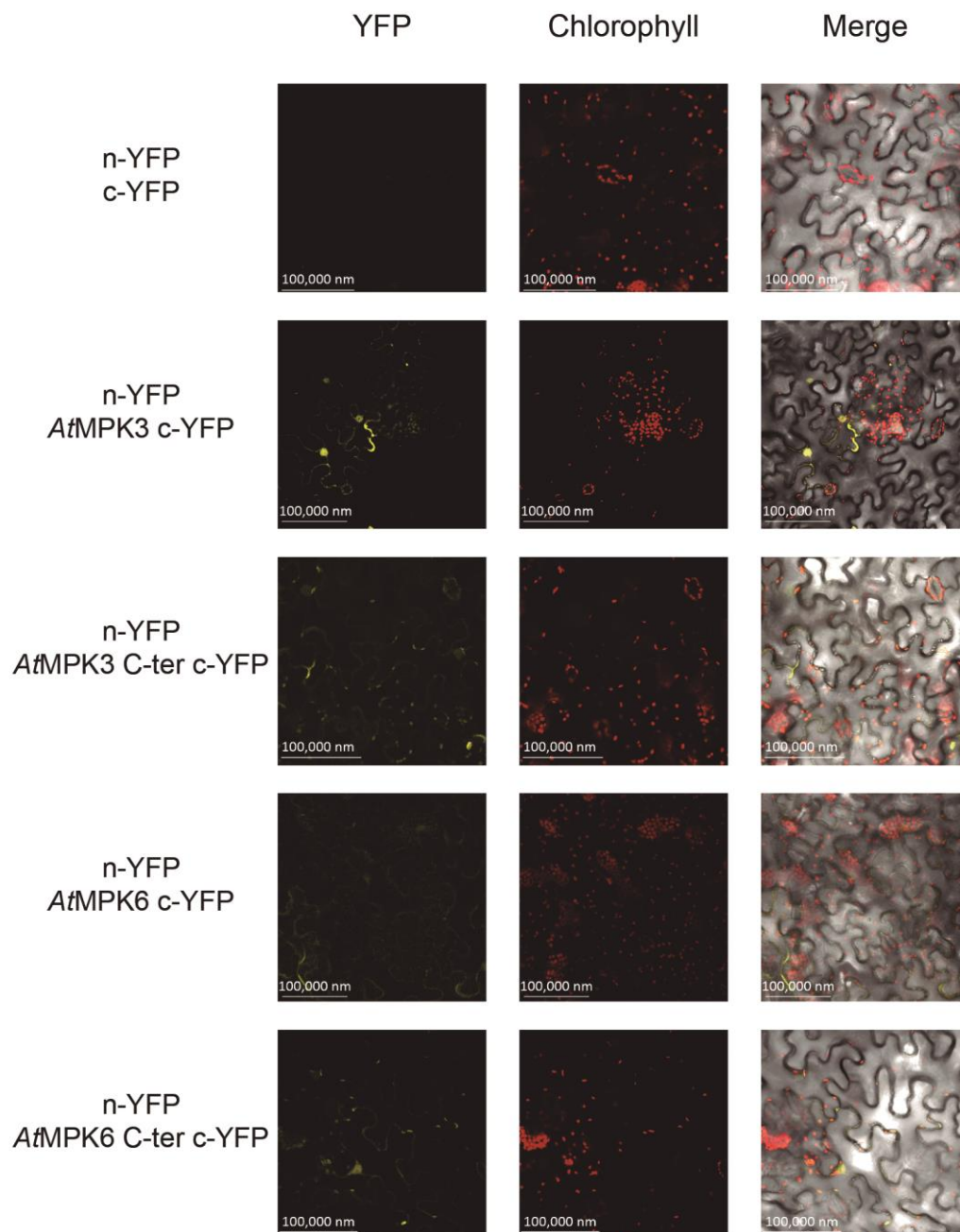
Zipfel, C., Kunze, G., Chinchilla, D., Caniard, A., Jones, J.D.G., Boller, T., and Felix, G. (2006). Perception of the bacterial PAMP EF-Tu by the receptor EFR restricts *Agrobacterium*-mediated transformation. *Cell* *125*, 749–760.

6. Supplementary Material



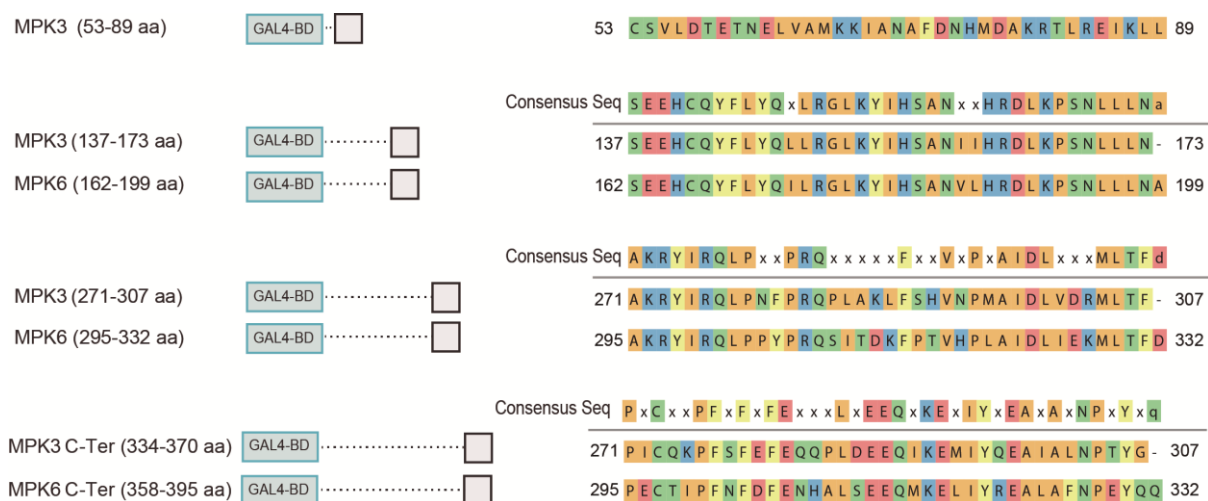
Supplementary Figure 1: *At*MPK3 and *At*MPK6 show autoactivity in Y2H LexA system

The combination of the bait expressing the TF TL1-binding factor (*At*TBF1) and the empty prey with the AD was used as a negative control. Autoactivity of the bait containing the full-length *At*MPK3 or *At*MPK6 was detected in combination with the empty prey containing only AD, as indicated by yeast growth on SD (-WLH) with 10mM and 40mM of 3-amino-1,2,4-triazole (3-AT), a histidine biosynthesis inhibitor. Data was obtained in collaboration with Dr. Nobutaka Mitsuda (AIST, Japan).



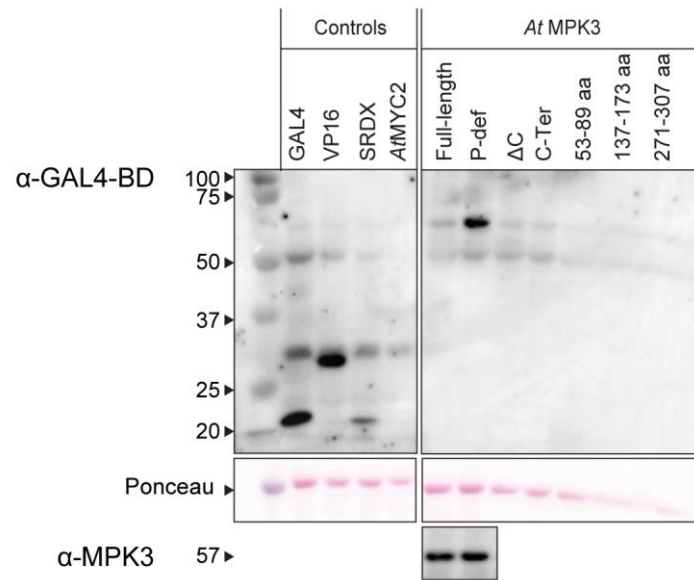
Supplementary Figure 2: YFP fluorescence caused by expression of n-YFP and AtMPK3 and AtMPK6 fused to c-YFP in BiFC assay

Bimolecular fluorescence complementation BiFC control assays. Empty vector pE-SPYNE expressing the n-YFP alone, and the pE-SPYCE vector expressing the MAPKs constructs AtMPK3/6 full-length or C-terminal fused to the c-YFP, were infiltrated in *Nicotiana benthamiana* leaves. YFP fluorescence was analyzed by confocal microscopy 48 h post infiltration.



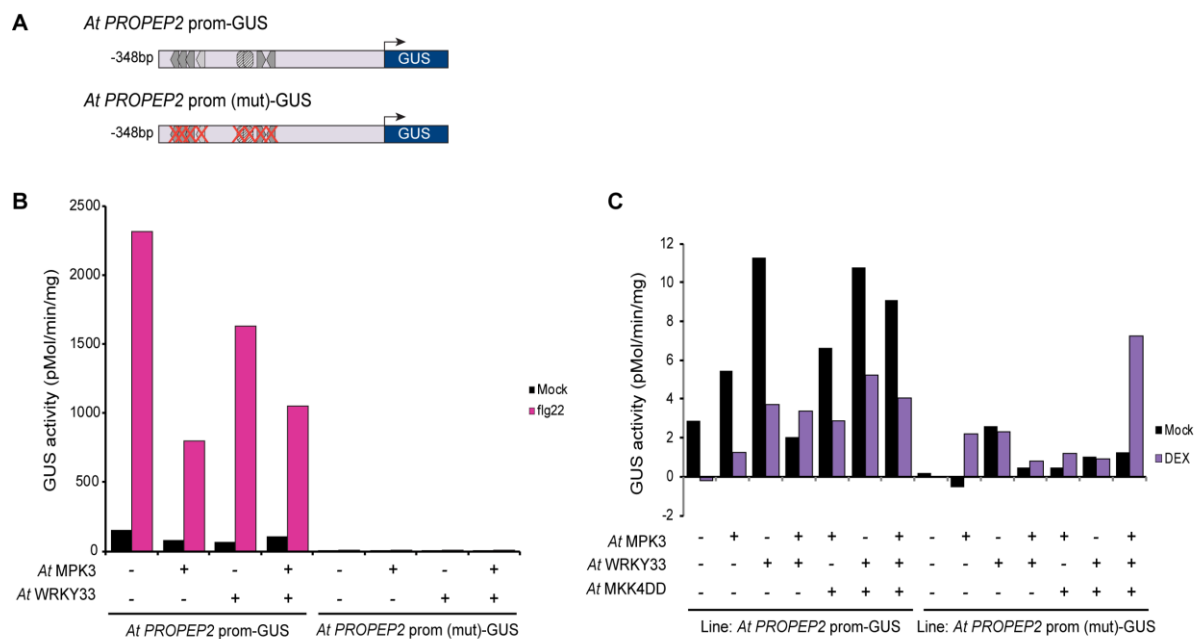
Supplementary Figure 3: Amino sequences of the new *At*MPK3 and *At*MPK6 deletion constructs

Full-length *At*MPK3/6 protein alignment performed by ClustalW (MEGA 5.2.2.) was used for selection of the new deletion constructs. *At*MPK3 constructs were 37aa long, and *At*MPK6 constructs were 38 aa long, comparable to the *At*MPK3/6 C-termini size. Consensus sequences were obtained from MegaAlignPro.



Supplementary Figure 4: Protein accumulations of effector proteins are not detectable by α-GAL4-DBD antibody

Protein accumulation levels of effectors used for transcriptional activity assays in *Arabidopsis* protoplasts were analyzed by western blot (WB) with α-GAL4-DBD (top panel), and α-MPK3 (lower panel) antibodies. Ponceau staining was used for protein loading control.



Supplementary Figure 5: Co-expression of *AtMPK3* and *AtWRKY33* does not lead to *AtPROPEP2* promoter induction

(A) *AtPROPEP2* prom-GUS contains the promoter sequence fused to the GUS reporter. Within the promoter, the W-box elements (T/CTGACC/T), W-box-like motifs (TGACC/T), and the *activation sequence-1/octopine synthase (as-1/OCS)* are shown in dark grey, light grey, and ovals with dash lines, respectively. The red × present in *AtPROPEP2* prom (mut)-GUS indicate the mutation in the DNA binding element as described by (Logemann et al., 2013) (B) GUS activity assays performed in *Arabidopsis* Col-0 protoplasts expressing the *AtMPK3*, *AtWRKY33*, and *AtPROPEP2* prom-GUS or *AtPROPEP2* prom (mut)-GUS for mock and flg22 treatment (100nM flg22). (C) GUS activity assays performed in protoplasts from *AtPROPEP2* prom-GUS, and *AtPROPEP2* prom (mut)-GUS transgenic lines, expressing *AtMPK3*, *AtWRKY33*, and the phosphomimetic version of *AtMKK4* (*AtMKK4DD*) induced by dexamethasone (DEX) treatment (2μM DEX). *AtPROPEP2* promoter constructs, as well as transgenic lines, were obtained from Elke Logemann (Max Planck Institute for Plant Breeding Research, Cologne, Germany).

Supplementary Material

Supplementary Table 1: Molecular weight of effectors containing HA tag

Effector	DNA Size (bp)	Length (aa)	Molecular weight (kDa)
GAL4-HA	582	194	21.53
GAL4-VP16 - HA	867	289	32.08
GAL4-SRDX - HA	675	225	24.98
GAL4-MYC2 - HA	2553	851	94.46
GAL4-MPK3 (53-89 aa) - HA	777	259	28.75
GAL4-MPK3 (137-173 aa) - HA	777	259	28.75
GAL4-MPK3 (271-307 aa) - HA	777	259	28.75
GAL4-MPK3 C-Term - HA	777	259	28.75
GAL4-MPK6 (162-199 aa) - HA	780	260	28.86
GAL4-MPK6 (295-332 aa) - HA	780	260	28.86
GAL4-MPK6 C-Term - HA	780	260	28.86

Acknowledgments

I would like to thank my direct supervisor Dr. Kenichi Tsuda for providing me the opportunity to develop as a scientist in his laboratory. I highly appreciated that your office was always open and that you always make time for discussing my scientific inquiries. I am thankful for your patience and guidance through my Ph.D., especially during my thesis writing. I highly appreciate all the scientific input, advice, and time that you gave me.

I also want to thank Prof. Dr. Jane E. Parker for the scientific input, advice, and constructive criticism during my TAC meetings, as well as her participation in my thesis committee as my first examiner. Moreover, I would like to thank Prof. Dr. Alga Zuccaro for accepting and taking over the work as the second examiner for my thesis. I also would like to thank Prof. Dr. Stanislav Kopriva for accepting, and participating as chair of my defense.

A special thanks to my other thesis committee advisor Dr. Hirofumi Nakagami for his engagement, vivid discussions, and scientific input he provided for my project during the meetings.

The last years at the MPIPZ enriched not only my scientific career, but also provided me the possibility to work, learn, and know people from different places of the world, and for that, I will always be grateful. I would like to thank all the Tsuda lab members: Caro, Matthias, Tom, Tatsi, Kaori, Sayan, Kasia, Yiming, Akira, Ping, Yu, Fred Dieter, Yayoi, and the three little Tsuda boys how made my days at the institute full of joy and happiness. A special thanks to Caro, Matthias, and Tom, all of you are not only great dancers and funny people, but also amazing friends. Moreover, I would like to thank Jonas, Sam, Alfredo, and Paul for all the great moments we shared together. I would also like to thank Saskia for translating my abstract, and to Patrick for all the coffee breaks we shared. Last but definitely not least, I would like to thank all my lovely Spartans for all the support during the last days, you guys remained me how strong people can be when they set a goal, and work in a team.

I would also like to thank my friends Alicia, Marcos, Santiago, Tere, Angela, Diani, Toa, and Rochi for been a great support during the last years. You are like family to me.

Por último quisiera agradecer a mi familia por compartir, disfrutar, sufrir y próximamente celebrar cada etapa de este doctorado. A mi papá, Stellita, mi hermana y Terrance, solo les puedo decir gracias. Gracias por darme la oportunidad de crecer y aprender

que la vida está compuesta de pequeños momentos que hay que atesorar. Su fortaleza, tenacidad, amor y convicción son algunas de las virtudes que admiro más de ustedes. Gracias por apoyarme en cada momento de mi vida y por estar siempre junto a mí.

Erklärung

Ich versichere, dass ich die von mir vorgelegte Dissertation selbständig angefertigt, die benutzten Quellen und Hilfsmittel vollständig angegeben und die Stellen der Arbeit – einschließlich Tabellen, Karten und Abbildungen –, die anderen Werken im Wortlaut oder dem Sinn nach entnommen sind, in jedem Einzelfall als Entlehnung kenntlich gemacht habe; dass diese Dissertation noch keiner anderen Fakultät oder Universität zur Prüfung vorgelegt worden ist, sowie, dass ich eine solche Veröffentlichung vor Abschluss des Promotionsverfahrens nicht vornehmen werde.

Die Bestimmungen dieser Promotionsordnung sind mir bekannt. Die von mir vorgelegte Dissertation ist von Prof. Dr. Jane E. Parker betreut worden.

Ich versichere, dass ich alle Angaben wahrheitsgemäß nach bestem Wissen und Gewissen gemacht habe und verpflichte mich, jedmögliche, die obigen Angaben betreffenden Veränderungen, dem Dekanat unverzüglich mitzuteilen.

Köln, 20. 05. 2019

MARÍA C. SALAZAR R.

María Claudia Salazar Rondón

Curriculum Vitae

María Claudia Salazar Rondón

Adress: Vondelstr. 28,
50677, Köln
Mobil: +004915755034015
Mail: mariac.salazar.rondon@gmail.com
Nationality: Colombian
Date of birth: 30 April 1988

Education and Research Experience

- Nov 2015 – Present **Ph.D. Candidate**
Max Planck Institute for Plant Breeding Research
Cologne, Germany
Supervisor: Dr. Kenichi Tsuda
Role of evolutionary conserved MAP kinase C-terminal regions in transcriptional activation in *Arabidopsis thaliana*.
- Oct 2013 – Sep 2015 **Master of Science Rheinische Friedrich-Wilhelms-Universität Bonn, Germany**
Focus on Plant Molecular Biology.
Master Thesis: Identification of novel transcription factor substrates of the Arabidopsis MAP kinases MPK3 and MPK6 by yeast two-hybrid assays.
- Jan 2008 – Dic 2012 **Bachelor of Science in Biology**
Universidad de los Andes. Bogota, Colombia
Specialization module: Developmental Biology, Systematics and Evolutionary Genetics, and Molecular Plant-Pathogen Interaction
- Aug 2007 – Dic 2012 **Bachelor of Science in Microbiology**
Universidad de los Andes. Bogota, Colombia
Specialization module: Molecular Cell Biology of Prokaryotes, Molecular Genetics of Eukaryotes, and Bacteriophages Biology
- Feb 2010 – Oct 2010 **Bachelor Internship**
Leibniz-Institut für Gemüse-und Zierpflanzenbau, Grossbeeren/Erfurt e.V, Germany
Analyzing the pathosystem *Rhizoctonia solani* AG3 and tomato plants; and *Rhizoctonia solani* AG1 and lettuce plants
- Jan 1995 – Jun 2006 **High School**

Colegio CIEDI. Bogota, Colombia

Publications

2017 **An incoherent feed-forward loop mediates robustness and tunability in a plant immune network**
Mine, A., Nobori, T., **Salazar-Rondon, M.C.**, Winkelmüller, T.M., Anver, S., Becker, D., and Tsuda, K.
EMBO Reports

Work Experience

Jun 2013 – Aug 2013 **Research Assistance**
Jardines de los Andes, El Cartucho S.A. Bogota, Colombia
Plant resistance and pathogen control

Languages

Spanish Mother tongue

Other language(s)	UNDERSTANDING		SPEAKING		WRITING
	Listening	Reading	Spoken interaction	Spoken production	
English	C2	C2	C2	C2	C1
Internet-based TOEFL test score (97/120)					
German	A2	A2	A2	A2	A1
Italian	B2	B2	B1	B1	B2

Levels: A1/A2: Basic user - B1/B2: Independent user - C1/C2: Proficient user
Common European Framework of Reference for Languages